



Effects of Chromium and Diclofenac on tomato's N and C primary metabolisms. Glutamine Synthetase as a key metabolic point to enhance plant stress tolerance

Maria João de Araújo Martins
Dissertação de Mestrado apresentada à
Faculdade de Ciências da Universidade do Porto em
Área Científica
2018



Effects of Chromium and Diclofenac on tomato's N and C primary metabolisms. Glutamine Synthetase as a key metabolic point to enhance plant stress tolerance

Maria João de Araújo Martins

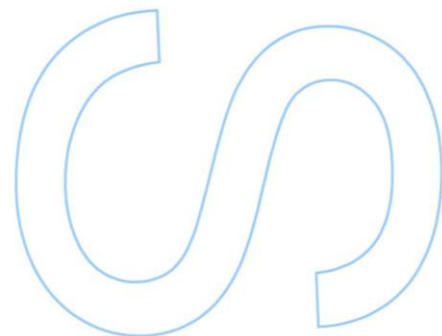
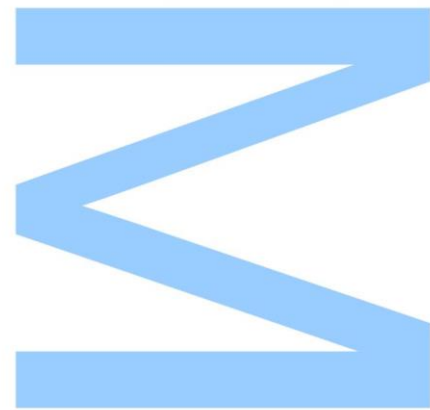
Mestrado em Biologia Funcional e Biotecnologia de Plantas
Departamento de Biologia
2018

Orientador

Jorge Teixeira, Professor Auxiliar, Faculdade de Ciências da Universidade do Porto

Coorientador

Fernanda Fidalgo, Professora Auxiliar, Faculdade de Ciências da Universidade do Porto

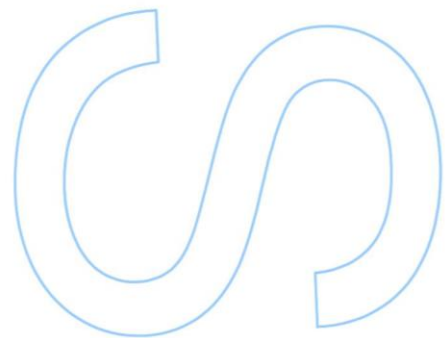
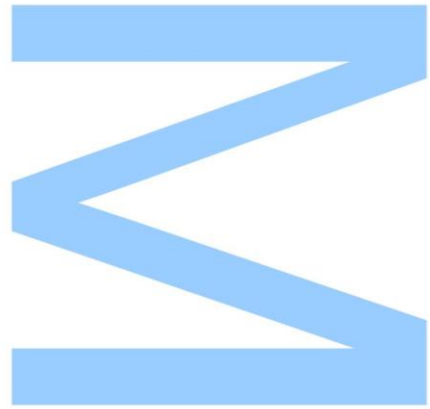




Todas as correções determinadas pelo júri, e só essas, foram efetuadas.

O Presidente do Júri,

Porto, ____ / ____ / ____



***“The only place success comes before work
is in the dictionary” - Vince Lombardi***

Aknowledgements

Terminado este trabalho e este longo ano, resta-me agora agradecer a todas as pessoas que fizeram parte do meu percurso.

Antes de mais, quero primeiramente agradecer ao Professor Jorge! O professor desde cedo acompanhou o meu percurso e foi essencial para o sucesso deste trabalho. O professor foi a primeira pessoa que me levou a descobrir o maravilhoso mundo das plantas e agradeço-lhe por isso. Obrigada por toda a confiança que o professor me transmitiu ao longo do tempo, pela paciência quando eu desanimava, por me ter sempre tentado motivar a fazer mais e melhor nas horas e horas de conversas.

À Professora Fernanda, co-orientadora deste trabalho, muito obrigada pelo rigor, pela disponibilidade, por todos os conselhos e conhecimentos transmitidos e por toda a motivação que sempre me deu.

Aos meus “mini-bosses” Leonor e Cris: nem tenho palavras para vos agradecer o vosso apoio, ajuda, transmissão de conhecimentos, pelo carinho e pela amizade desenvolvida. Sem vocês, tenho a certeza que este trabalho não era o mesmo. Vocês são o meu exemplo de cientistas e fazem de mim uma cientista melhor!

Aos colegas de laboratório Jorge e Bruno, muito obrigada por todos estes anos (que já são alguns) de partilha, alegria, viagens de comboio e muita, muita luta diária no 2.62! Para além disto, muito obrigada pelas plantinhas, sem o vosso cuidado, este trabalho, garantidamente, não estaria feito. Aos meus “escravos” Miguel, David e João, muito obrigada pelo apoio e confiança nos meus conhecimentos.

À Ana Marta, muito obrigada pela ajuda, pela paciência a aturares os meus desesperos com o real-time (mas consegui!), pelas “regras da Marta” (prometo não me esquecer!), por toda a motivação e pelos conhecimentos.

Às “girls das plantas” Diana e Bruna, obrigada por estes 2 anos, foram muito mais fáceis com vocês do meu lado. Obrigada pelas conversas, pelos desabafos, pelo estudo e por toda a motivação! À Diana só tenho a dizer que sem ti, as horas de almoço a falar da vida não seriam a mesma coisa (:D).

Às duas meninas que na fase mais difícil estiveram lá, incondicionalmente, para me dar uma palavra de conforto e carinho: Maling e Catarina, muito obrigada! Que esta amizade se mantenha por muitos anos.

À Inês (ou Tina), que, embora longe, estará sempre por perto, obrigada por tudo! Foi um enorme gosto partilhar contigo todos estes anos e desejo que o futuro nos reserve o melhor!

Sara, obrigada por seres a minha pessoa, o meu juízo e a minha inspiração durante estes anos. Foste, és e serás das melhores amizades que eu levo destes 5 anos!

Ao Pedro e à Joana, obrigada por não se limitarem a ser meros amigos, mas sim, realmente, a família que eu escolhi! Obrigada pela paciência, pelo orgulho que têm em mim e por todos os momentos que ao longo destes anos partilhamos juntos.

Ao Micael, que ao longo destes 3 anos me tem aturado mais do que qualquer um e faz de mim uma melhor pessoa e melhor cientista. Não há palavras para ti, mas sei que não preciso de dizer nada. Obrigada, por tudo!

Para terminar, como não poderia deixar de ser, um último (e talvez o maior) agradecimento à minha família por sempre me apoiarem, motivarem e educarem a querer fazer sempre mais e melhor. Obrigada por sempre me deixarem lutar pelos meus objetivos e por estarem lá quando eu os conquisto. Pai, avós, tios, irmãs e primos, e em especial mãe: esta é para vocês!

A todos vocês que, de alguma maneira, contribuíram para este trabalho: MUITO OBRIGADA!

Resumo

O crescimento mundial da população humana, bem como as atividades antropogénicas, têm levado a um aumento na utilização de metais pesados e produtos farmacêuticos, causando sérias perturbações no meio ambiente. O crómio (Cr) é um metal pesado muito perigoso, sendo libertado para o meio ambiente em largas quantidades e com efeitos nefastos conhecidos em vários organismos, incluindo nas plantas. O diclofenac (DCF) é um medicamento anti-inflamatório não esteroide extremamente utilizado, que não é totalmente removido nos processos de tratamento de águas residuais, atingindo assim todos os ecossistemas e apresentando-se como uma ameaça a todos os organismos. Através de uma abordagem integrada, combinando parâmetros bioquímicos com técnicas de biologia molecular, este trabalho teve como objetivo avaliar a fitotoxicidade de Cr e DCF em tomateiro, focando-se em dois processos primários das plantas: a assimilação de azoto e a fotossíntese. Além disso, pretendeu-se sobreexpressar o cDNA que codifica a GS2, como uma ferramenta para aumentar a tolerância das plantas. A exposição a concentrações crescentes de Cr (0, 5 e 10 μM) e DCF (0, 0,5 e 5 mg L^{-1}) revelou que a glutamina sintetase (GS) foi diferencialmente afetada por ambos contaminantes ao nível da expressão génica, atividade e proteína, e que a atividade da enzima glutamato desidrogenase (GDH) aumentou, bem como os níveis de prolina. De um modo geral, após exposição ao Cr e DCF, foi observada uma diminuição nos transcritos dos genes relacionados com a fotossíntese, bem como uma redução na quantidade de amido. No entanto, nas plantas tratadas com Cr e DCF, os níveis de pigmentos fotossintéticos e o aparelho fotossintético não sofreram alterações. Adicionalmente, estes contaminantes induziram alterações no perfil do conteúdo polipeptídico solúvel. Os resultados obtidos sugerem que a GDH tem um papel importante e alternativo na assimilação do azoto, bem como na produção de prolina, em resposta ao stress. Além disso, o aparecimento de polipeptídeos de baixa massa molecular aponta para o papel de proteínas relacionadas com o stress na tolerância ao Cr e DCF. A clonagem do cDNA que codifica a GS2 em orientações opostas foi bem-sucedida, sendo este o primeiro passo para obtenção das primeiras plantas de tomateiro a sobreexpressar a GS2 com um aumento da tolerância ao stress.

Abstract

The growing of human population worldwide, as well as human activities, led to an increase in heavy metals (HMs) and pharmaceuticals utilization, causing serious disturbances in the environment. Cr is a dangerous HM, that is discharged to the environment in huge quantities and with known negative effects in various organisms, including plants. DCF is an extremely used non-steroidal anti-inflammatory drug (NSAID) that is not entirely removed by wastewater treatment processes, thus reaching all ecosystems and being a serious threat to all organisms. Through an integrated approach, where biochemical parameters and molecular biology techniques were combined, this work aimed to evaluate the phytotoxicity of Cr and DCF on tomato plants, focusing on two primary plant processes: nitrogen assimilation and photosynthesis. Moreover, the overexpression the GS2-encoding cDNA as a tool to increase plant tolerance was started. The exposure to increased concentrations of Cr (0, 5 and 10 μM) and DCF (0, 0.5 and 5 mg L^{-1}) revealed that GS was differentially affected by both contaminants at the gene expression, activity and protein levels, and that GDH activity was enhanced, followed by an increase in proline levels. Upon exposure to Cr (VI) and DCF, an overall decrease in photosynthetic-related genes' transcripts accumulation was observed paired with a reduction in the starch content. However, the pigments' contents and the photosynthetic apparatus did not alter in Cr (VI)- and DCF-treated plants. Additionally, these contaminants induced some alterations in the soluble polypeptide content profile. The obtained results suggest that GDH plays an important and alternative role in N assimilation, as well as in proline production, in response to stress. Furthermore, the appearance of low molecular weight polypeptides indicates a role of some stress-related proteins in Cr (VI)- and DCF-induced stress tolerance. The cloning of S/GS2-encoding cDNA in opposite directions was successfully achieved, being the first step to obtain the first tomato plants overexpressing GS2 and with increased tolerance to stress.

Keywords

Nitrogen assimilation, glutamate dehydrogenase, heavy metals, pharmaceuticals, photosynthesis, overexpression (glutamine synthetase), abiotic stress; *Solanum lycopersicum* L.

Table of Contents

Aknowledgements	II
Resumo	IV
Abstract	V
Keywords.....	V
Figure Index.....	X
Table Index.....	XIV
1. Introduction.....	1
1.1 Heavy metal contamination.....	1
1.1.1 Chromium VI [Cr (VI)] and its phytotoxicity	2
1.2 Pharmaceuticals contamination	4
1.2.1 Diclofenac (DCF) and its phytotoxicity	6
1.3 Nitrogen (N) metabolism.....	8
1.3.1 Glutamine synthetase and its role in NUE improvement	9
1.3.2 Glutamate Dehydrogenase	11
1.4 GS and GDH - a role in proline production under stress	12
1.5 <i>Solanum lycopersicum</i> L. cv Micro-Tom as a perfect model species for molecular biology studies	12
1.6 Main Objectives	14
2. Material and Methods	15
2.1 Plant material and growth conditions	15
2.2 Analytical determinations	15
2.2.1 Determination of Cr content in plant tissues.....	15
2.3 Biochemical determinations	16
2.3.1 Glutamine synthetase activity determination (GS; EC 6.3.1.2).....	16
2.3.2 GDH activity determination (GDH, EC 1.4.1.2)	16
2.3.3 Sodium dodecyl sulphate polyacrylamide gel electrophoresis (SDS-PAGE) 17	
2.3.4 Western Blotting analysis.....	17

2.3.5	Evaluation of photosynthesis-related parameters	18
2.3.5.1	Photosynthetic pigments evaluation.....	18
2.3.5.2	Gas exchange analysis.....	19
2.3.5.3	Histochemical coloration of starch	19
2.3.6	Proline quantification	19
2.4	Bioinformatics characterisation of <i>Solanum lycopersicum</i> GS-encoding gene family (<i>S/GSs</i>)	20
2.5	Evaluation of expression of <i>Solanum lycopersicum</i> GS gene family	20
2.5.1	RNA extraction, quantification and assessment of its purity	20
2.5.2	Reverse Transcription (cDNA Synthesis).....	21
2.5.3	Primer design	21
2.5.4	Gene Sequencing.....	22
2.5.5	Expression of <i>S/GS</i> genes by Semi-quantitative RT-PCR.....	23
2.5.6	Evaluation of <i>S/GS</i> gene expression by Real-time PCR (qPCR).....	23
2.6	Evaluation of photosynthetic-related genes expression by qPCR	24
2.7	Overexpression of GS2-encoding cDNA.....	24
2.7.1	Obtaining <i>S/GS2</i> -encoding cDNA sequence.....	24
2.7.1.1	Genomic DNA extraction	24
2.7.1.2	Obtaining the <i>S/GS2</i> gene	25
2.7.1.3	Obtaining <i>S/GS2</i> -encoding cDNA	25
2.7.2	Bacterial strains and culture conditions.....	26
2.7.3	Induction of chemical competency in <i>E. coli</i> DH5 α	26
2.7.4	Induction of electro competency in <i>E. coli</i> DH5 α	26
2.7.5	Ligation to the pJET 1.2 plasmid.....	26
2.7.6	Transformation of chemical competent <i>E. coli</i> DH5 α	27
2.7.7	Electro Transformation of <i>E. coli</i> DH5 α	27
2.7.8	Plasmid Isolation	27
2.7.9	Plasmid DNA extraction using NZYMiniprep kit	28
2.7.10	Restriction Analysis	28

2.8	Statistical Analysis	29
3.	Results	30
3.1	Cr accumulation on tomato plants' shoots and roots	30
3.2	Effects of Cr (VI) and DCF on nitrogen assimilation	30
3.2.1	GS and GDH activity	30
3.2.2	Western Blotting Analysis	32
3.3	Soluble polypeptide accumulation analysis after Cr (VI) and DCF exposure	33
3.4	Evaluation of Cr (VI) and DCF impact on physiological parameters associated with nitrogen metabolism	35
3.5	Assessment of the Cr (VI) and DCF effects on several photosynthetic endpoints	35
3.5.1	Photosynthetic pigments	36
3.5.2	Photosynthetic apparatus	36
3.5.3	Photosynthesis-related gene expression	37
3.5.4	Starch accumulation	38
3.6	Bioinformatics characterisation of <i>Solanum lycopersicum</i> L.'s GS-encoding gene family	39
3.6.1	Phylogenetic analysis of <i>S. lycopersicum</i> cDNAs coding for GS (<i>SIGSs</i>)	39
3.6.2	<i>SIGSs</i> relative expression analysis using the eFP browser	40
3.6.3	<i>SIGS</i> gene family relative expression analysis by RT-PCR	41
3.7	Study of Cr (VI) and DCF impact on <i>SIGS</i> gene family expression	43
3.7.1	Changes in transcript levels of tomato GS genes under Cr (VI)- and DCF-induced stress	43
3.8	Cloning of the <i>SIGS2</i> -encoding cDNA	46
4.	Discussion	49
4.1	The accumulation of Cr occurs predominately in roots	49
4.2	GS – from gene to protein	49
4.3	Cr (VI) and DCF differentially influenced N metabolism at gene expression, enzyme activity and polypeptide levels	50

4.4	Proline accumulation is positively affected by both contaminants	54
4.4.1	GDH - An alternative pathway that allow proline accumulation under stressful conditions	55
4.5	The exposure of tomato plants to Cr (VI) and DCF did not impair photosynthetic activity	56
4.6	Both Cr (VI) and DCF induced changes in soluble polypeptide content and profile	59
4.7	Development of new tools that will allow the overexpression of <i>SIGS2</i> -encoding cDNA	60
5.	Concluding remarks	62
6.	Future Perspectives	63
7.	References	64
	Supplemental Data	82

Figure Index

Figure 1. Sources of Cr (VI) in the environment and some effect of Cr (VI) in plants. ...	4
Figure 2. Different sources of pharmaceuticals and the pathways used to reach the aquatic environment (based on Lapworth et al. (2012)).	5
Figure 3. Diclofenac chemical structure (from: Vieno and Sillanpää (2014)).....	7
Figure 4. Biochemical reactions catalysed by GS and GOGAT (Adapted from Hodges (2002)).....	9
Figure 5. <i>Solanum lycopersicum</i> L. cv Micro-Tom.	13
Figure 6. Chromium accumulation levels in shoots (A) and roots (B) of tomato plants. CTL: Control; Cr 5: 5 µM Chromium (VI); Cr 10: 10 µM Chromium (VI); n.d.: non-detected. Values presented are mean plus SD. **** above bars indicate significant statistical differences from control at $p \leq 0.0001$	30
Figure 7. GS activity in shoots (A) and roots (B) of tomato plants exposed to Cr (VI) and DCF expressed as nkat mg ⁻¹ protein. CTL: Control; Cr 5: 5 µM Chromium (VI); Cr 10: 10 µM Chromium (VI); DCF 0.5: 0.5 mg L ⁻¹ Diclofenac; DCF 5: 5 mg L ⁻¹ Diclofenac. Values presented are mean ± SD. *** and **** above bars indicate significant statistical differences from control at $p \leq 0.001$ and $p \leq 0.0001$, respectively.....	31
Figure 8. Typical GDH activity results for shoots and roots by native PAGE analysis. CTL: Control; Cr 5: 5 µM Chromium (VI); Cr 10: 10 µM Chromium (VI); DCF 0.5: 0.5 mg L ⁻¹ Diclofenac; DCF 5: 5 mg L ⁻¹ Diclofenac.....	32
Figure 9. One-dimensional western blotting analysis of shoot (A) and root (B) tomato GS using GS antibodies raised to <i>Pinus</i> cytosolic GS. CTL: Control; Cr 5: 5 µM Chromium (VI); Cr 10: 10 µM Chromium (VI); DCF 0.5: 0.5 mg L ⁻¹ Diclofenac; DCF 5: 5 mg L ⁻¹ Diclofenac.....	33
Figure 10. One-dimensional western blotting analysis of shoot (A) and root (B) tomato NAD-GDH using antibodies raised to <i>Vitis vinifera</i> NAD-GDH. CTL: Control; Cr 5: 5 µM Chromium (VI); Cr 10: 10 µM Chromium (VI); DCF 0.5: 0.5 mg L ⁻¹ Diclofenac; DCF 5: 5 mg L ⁻¹ Diclofenac.	33
Figure 11. Typical SDS-PAGE analysis of soluble proteins on shoots (A) and roots (B) of <i>S. lycopersicum</i> . CTL: Control; Cr 5: 5 µM Chromium (VI); Cr 10: 10 µM Chromium (VI); DCF 0.5: 0.5 mg L ⁻¹ Diclofenac; DCF 5: 5 mg L ⁻¹ Diclofenac. Arrows indicate common bands that suffered a decreased (red) or an increased accumulation; - indicates qualitative changes: red – disappearance; green – de novo polypeptide. The used ladder was BLUE Wide Range CSL-BBL Prestained Protein Ladder (Clever Scientific Ltd).	34
Figure 12. Proline levels in shoots (A) and roots (B) of tomato plants exposed to Cr (VI) and DCF. CTL: Control; Cr 5: 5 µM Chromium (VI); Cr 10: 10 µM Chromium (VI); DCF	

0.5: 0.5 mg L⁻¹ Diclofenac; DCF 5: 5 mg L⁻¹ Diclofenac. Values presented are mean ± SD. *, ** and *** above bars indicate significant statistical differences from control at p ≤ 0.05, p ≤ 0.01 and p ≤ 0.001, respectively..... 35

Figure 13. Total chlorophylls (A) and carotenoids (B) levels of tomato plants exposed to Cr (VI) and DCF. CTL: Control; Cr 5: 5 µM Chromium; Cr 10: 10 µM Chromium; DCF 0.5: 0.5 mg L⁻¹ Diclofenac; DCF 5: 5 mg L⁻¹ Diclofenac. Values presented are mean ± SD. **, *** and **** above bars indicate significant statistical differences from control at p ≤ 0.01, p ≤ 0.001 and p ≤ 0.0001, respectively..... 36

Figure 14. Expression profile of two genes coding for protein subunits of PSII, D1 protein (PSIIa) and CP47 (PSIIb), respectively, of tomato leaves exposed to Cr (VI) and DCF. CTL: Control; Cr 5: 5 µM Chromium; Cr 10: 10 µM Cr (VI); DCF 0.5: 0.5 mg L⁻¹ Diclofenac; DCF 5: 5 mg L⁻¹ Diclofenac. Values presented are mean ± SD. ** and **** above bars indicate significant statistical differences from control at p ≤ 0.01 and p ≤ 0.0001, respectively..... 37

Figure 15. Expression profile of the small and large subunits of RuBisCO, rbcS and rbcL, respectively, of tomato leaves exposed to Cr (VI) and DCF. CTL: Control; Cr 5: 5 µM Chromium; Cr 10: 10 µM Cr (VI); DCF 0.5: 0.5 mg L⁻¹ Diclofenac; DCF 5: 5 mg L⁻¹ Diclofenac. Values presented are mean ± SD. * and **** above bars indicate significant statistical differences from control at p ≤ 0.05 and p ≤ 0.0001, respectively. 38

Figure 16. Lugol staining of starch in tomato leaves exposed to Cr (VI) and DCF. CTL: Control; Cr 5: 5 µM Chromium (VI); Cr 10: 10 µM Chromium (VI); DCF 0.5: 0.5 mg L⁻¹ Diclofenac; DCF 5: 5 mg L⁻¹ Diclofenac. 39

Figure 17. Phylogenetic tree constructed with all *S. lycopersicum* GS cDNA sequences recovered from the databases referred in the text. The bootstrap consensus tree was generated using the Neighbour-Joining method with MEGA7, with 1000 bootstrap replicates. The percentage of replicate trees in which the associated taxa clustered together in the bootstrap test are shown next to the branches. Bar represents the scale length..... 40

Figure 18. Agarose gel (0.8% (w/v)) electrophoresis evidencing the PCR products of GS2, GS1.1, GS1.2, GS1.3 and GS1.4 of *S. lycopersicum* when gDNA was used as template. The used ladder was NZYDNA Ladder III (Nzytech®, Portugal). 42

Figure 19. Results for GS2, GS1.1, GS1.2, GS1.3 and GS1.4 RT-PCR analysis by 0.8 % (w/v) agarose gel electrophoresis in both shoots and roots; Expected sizes: 189 bp; 178 bp, 191 bp; 164 bp; 192 bp, respectively. GS1.1- corresponds to the negative control reaction for GS1.1..... 43

Figure 20. Total RNA extracted from shoots and roots of tomato plants exposed to Cr (VI) and DCF. For quality assessment of total RNA, it was separated on agarose gel at 0.8 % (w/v). CTL: Control; Cr 5: 5 μM Chromium (VI); Cr 10: 10 μM Chromium; DCF 0.5: 0.5 mg L^{-1} Diclofenac; DCF 5: 5 mg L^{-1} Diclofenac. 43

Figure 21. Expression profile of GS2 gene in shoots (A) and roots (B), of tomato leaves exposed to Cr (VI) and DCF. CTL: Control; Cr 5: 5 μM Chromium (VI); Cr 10: 10 μM Chromium (VI); DCF 0.5: 0.5 mg L^{-1} Diclofenac; DCF 5: 5 mg L^{-1} Diclofenac. Values presented are mean \pm SD. * and *** above bars indicate significant statistical differences from control at $p \leq 0.05$ and $p \leq 0.001$, respectively. 44

Figure 22. Expression profile of GS1.1 gene in shoots (A) and roots (B), of tomato leaves exposed to Cr (VI) and DCF. CTL: Control; Cr 5: 5 μM Chromium (VI); Cr 10: 10 μM Chromium (VI); DCF 0.5: 0.5 mg L^{-1} Diclofenac; DCF 5: 5 mg L^{-1} Diclofenac. Values presented are mean \pm SD. * and **** above bars indicate significant statistical differences from control at $p \leq 0.05$ and $p \leq 0.0001$, respectively. 45

Figure 23. Typical results for GS1.2, GS1.3 and GS1.4 semi-quantitative RT-PCR analysis by 2 % (w/v) agarose gel electrophoresis in both shoots (A) and roots (B) of tomato plants exposed to increasing concentrations of Cr (VI); Expected sizes: 191 bp; 164 bp; 192 bp, respectively. CTL: Control; T1: 5 μM Cr (VI); T2: 10 μM Cr (VI). 45

Figure 24. Typical results for GS1.2, GS1.3 and GS1.4 semi quantitative RT-PCR analysis by 2 % (w/v) agarose gel electrophoresis in both shoots (A) and roots (B) of tomato plants exposed to increasing concentrations of DCF; Expected sizes: 191 bp; 164 bp; 192 bp, respectively. CTL: Control; T1: 0.5 mg L^{-1} DCF; T2: 5 mg L^{-1} DCF. 46

Figure 25. Agarose gel (0.8% (w/v)) electrophoresis evidencing the PCR products of GS2 of *S. lycopersicum* when gDNA was used as template, using 54.7, 53.4 and 51 $^{\circ}\text{C}$ as annealing temperatures (lanes 1 to 3, respectively). The chosen temperature is highlighted. The ladder used was NZYDNA Ladder III (Nzytech®, Portugal). 46

Figure 26. Schematic representation of the GS2 cDNA insert depicting the sites for the restriction enzymes *SacI*, *NcoI* and *XhoI*. The cDNA size is 1684 bp. 47

Figure 27. Agarose gel (0.8 % (w/v)) electrophoresis evidencing three distinct minipreps digested with *XhoI* (A) and *NcoI* (B). The green and red arrows highlight the SIGS2-encoding cDNA in the sense and antisense orientations, respectively. 1, 2 and 3 represent the three distinct minipreps. The ladder used was GeneRuler 100 bp Plus DNA ladder, ready-to-use (ThermoFisher Scientific). 47

Figure 28. Agarose gel (0.8 % (w/v)) electrophoresis evidencing two distinct minipreps digested with *SacI*. 1 and 2 represent minipreps 1 and 2, respectively. The arrows

evidence two bands resulting from the restriction. The used ladder was GeneRuler 100 bp Plus DNA ladder, ready-to-use (ThermoFisher Scientific). 48

Figure 29. Two pathways that provide the glutamate for proline production and accumulation, under stressful conditions. The dashed arrow corresponds to the GDH pathway, which is an alternative route for amino acid's production, while the GS/GOGAT cycle corresponds to the principal pathway of glutamate, and thus, proline production. 56

Table Index

Table 1. Concentrations of different pharmaceuticals in crops from agricultural fields and subsequent phytotoxicities of each compound (adapted from Bartrons and Peñuelas (2017)).	6
Table 2. Summary of properties of Diclofenac (Feito et al., 2012).	7
Table 3. Gene-specific primers, their T_m and respective expected amplicon sizes for the performed RT-PCR reactions.	22
Table 4. Photosynthetic gene-specific primers and respective expected amplicon sizes.	24
Table 5. Gas exchange measurement of plants exposed to Cr (VI) and DCF, considering the following parameters: A, CO ₂ uptake ($\mu\text{mol m}^{-2} \text{s}^{-1}$); E, transpiration rate ($\text{mmol m}^{-2} \text{s}^{-1}$); Gs, stomatal conductance ($\text{mmol m}^{-2} \text{s}^{-1}$); WUE, water use efficiency (nmol mol^{-1}); Ci/Ca, internal and environmental CO ₂ ratio. CTL: Control; Cr 5: 5 μM Chromium (VI); Cr 10: 10 μM Cr (VI); DCF 0.5: 0.5 mg L^{-1} Diclofenac; DCF 5: 5 mg L^{-1} Diclofenac. Values presented are mean \pm SD. ** above bars indicate significant statistical differences from control at $p \leq 0.01$.	37
Table 6. Effects of Cr (VI) treatments on photosynthetic-related genes expression. It was considered up regulated or down regulated if expression increased, or decreased (respectively) with $p < 0.05$, and no change if $p > 0.05$; CTL: Control; Cr 5: 5 μM Chromium (VI); Cr 10: 10 μM Chromium (VI); DCF 0.5: 0.5 mg L^{-1} Diclofenac; DCF 5: 5 mg L^{-1} Diclofenac.	38
Table 7. Relative expression levels of the tomato GS-encoding genes on leaves and roots.	40
Table 8. Summary of chosen temperatures, expected sizes and intron presence of all SIGS-encoding genes.	42
Table 9. Summary of the effects of Cr (VI) and DCF exposure on the mRNA accumulation of the tomato GS-encoding genes. (=) means no changes, (-) means decreased accumulation and (+) means increased accumulation relative to the control. (x) means no mRNA accumulation.	52

Abbreviations and Acronyms

2-OG – 2- oxoglutarate;

ADP – adenosine diphosphate;

ALAD – δ-aminolevulinic acid dehydratase;

AMP – ampicillin;

Ca – calcium;

Car – carotenoid;

Chla – chlorophyll a;

Chlb – chlorophyll b;

Cr – chromium;

DCF – 2-(2-(2,6-dichlorophenylamino)phenyl) acetic acid; diclofenac;

DTT – 1,4-dithioereitol;

EC – emerging contaminants;

FW – fresh weight;

gDNA – genomic DNA;

GDH – glutamate dehydrogenase;

GOGAT – glutamate synthase;

GS – glutamine synthetase;

GS1 – cytosolic glutamine synthetase;

GS2 – plastidic glutamine synthetase;

HM – heavy metal;

HS – Hoagland solution;

LB – Luria Broth;

MTT-3-(4,5-dimethylthiazol-2-yl)-2,5-diphenyltetrazolium bromide

NR – nitrate reductase;

NUE – Nitrogen Use Efficiency;

ON – Overnight;

PPCP – pharmaceutical and personal care product;

PSII – photosystem II;

PVPP – polyvinylpyrrolidone;

ROS – reactive oxygen species;

RT – room temperature;

RT-qPCR – reverse transcription coupled to real time PCR;

RuBisCO – ribulose-1,5-biphosphate carboxylase oxygenase;

SDS – sodium dodecyl sulphate;

SN – supernatant;

TEMED – N,N,N',N'-Tetramethylethylenediamine;

Tm – melting temperature;

WWTP – wastewater treatment plant;

1. Introduction

The exponential growth of the world population, as well as anthropogenic activities, such as accelerated industrialization, intensive agriculture and extensive mining, is resulting in several disturbances in the environmental compartments (air, water, soil and biota). The contamination of the environment became an important public health problem and raised concern over the last years (Cristaldi et al., 2017; Gorito et al., 2017). By definition, a contaminant is a substance that is present in non-expected locations and in concentrations that overcome a set limit (Chapman, 2007). Well-known contaminants include toxic HMs, some pesticides, asbestos and petroleum and polyaromatic hydrocarbons. However, over 80,000 synthetic substances are released into the environment per year, either as industrial waste or as part of production processes. Some of these substances are considered emerging contaminants (ECs), either due to their recent development or the discovery of their presence in the environment, and they include pharmaceuticals and personal care products (PPCP's) (Naidu et al., 2016; Bartrons and Peñuelas, 2017). Since plants are the basis of food chains and have the ability to uptake some contaminants into their tissues, the study of the impact of ECs on these organisms has become a matter of special interest, not only because of the effects of these substances on plant physiology, but also due to food quality and safety (Zhuang et al., 2009; Lajayer et al., 2017; Al-Farsi et al., 2018).

1.1 Heavy metal contamination

Various anthropogenic activities can cause a vast amount of perturbations in the biosphere. Consequently, these activities increase the accumulation of HMs, causing serious concerns of ecological, nutritional and environmental motives. HMs are a group of metals and metalloids that possess high atomic mass (over 20 g cm^{-3}) and density (more than 5 g cm^{-3}) (Emamverdian et al., 2015; Lajayer et al., 2017). HMs enter the environment mainly through two sources: natural and anthropogenic sources. Natural sources include volcanic activities, soil erosion and rock and mineral disaggregation, while anthropogenic ones comprise agricultural and industrial activities, fuel combustion, street run-off, mineral processing and landfills (Burakov et al., 2018). HMs have genotoxic, cytotoxic and mutagenic effects on humans, animals and plants. Despite these severe effects, some of these substances are essential elements for plants and animals due to their important biochemical and physiological roles in these living beings. Indeed, some HMs are an integral part of several enzymes and participate in redox reactions (Nagajyoti et al., 2010).

1.1.1 Chromium VI [Cr (VI)] and its phytotoxicity

Cr is a silver-coloured HM belonging to the group VI-B of the periodic table with atomic number 24, molecular weight 51.1 g mol^{-1} and density 7.19 g cm^{-3} and is the 21st most abundant metal of the Earth's crust (Shanker et al., 2005; Shahid et al., 2017). This metal is one of the 18 main hazardous air pollutants (HAPs), 33 urban air toxicants, and the Agency for Toxic Substances and Disease Registry classified Cr as 7th among the top 20 hazardous substances (Oh et al., 2007). Furthermore, Cr has the 5th place within the HMs in the Comprehensive Environmental Response, Compensation, and Liability Act (Ma et al., 2007) and it is also considered as the 1st carcinogen, according to the International Agency for Research on Cancer (Cancer, 1987) and the National Toxicology Program (Shahid et al., 2017).

Despite having several valence states (from -2 to +6), the most common and stable forms of Cr are the trivalent - Cr (III) - and the hexavalent - Cr (VI) - forms (Ashraf et al., 2017; Shahid et al., 2017). These two states differ in bioavailability, mobility and toxicity (Panda and Choudhury, 2005). Cr (VI) is the most toxic form due to its high reactivity with other elements (Shahid et al., 2017), and it generally associates with oxygen, resulting in chromate (CrO_4^{2-}) or dichromate ($\text{Cr}_2\text{O}_7^{2-}$) oxyanions. Cr (III) is less mobile and toxic, and forms complexes with organic matter in soil and aquatic environments. Cr (III) plays an important role on lipid and sugar metabolism of animals, including humans (Oliveira, 2012), however, it is not essential for plants (Shanker et al., 2005).

The release of high levels of Cr in soils and ground waters leads to environmental contamination. Consequently, crops growing in contaminated soils may accumulate this metal in their tissues, allowing Cr's entrance in food chains, ultimately affecting human health (Broadway et al., 2010; Ahmed et al., 2016). This problem raised the attention of the scientific community worldwide over the years (Shanker et al., 2005; Shahid et al., 2017). Cr occurs naturally in rocks, soil, water, plants, animals, and volcanic dust and gases (Shanker et al., 2005). The main sources of Cr are industrial activities such as leather tanning, metallurgical, Cr plating, wood processing and preservation, anodizing aluminium, catalytic manufacture, cleaning agents, organic synthesis, textile dyeing and textile pigment production, and alloy preparation industries (Sinha et al., 2018). According to Santos and Rodriguez (2012), the most important sources of this element in the environment are Cr fugitive emissions from industrial cooling towers and road dust. Mohan and Pittman Jr (2006) found that 30, 896 and 146 metric tons/year of Cr were discharged worldwide in air, soil and water, respectively. In 2012, Cr concentration varied

from 0.1 to 0.5 mg L⁻¹ in fresh water and from 0.0016 to 0.05 mg L⁻¹ in sea waters (Kumar and Puri, 2012).

Plants' contamination by Cr is dependent on the speciation of the metal, which defines its mobilization, uptake and phytotoxicity. Because Cr is not an essential element for plant metabolism, these organisms do not possess any specific mechanism for its uptake (Shanker et al., 2005; Oliveira, 2012). Even yet, plants can uptake Cr (III), through a passive mechanism that does not require energy consumption. Moreover, due to its structural similarity with phosphate and sulphate, the uptake of Cr (VI) can be achieved by an active process mediated by phosphate or sulphate carriers (de Oliveira et al., 2014; de Oliveira et al., 2016). Besides, Cr (VI) also affects the uptake of Ca, Fe, K, Mg, Mn and P (Gardea-Torresdey et al., 2004).

The majority of Cr is accumulated in roots, since this metal is poorly translocated to the aerial parts of the plant. In fact, the concentration of Cr in roots can be 100-fold higher than in shoots (Shanker et al., 2005; Oliveira, 2012). Cr is highly toxic to plants as it affects not only plant morphology but also several crucial processes. For example, root growth is strongly disturbed by Cr, due to the low translocation index of this metal to the aerial parts of plants. Consequently, this process disrupts some other processes such as water and nutrient absorption and their transportation to shoots, thus impairing shoot growth. On the other side, Cr (VI) directly influences foliar tissues by reducing leaf number and area, which is associated to the decrease in cell division and number of cells in leaves. In addition, at long-term exposure, this HM can cause chlorosis and tissue necrosis (Singh et al., 2013; Shahid et al., 2017).

Cr (VI)-induced stress culminates in several photosynthetic damages. It is well documented that Cr (VI) decreases chlorophyll a (chl a), chlorophyll b (chl b) and carotenoids contents (Singh et al., 2013). The decrease in chlorophyll content in response to Cr (VI) exposure is related to the degradation of key enzymes involved in chlorophyll biosynthesis, such as δ -aminolevulinic acid dehydratase (ALAD or porphobilinogen synthase, EC 4.2.1.24) and protochlorophyllide reductase (EC 1.3.1.33) (Ganesh et al., 2008). Moreover, Cr-induced reduction in absorption of Mg and N, which are fundamental components of the chlorophyll molecule, can also contribute to its negative effects on chlorophyll content (Sela et al., 1989). Since the production of photosynthetic pigments is affected, CO₂ assimilation is also committed. Cr (VI) also inhibits the electron transport chain, therefore affecting the photosynthetic rate (Vernay et al., 2007; Liu et al., 2008; Subrahmanyam, 2008). Some authors report that this metal also prejudices Calvin cycle enzymes such as ribulose-1,5-biphosphate carboxylase

oxygenase (RuBisCO), stomatal conductance, transpiration rate and substomatal CO₂ concentration (Rodriguez et al., 2011; Santos and Rodriguez, 2012).

Cr (VI) can affect mineral nutrition of plants in a complex manner, due to its similar structure to other essential elements (Shanker et al., 2005; Oliveira, 2012; Shahid et al., 2017). The Cr (VI)'s competitive binding to common carriers, as above described, can reduce the uptake of many essential nutrients. Moreover, Cr-induced stress causes the inhibition of the activity of plasma membrane H⁺-ATPase (Shanker et al., 2005). High levels of Cr (VI) might displace some essential nutrients from their physiological binding sites which, consequently, decreases their uptake and translocation (Oliveira, 2012; Shahid et al., 2017). In fact, it is well documented that Cr (VI) can interfere with the uptake of some macronutrients such as N, P, K, and Mg. Given that N is an essential macronutrient for plants and being its uptake compromised by Cr (VI)-induced stress, N metabolism can also be negatively influenced by the presence of this HM. Indeed, some authors reported that Cr (VI) affects key enzymes involved in N metabolism such as nitrate reductase (NR, EC 1.6.6.1), nitrite reductase (NiR, EC 1.7.7.1) glutamine synthetase (GS, EC 6.3.1.2), glutamate synthase (GOGAT, EC 1.4.1.14; EC 1.2.7.1) and glutamate dehydrogenase (GDH, EC 1.4.1.2) (Dubey and Rai, 1987; Kumar and Joshi, 2008; Gangwar and Singh, 2011; Singh et al., 2013). As well as N, C and starch metabolism are also negatively affected by Cr (VI) (Singh et al., 2013). All the effects provoked by Cr (VI), indirectly affect plant yield and crop productivity (Figure 1) (Shanker et al., 2005; Oliveira, 2012).

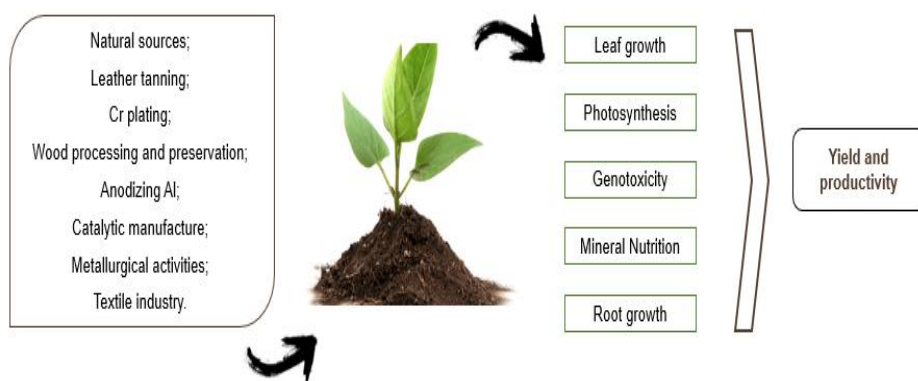


Figure 1. Sources of Cr (VI) in the environment and some effect of Cr (VI) in plants.

1.2 Pharmaceuticals contamination

Over the last years, increasing urbanisation, growing *per-capita* income, ageing population and other factors have contributed to a major increase in the production and the consumption of pharmaceuticals worldwide, a problem that tends to continue in the

future. Pharmaceuticals, used in both human and animal medicine, agriculture and aquaculture facilities, are a wide range of chemical compounds frequently used in illnesses' prevention, diagnosis, treatment or cure. The intensive usage of these substances enabled their presence in the environment, particularly in the aquatic compartment (Fatta-Kassinos et al., 2011; Bartrons and Peñuelas, 2017). Indeed, the presence of pharmaceuticals in aquatic environment was detected many decades ago by several authors (Tabak and Bunch, 1970; Norpoth et al., 1973). Different pathways allow the entrance of pharmaceuticals into the aquatic environment (Figure 2), but all of them result from human activities.

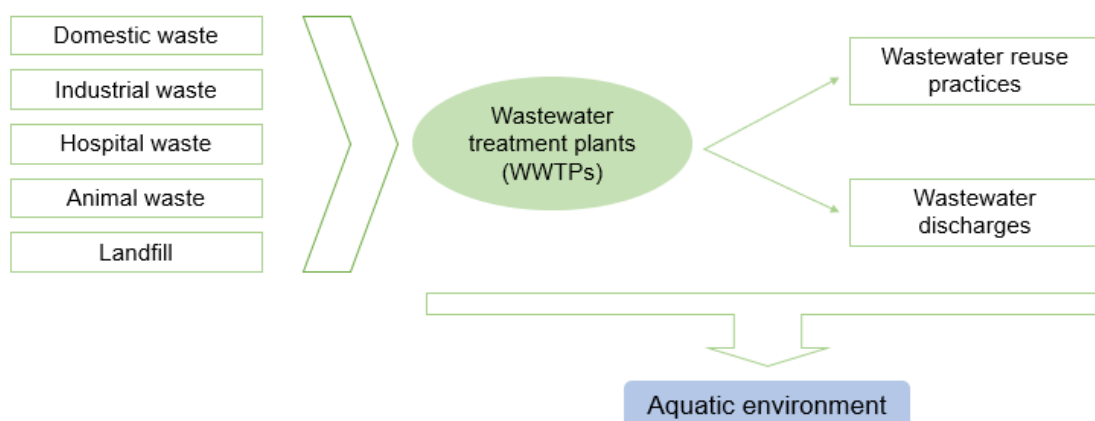


Figure 2. Different sources of pharmaceuticals and the pathways used to reach the aquatic environment (based on Lapworth et al. (2012)).

Human bodies cannot completely metabolise some pharmaceuticals, being these compounds excreted as the parent drug or as its derived metabolites via urine and faeces, therefore reaching conventional wastewater treatments plants (WWTPs) (Ribeiro et al., 2016). Conventional WWTPs were not planned to completely remove organic substances, like pharmaceuticals, from wastewater effluents. Consequently, some of these substances can pass through the wastewater treatment process without being treated (Christou et al., 2017; Gorito et al., 2017) and reach several aquatic systems such as wastewater, ground water, surface water and drinking water (Odendaal et al., 2015; Balakrishna et al., 2017; Yang et al., 2017).

The re-use of wastewater effluents for crop irrigation, of manure for the fertilization of agricultural soils, as well as the application of biosolids, are considered serious threats to human health. In fact, these compounds are absorbed by plants, which are the basis of food chains, thus affecting humans by food ingestion (Bartrons and Peñuelas, 2017; Madikizela et al., 2018). Upon exposure to pharmaceuticals, plant growth and development can be directly or indirectly affected by disturbing plant's microbiota

(Madikizela et al., 2018). As shown in Table 1, several studies reported phytotoxicity caused by pharmaceuticals in important crop plants (Table 1).

Table 1. Concentrations of different pharmaceuticals in crops from agricultural fields and subsequent phytotoxicities of each compound (adapted from Bartrons and Peñuelas (2017)).

Pharmaceuticals	Concentration	Plant Species	Effect on plants	Reference
Ibuprofen	83 mg kg ⁻¹ dry weight, spiked soil	Great millet (<i>Sorghum bicolor</i>)	Decreased quantum efficiency of photosystem II and photochemical quenching coefficient	(González-Naranjo et al., 2015)
Metformin	10 mg kg ⁻¹ dry weight, spiked soil	Carrot (<i>Daucus carota</i>)	Reduction of growth and development	(Eggen et al., 2011)
Amoxicilin, Chlortetracycline and Tetracycline	0.001-10 mg L ⁻¹	Alfafa (<i>Medicago sativa</i>), carrot (<i>Daucus carota</i>), lettuce (<i>Lactuca sativa</i>)	Reduction of growth and germination	(Hillis et al., 2011; Huber et al., 2016)
Sulfadiazine	10 and 200 mg kg ⁻¹ dry weight, spiked soil	Maize (<i>Zea mays</i>)	Death	(Michelini et al., 2012)
Tetracycline	0-500 mg L ⁻¹	Cucumber (<i>Cucumis sativus</i>), rice (<i>Oryza sativa</i>), sweet oat (<i>Cichorium endivia</i>)	Reduction of growth and germination	(Liu et al., 2009)
Acetaminophen	400 mg kg ⁻¹ dry weight, spiked soil	Barley (<i>Hordeum vulgare</i> L.)	Reduction of growth and development	(Soares et al., 2018)

As it is clear from the data in Table 1, plant growth and development can be differently affected by pharmaceuticals, depending on the compound and its concentration, and the plant species (Madikizela et al., 2018).

1.2.1 Diclofenac (DCF) and its phytotoxicity

Diclofenac (2-(2-(2,6-dichlorophenylamino)phenyl)acetic acid) (DCF) is a non-steroidal anti-inflammatory drug (NSAID) (Figure 3), which is used as a pain killer or as an anti-inflammatory, and it is marketed under various trade names, being Voltaren the most known (Vieno and Sillanpää, 2014). Furthermore, it is consumed in large quantities worldwide (Zhang et al., 2008).

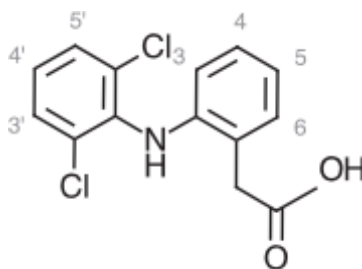


Figure 3. Diclofenac chemical structure (from: Vieno and Sillanpää (2014)).

This drug is administered as oral tablets or topical gel and, once in the human body, DCF is not completely metabolised, as 1 to 10% is excreted in its native ingested form (Davies and Anderson, 1997). Some properties of this substance are summarised in Table 2.

Table 2. Summary of properties of Diclofenac (Feito et al., 2012).

Diclofenac	
Cas NO.	15307-79-6
Molecular formula	C ₁₄ H ₁₀ Cl ₂ NNaO ₂
Molecular weight	318.13
Water solubility	50 mg L ⁻¹
Main metabolites	4'-hydroxydiclofenac
	3'-hydroxydiclofenac
	4',5-hydroxydiclofenac
Excretion without metabolization	1-10%
Excretion	65-70% in urine, 20-30% in faeces
Biodisponibility	54%
Daily consumption per patient	200-300 mg
Annual world consumption	940 tons

Like other PPCP's, upon being excreted via urine or faeces, DCF enters the environment through WWTP's, being one of the most detected pharmaceuticals (aus der Beek et al., 2016; He et al., 2017), as well as one of the lowest removed (Vieno and Sillanpää, 2014). In WWTP's, DCF reaches concentrations of nearly µg L⁻¹, whereas in surface water bodies it is detected in ng L⁻¹ levels (Lonappan et al., 2016). Within the aquatic

environment, DCF has been noticed in rivers, estuaries, lakes (Buser et al., 1998; Öllers et al., 2001; Metcalfe et al., 2003; Kim et al., 2007), in groundwater and even in drinking water (Rabiet et al., 2006; Benotti et al., 2008).

The ecological concern of DCF started in the beginning of the current century when, due to its usage for cattle treatments, this drug was associated with the massive decline of a vulture population in India (Oaks et al., 2004).

So far, numerous studies on the ecotoxicological effects of DCF have been conducted, mostly from animal and aquatic invertebrates and different biomarkers and endpoints have been used in these organisms to clarify and monitor the ecotoxicological effects of this drug (Huber et al., 2016). Comparing to animals, not much is known regarding the effects of DCF on plants.

In 2012, Huber et al., firstly reported the metabolism of DCF on plants, using *Hordeum vulgare* L. and *Armoracia rusticana* L. cultures. Later, the same authors revealed the role of peroxidases on the metabolism of DCF in cultures of *Armoracia rusticana* L. (Huber et al., 2016) and Fu et al. (2017) studied the uptake and metabolism of DCF on *Arabidopsis thaliana*. Concerning the effects of DCF on plant physiology and development, there is an even more accentuated gap in knowledge. Kummerová et al. (2016) reported the negative effects of this drug on biomass production, pigments content and oxidative stress in *Lemna minor* and, a recent work of Pierattini et al. (2018), besides studying the plant uptake of DCF, also evaluated some physiological responses such as growth parameters and stress enzymes activity. Yet, further investigation is required for adequately unveil the consequences of DCF in plant metabolism and development, especially regarding N and C assimilation processes, once they are part of the plants' primary metabolism.

1.3 Nitrogen (N) metabolism

It is well-known that N is a vital macronutrient and an essential component of biomolecules like proteins, chlorophylls, nucleic acids, pyrimidines, purines, porphyrins, and co-enzymes. For this reason, N is indispensable for plant growth, development and productivity (Singh et al., 2013). N is obtained from the environment by three biological processes: nitrate (NO_3^-) reduction, ammonia uptake or N fixation (Hoffman et al., 2014). Most of plants acquire NO_3^- as the preferred source of N available forms to plants (Pathak et al., 2008). Then, NO_3^- is reduced to ammonium (NH_4^+) by NR and NiR, which is assimilated into the amino acids glutamine and glutamate by GS and GOGAT, respectively, through the GS/GOGAT cycle (Cren and Hirel, 1999). GDH also catalyses

the formation of glutamate, from NH_4^+ and 2-oxoglutarate (2-OG), when the concentration of NH_4^+ is high (Fontaine et al., 2012).

Knowing the importance of N to plant productivity and with the continuous increase of human population, the application of N fertilisers in crops became an important issue nowadays. The high costs of N fertiliser applications, along with the observed negative impact of this practise on natural ecosystems, is concerning the scientific community, which has been committed in improving the N use efficiency (NUE) (Miyashita and Good, 2008; Nguyen and Kant, 2018; Tiwari et al., 2018). This index, according to some authors, is defined as the biomass/grain yield per unit N accessible for uptake (Brauer and Shelp, 2010). So far, many strategies to improve NUE have been proposed, some of them being related to N metabolism (Tiwari et al., 2018).

1.3.1 Glutamine synthetase and its role in NUE improvement

Glutamine synthetase, also known as glutamate-ammonia ligase, is an enzyme that is involved in the first step of ammonium assimilation into glutamine (Thomsen et al., 2014). This enzyme catalyses the ATP-dependent fixation of NH_4^+ to the D-carboxyl group of glutamate to produce one molecule of glutamine, which, together with one molecule of 2-OG, originates two molecules of glutamate by the action of GOGAT. At the end of the GS-GOGAT cycle (Figure 4), through the catalytic action of GOGAT, two molecules of glutamate, at the expense of reducing power, as well as one molecule of glutamine are formed. One of them provides nitrogen groups for the biosynthesis of all nitrogenous compounds in the plant, while the other is recycled back to the GS-GOGAT cycle. Moreover, GS is responsible for the reassimilation of the NH_4^+ released during photorespiration in C_3 plants (Lea and Mifflin, 2003; Thomsen et al., 2014).

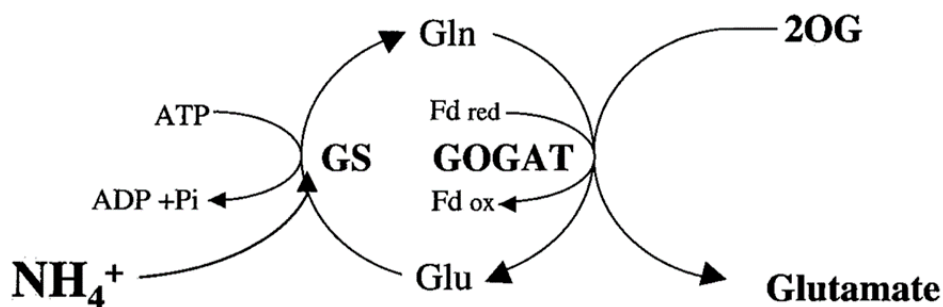


Figure 4. Biochemical reactions catalysed by GS and GOGAT (Adapted from Hodges (2002)).

GS-encoding genes, due to their old existence and function, act as a good molecular clock for phylogenetic analysis (Pesole et al., 1991; Kumada et al., 1993). In prokaryotes and eukaryotes, based on their gene sequence, molecular weight and quaternary structure, the GS superfamily is divided into three distinct types - GSI, GSII and GSIII

(Swarbreck et al., 2010; James et al., 2018). The GSI, GSII and GSIII proteins possess, on average, 360, 450 and 730 amino acids, respectively (van Rooyen et al., 2011). According to a research based on sequence similarity, the GSIII family does not exist in plants. Indeed, this GS isoenzyme is only described in various prokaryotes, whereas GSI and GSII are present in both eukaryotes and prokaryotes. Up to now, GSI function and role in plants is not well-established. However, recent studies proposed an association of this GS type with N and biotic stress signalling (Doskočilová et al., 2011; Silva et al., 2015).

The most predominant GS type in higher plants is the GSII (Bernard and Habash, 2009; Swarbreck et al., 2010). Within GSII, two types are identified in higher plants: a cytosolic (GS1) form and a plastidic (GS2) one (Cren and Hirel, 1999; Habash et al., 2001; Miflin and Habash, 2002). This GS type presents a decameric structure with two pentameric rings (Unno et al., 2006; Seabra et al., 2009; Torreira et al., 2014). Regarding the GSII gene family in plants, the majority of studies conducted to date revealed that most plant species possess only one nuclear gene encoding GS2, while GS1 seems to be encoded by two to five genes (Lam et al., 1996; Swarbreck et al., 2010). The GS2 polypeptide has an *N*-terminal transit peptide with almost 50 amino acids, which targets it to the chloroplast, and a 16-amino acid conserved region at the *C*-terminal part of the subunit, that is exclusive to this isoenzyme. GS1 is localised to the cytosol and possesses none of the above-mentioned conserved regions (Lightfoot et al., 1988; Cren and Hirel, 1999). Different localization of the GS genes' expressions to specific cell and tissue types suggests distinct specific physiological functions (Swarbreck et al., 2010). GS1 (polypeptide molecular weight ~ 38-40 kDa) is a key factor in primary NH_4^+ assimilation in roots and re-assimilation of NH_4^+ released during leaf senescence and from protein breakdown during seed germination, while GS2 (polypeptide molecular weight ~ 42-45 kDa) is involved in the primary assimilation of NH_4^+ resulting from NO_3^- reduction in chloroplasts and in the re-assimilation of NH_4^+ released during photorespiration. Previous studies suggested that GS2 also has a protective role against biotic and abiotic stresses (Lam et al., 1996; Miflin and Habash, 2002; Masclaux-Daubresse et al., 2010).

Taking into account the role of GS in N metabolism and the importance of this macronutrient in plant growth and development, it can be assumed that GS might be the rate-limiting enzyme during N incorporation into organic forms (Lam et al., 1996). In this way, GS can be considered as a good candidate to NUE improvement through genetic manipulations (James et al., 2018). Furthermore, due to the role of GS in the tolerance to abiotic and biotic stresses, the overexpression of GS-encoding genes appears to be

a good molecular approach to obtain genetically modified plants with an optimized NUE. Actually, up to date, numerous studies have already been carried out and the results are quite promising. For instance, in transgenic *Lotus corniculatus* plants overexpressing a soybean *GS1* gene under the control of a cauliflower mosaic virus (CaMV) 35S promoter, it was observed an accelerated growth rate (Vincent et al., 1997). In addition, poplar trees (Gallardo et al., 1999; Fuentes et al., 2001; Pascual et al., 2008) and tobacco plants (Fuentes et al., 2001) with an overexpressed *GS1* gene improved their vegetative growth and photosynthetic capacity. Also, it was observed an earlier flowering and seed development in transgenic wheat plants transformed with a *Phaseolus vulgaris* *GS1* gene driven by the RuBisCO small subunit promoter (*rbcS*) (Habash et al., 2001). There are less studies regarding the overexpression of *GS2*, when compared to *GS1*. In 2000, (Migge et al.) reported a higher growth rate in transgenic tobacco seedlings overexpressing a *GS2* cDNA. In rice leaves (Takabe et al., 2001) and protoplasts (Hoshida et al., 2000), the overexpression of a *GS2* cDNA increased their photorespiration capacity and conferred salt and chilling tolerance. Moreover, Wang et al. (2013) reported an increase in leaf surface area, total protein and amino acid content, chlorophyll content, glucose and sucrose contents, and plant length in transgenic tobacco plants overexpressing the Arabidopsis *Dof1* (a transcription factor that regulates *GS* gene expression) and *GS1* and *GS2* genes.

1.3.2 Glutamate Dehydrogenase

GDH is an enzyme that catalyses the deamination of glutamate to produce 2-OG and NH_4^+ , with the production of reducing power, as well as the production of glutamate from NH_4^+ and 2-OG, using NADH or NADPH as a coenzyme (amination reaction). According to Ferraro et al. (2012), there are three to four genes in the GDH gene family, encoding two subunits (α and β), which can be randomly combined to form many NADH-GDH hexameric isoenzymes (Melo-Oliveira et al., 1996; Turano et al., 1997; Dubois et al., 2003; Purnell et al., 2005; Miyashita and Good, 2008). GDH is present in several plant organs, being located at several cell compartments, such as the cytosol, mitochondria and chloroplasts (Dubois et al., 2003).

The physiological role of GDH is not clearly understood yet, despite the efforts of the scientists to reveal it (Dubois et al., 2003; Purnell and Botella, 2007; Skopelitis et al., 2007; Lehmann and Ratajczak, 2008; Miyashita and Good, 2008; Masclaux-Daubresse et al., 2010). So far, it is known that under stressful conditions, the *GS/GOGAT* cycle is not completely enough neither to reduce the toxic levels of NH_4^+ , nor to provide the necessary glutamate for the biosynthesis of some protective biomolecules. In this case, the dual role of GDH is crucial because the amination reaction leads to a reduction of

toxic amounts of NH_4^+ that are accumulated during stress, plus providing glutamate for the synthesis of other nitrogenous compounds (Forde and Lea, 2007), while the deamination activity is required to supply carbon skeletons for the tricarboxylic cycle (Chiraz et al., 2003; Jha and Dubey, 2004).

1.4 GS and GDH - a role in proline production under stress

When subjected to various abiotic stresses, plants usually enhance the production of the amino acid proline, which has been proved to have multiple roles in response to abiotic stresses (Hare and Cress, 1997; Hellmann et al., 2000; Verbruggen and Hermans, 2008; Szabados and Savoure, 2010). Plants under stressful conditions can accumulate proline through two ways: either by a stimulation of its biosynthesis, or by inhibiting its oxidation/degradation. The major precursor for proline biosynthesis in stress-induced plants is glutamate, which results from the GS/GOGAT cycle (Díaz et al., 2010). Indeed, it was showed that the phloem-located GS is essential for controlling proline production and that a higher GS activity had a positive influence in proline synthesis in plants under water stress (Brugière et al., 1999). Also, in the previous year, Larher et al. reported that the conversion of amino acids into proline was compromised by the application of a GS inhibitor in rapeseed leaf discs (Larher et al., 1998). Moreover, a decrease in proline content was observed in *gs2* mutants of *Lotus japonicus* under drought stress (Díaz et al., 2010). However, some studies showed that GS-GOGAT cycle was not the only source of glutamate for proline biosynthesis under stress-induced conditions (Lutts et al., 1999; Wang et al., 2007). These authors suggested that NAD-GDH is an alternative pathway to provide glutamate, since this enzyme is responsible for the conversion of 2-OG into glutamate by the amination reaction.

1.5 *Solanum lycopersicum* L. cv Micro-Tom as a perfect model species for molecular biology studies

Tomato (*Solanum lycopersicum* L.), native from South America, belongs to the Solanaceae family which includes many economically important species like potato (*Solanum tuberosum* L.), tobacco (*Nicotiana tabacum* L.) and eggplant (*Solanum melongena* L.). According to FAO, in 2014 tomato production reached ~160 millions of tons year⁻¹ and it is predicted that production of this crop continues to increase (Gerszberg and Hnatuszko-Konka, 2017). Nowadays, tomato not only has an agricultural and economic importance worldwide but is also considered a model system for genetic studies in plants (Bergounoux, 2014).

Solanum lycopersicum cv. Micro-Tom (Figure 5) is a dwarf miniature tomato cultivar which was originally created for gardening purposes. The phenotype of this cultivar derived from three mutations: *self-pruning* (producing a determinate phenotype), *dwarf* (reducing internode length and producing smaller, rugose, and dark-green leaves) and *miniature* (likely to be associated with gibberellin signalling) (Meissner et al., 1997; Martí et al., 2006).



Figure 5. *Solanum lycopersicum* L. cv Micro-Tom.

Due to its special characteristics such as small size, rapid life cycle (fruits mature in 70-90 days), a large number of plants per square meter (can reach 1357 plants m⁻²), easy to grow under laboratory conditions, a well-studied small diploid genome and high transformation frequencies, Micro-Tom became a good model system for agronomic and genetic studies. In fact, this cultivar is also named as “the laboratory tomato” (Meissner et al., 1997; Shibata, 2005). Up to now, there are many reports on Solanaceae and tomato genetics (Meissner et al., 1997; Shibata, 2005; Aoki et al., 2010), hormonal functions and interactions (Campos et al., 2010), microbial plant interaction (Park et al., 2007), carbohydrate and amino acids metabolisms (Obiadalla-Ali et al., 2004; Scarpeci et al., 2007; Sorrequieta et al., 2010; Ferraro et al., 2012) and in molecular breeding of tomato fruit shelf-life (Okabe et al., 2012).

Thus, altogether, these characteristics, allied to the great economic importance, makes *S. lycopersicum* an excellent tool for biochemical, physiological and molecular studies.

1.6 Main Objectives

As previously stated, worldwide contamination by HMs and pharmaceuticals are fast-growing issues, posing important and determinant consequences to the dynamics of the agroecosystems, including the development of important crops, like tomato. Moreover, knowing that N is the major mineral nutrient influencing plant growth, this dissertation firstly aimed to uncover the effects of HM- and xenobiotic-exposure on the N metabolism and photosynthesis in *S. lycopersicum* plants. Given the recognized importance of GS, particular focus was given to the regulation and performance of this enzyme, at transcript, protein and activity levels.

In this way, to meet these goals, this work had several specific objectives:

- i) To assess the impact of Cr (VI) and DCF in N metabolism, particularly on GS gene expression and protein accumulation and activity, as well as to investigate the role of GDH in N metabolism in tomato plants under these types of stresses, and check how these enzymes cooperate in proline biosynthesis;
- ii) To evaluate the effects of these contaminants on photosynthesis and photosynthetic-related parameters;
- iii) To overexpress the *S/GS2* cDNA as a tool to increase plant abiotic stress tolerance and NUE.

By combining diverse and complementary approaches, through the application of several physiological, biochemical and molecular tools, this work will help to unravel the direct consequences of DCF and Cr (VI) in the growth and development of *S. lycopersicum*, shedding some light on the phytotoxicity of DCF and strengthening the scientific basis of Cr contamination risks for crops. Furthermore, this dissertation will be the first study reporting the overexpression of GS2 in tomato plants in an attempt to increase its tolerance to environmental contamination with EC and metals.

2. Material and Methods

2.1 Plant material and growth conditions

All experiments of this work were performed using certified *Solanum lycopersicum* L. cv. Micro-Tom (Tomato Genetics Resource Center (TGCR); germplasm LA3911) seeds. Prior to their use, the seeds were surface-sterilized with 70% ethanol for 10 min, followed by 20% commercial bleach containing 0.02% tween-20 for 5 min under constant agitation and then several washes with sterilized deionized water were done. After that, the seeds were distributed in Petri dishes (10 cm diameter) with Hoagland Solution (HS) solidified with 0.8% (w/v) agar (Taiz et al., 2015). To allow seed stratification, in order to synchronize the seed germination, the Petri dishes were placed at 4 °C for two days, and then, transferred to a growth chamber (16 h light/ 8 h dark) at 25 °C, with photosynthetically active radiation (PAR) of 60 $\mu\text{mol m}^{-2} \text{s}^{-1}$ for 10 days. After this period, seedlings were transplanted to individual pots and cultivated with a mixture of expanded vermiculite:perlite (2:1). At this point, the seedlings were split in five growth conditions and grown in a growth chamber under the same conditions described above for 21 days. The five growth conditions consisted in: Control (CTL) – watered with HS; Cr 5 - watered with HS and 5 μM Cr (VI); Cr 10 - watered with HS and 10 μM Cr (VI); DCF 0.5 – watered with HS and 0.5 g L^{-1} Diclofenac; DCF 5 – watered with HS and 5 g L^{-1} Diclofenac. For each treatment, 12 biological replicates were prepared. After 21 days, plants were picked, and the shoots were separated from roots. Roots were washed carefully with tap water, followed by a wash with deionized water. Part of the plant material was directly handled for biochemical assays, another part was dried for posterior Cr and DCF quantifications in plant tissues, and the remaining material was frozen and grounded in liquid nitrogen (N_2) and stored at -80 °C for posterior biochemical and molecular assays.

2.2 Analytical determinations

2.2.1 Determination of Cr content in plant tissues

The levels of Cr on tomato plants tissues were quantified to verify the preferential organ for Cr accumulation. Both shoots and roots were collected (as above described) and dried at 60 °C, until constant weight was registered. Then, the samples were ground to a fine powder and kept in a desiccator for further use. The samples were subjected to an acid digestion using a mixture of $\text{HCl}:\text{HNO}_3$ to release the metals bound to proteins or other biological structures. The resultant digests were dissolved in a precise volume of water and the quantification of Cr content was performed using a Flame atomic

absorption spectrometer, based on a suitable external standard solution (Perkin Elmer, AAnalyst 200 model, Shelton CT) according to manufacturer's instructions.

2.3 Biochemical determinations

2.3.1 Glutamine synthetase activity determination (GS; EC 6.3.1.2)

The activity of GS was determined using samples from frozen leaf and root tissues. With a mortar on ice, aliquots of about 300 mg were homogenized in extraction buffer (750 μL for shoots and 500 μL for roots) composed of 25 mM Tris-HCl (pH 6.4), 10 mM Magnesium Chloride (MgCl_2), 1 mM Dithiothreitol (DTT), 10% Glycerol, 0.05% Triton X-100 with quartz sand and 1% (w/v) Polyvinylpyrrolidone (PVPP). Posteriorly, homogenates were centrifuged at 15,000 g at 4 $^\circ\text{C}$ for 20 min and the supernatant (SN) was collected. The enzymatic reaction started when 50 μL of SN were mixed with 50 μL of 6.4% (w/v) Sodium arsenate (pH 6.4) and 400 μL of reaction mixture composed of 100 mM Trizma-Base, 125 mM L-glutamine, 157 mM Hydroxylamine, 0.26 mM Manganese chloride tetrahydrate and 1.25 μM Adenosine 5'-diphosphate sodium salt (ADP), pH 6.4. For each SN, three replicates were prepared. Simultaneously, a blank was set by replacing the protein extract by extraction buffer. All the reactions were incubated at 30 $^\circ\text{C}$ for 30 min and the reaction was stopped by adding 500 μL of Stop solution (0.16 M Iron Chloride (FeCl_3), 0.25 M Trichloroacetic acid in 3.33% chloridric acid (HCl)). The absorbances were measured at 500 nm and the transferase activity of GS was determinate according to the formula ($\mu\text{mol min}^{-1} \text{mL}^{-1}$):

$$\text{GS activity} = \frac{\text{Abs (500 nm)}}{0.4 \times \text{protein extract} \times \text{reaction time}}$$

The protein content of the extracts was determined by the Bradford method (Bradford, 1976) and GS activity was expressed as nkat mg^{-1} protein (1 kat = 60 mole min^{-1}) (Cullimore and Sims, 1980). The extracts were mixed with glycerol to a final concentration of 40% and stored at -80 $^\circ\text{C}$ until further use.

2.3.2 GDH activity determination (GDH, EC 1.4.1.2)

GDH activity was visualized in a non-denaturing 10% (w/v) resolving polyacrylamide gel (3.33 mL 30% Acrylamide stock, 1.25 mL 1.5 M Tris-HCl (pH 8.8), 1.15 mL 87% Glycerol, 75 μL 10% (w/v) Ammonium Persulfate (APS), 5 μL N,N,N'-Tetramethylethylenediamine (TEMED) and distilled water to a final volume of 10 mL) and 4% stacking gel (660 μL 30% Acrylamide stock, 1.25 mL 0.5 M Tris-HCl (pH 6.8), 570

µL 87% Glycerol, 12,5 µL 10% (w/v) APS, 25 µL TEMED and distilled water to a final volume of 5 mL). The protein extracts used were those obtained from the GS activity assays and 40 µg protein were loaded with 1x sample buffer (10x sample buffer consisting of 50% (w/v) Sucrose, 0.1% (w/v) Bromophenol blue). The buffer system consisted in 25 mM Tris-HCl (pH 8.3) and 192 mM Glycine. Running was performed at non-limiting voltage, 15 mA per stacking gel, 20 mA per resolving gel and non-limiting time, under refrigeration. GDH activity bands were detected after an incubation overnight (ON) with gentle rocking in a staining solution (100 mM Tris-HCl pH 9.3, 55 mM L-glutamate, 450 µM NAD⁺, 480 µM 3-(4,5-dimethylthiazol-2-yl)-2,5-diphenyltetrazolium bromide (MTT), 130 µM Phenazine methosulphate and 500 µM CaCl₂) (Loulakakis and Roubelakis-Angelakis, 1991). All images were captured with ChemiDoc™ XRS+ System (Bio-Rad®) and treated with Image Lab™ 5.2 (Bio-Rad®).

2.3.3 Sodium dodecyl sulphate polyacrylamide gel electrophoresis (SDS-PAGE)

SDS-PAGE (Laemmli, 1970) was carried out on 12.5% SDS-Polyacrilamide resolving gels (8.3 mL 30% Acrylamide stock, 5 mL 1.5 M Tris-HCl pH 8.8, 0.2 mL 10% SDS, 100 µL 10% (w/v) APS, 6.7 µL TEMED and distilled water to a final volume of 10 mL) and 5% SDS-Polyacrilamide stacking gels (670 µL 30% Acrylamide stock, 500 µL 1.0 M Tris-HCl pH 6.8, 40 µL 10% SDS, 40 µL 10% (w/v) APS, 4 µL TEMED and distilled water to a final volume of 4 mL). The extracts obtained from the GS activity assay were treated at 96 °C for 5 min with 1x SDS sample buffer (10x sample buffer composed of 0.375 g Tris-HCl pH 6.8, 5 mL 99% Glycerol; 0.5 g SDS, 20 mg Bromophenol blue and water up to 10 mL) and 0.5% (v/v) β-mercaptoethanol and 30 µg protein per lane were loaded. The running buffer consisted in 25 mM Tris, 192 mM Glycine and 1% (w/v) SDS and the electrophoresis occurred at non-limiting voltage, 15 mA per stacking gel, 20mA per resolving gel and non-limiting time. The gels were incubated ON in BlueSafe (Nzytech) with gentle rocking. Finally, the gels were rinsed with distilled water. The molecular weight of protein bands was estimated by comparison with a protein marker BLUE Wide Range CSL-BBL Prestained Protein Ladder (Cleaver Scientific Ltd). All images were captured with ChemiDoc™ XRS+ System (Bio-Rad®) and treated with Image Lab™ 5.2 (Bio-Rad®).

2.3.4 Western Blotting analysis

After separation by SDS-PAGE as described above, proteins were electroblotted onto a PVDF membrane (Protran, Whatman® Schleicher and Schuell), according to the

supplier's instructions. Transfers were performed in transfer buffer (192 mM Glycine, 25 mM Tris and 20% methanol) during 1 h at 200 mA. The membranes were saturated for 45 min in blocking solution [5% non-fat dry milk (w/v), in 0.05 M Tris, 0.2 M NaCl (TBS)] and then incubated ON at 4 °C with Anti-GS antibody raised to *Pinus* (Canton et al., 1996) or Anti-GDH antibody raised to *Vitis vinifera* L. (Loulakakis and Roubelakis-Angelakis, 1990) diluted to 1:500 and 1:1000, respectively, in blocking solution. After washing, blots were probed during 1 h at room temperature (RT) with anti-rabbit IgG-Alkaline Phosphatase diluted to 1:30000 (Sigma). Membranes were washed with distilled water for 1-2 min and with TBS during 5 min, and the washing was repeated twice. The reaction was revealed using Novex® Chromogenic Substrates (Invitrogen). The molecular weight of protein bands was estimated by comparison with a protein marker BLUE Wide Range BBL Prestained Protein Ladder (Cleaver Scientific Ltd). All images were captured with ChemiDoc™ XRS+ System (Bio-Rad®) and treated with Image Lab™ 5.2 (Bio-Rad®).

2.3.5 Evaluation of photosynthesis-related parameters

2.3.5.1 Photosynthetic pigments evaluation

The extraction and quantification of photosynthetic pigments was carried out according to Lichtenthaler (1987). All the procedure was performed under the lowest light conditions possible to avoid pigment photooxidation. For each tested situation, frozen aliquots of leaves (150-200 mg) were homogenized in 80% acetone with quartz sand. The homogenates were centrifuged at 3,500 g for 10 min. The last step was repeated, after the addition of 80% acetone and mixing vigorously, until the sediment lost the green colour. Later, all SNs were collected to 15 mL conic tubes and the volume was settled to a known final volume with 80% acetone. The absorbance at 470, 647 and 663 nm was recorded, using 80% acetone as blank. The chlorophyll a (Chl a), chlorophyll b (Chl b) and carotenoids (Car) concentrations were calculated using to the following formulas (Lichtenthaler, 1987):

$$Chl\ a\ (mg\ L^{-1}) = 12.25 \times Abs\ (663\ nm) - 2.79 \times Abs\ (647\ nm)$$

$$Chl\ b\ (mg\ L^{-1}) = 21.50 \times Abs\ (647\ nm) - 5.10 \times Abs\ (663\ nm)$$

$$Car\ (mg\ L^{-1}) = (1000 \times Abs\ (470\ nm) - 1.82 \times Chl\ a - 85.02 \times Chl\ b) / 198$$

The chlorophyll and carotenoids concentrations were expressed in mg g⁻¹ of fresh weight (F.W.).

2.3.5.2 Gas exchange analysis

The evaluation of gas exchange-related parameters was carried out with an open gas exchange system (Li-6400xt; LI-COR, Inc., Lincoln, Nebraska) coupled with an integrated chamber head (LI-6400-40 leaf chamber fluorometer; LI-COR, Inc.). All the measurements occurred from 10 to 11 a.m., under the following conditions: atmospheric CO₂ concentration of 400 μmol mol⁻¹ and saturating photosynthetic photon flux density of 500 μmol m⁻² s⁻¹ and the temperature was at 22 °C. Furthermore, all measurements were made in the terminal leaflet of the fourth or fifth leaf (counting from the apex) of each plant. The parameters net photosynthetic rate (A, μmol m⁻² s⁻¹), stomatal conductance of CO₂ (Gs, mmol m⁻² s⁻¹), leaf transpiration rate (E, mmol m⁻² s⁻¹) and CO₂ intercellular ratio (Ci/Ca) were then calculated (Von Caemmerer and Farquhar, 1981). Water use efficiency (WUE) was calculated as the ratio between A and E [mmol (CO₂ assimilated) mol⁻¹ (H₂O transpired)] (Nieva et al., 1999).

2.3.5.3 Histochemical coloration of starch

To detect possible alterations on starch storage of tomato leaves in response to Cr and DCF, a histochemical coloration of the starch grains was performed. To do that, leaf discs of about 1 cm diameter were collected and boiled in 80% ethanol, to allow leaf bleaching. Then, the samples were hydrated in distilled water followed by a 30 min incubation in Lugol solution (2 mM I₂, 6mM KI), in dark conditions. Finally, the samples were briefly destained in distilled water and the results were visualized and captured with a personal photographic camera.

2.3.6 Proline quantification

This assay was performed according to Bates et al. (1973). Samples of plant material of about 200 mg were homogenized with quartz sand in 1.5 mL and 1 mL of 3% (w/v) sulfosalicylic acid for shoots and roots, respectively. The homogenates were centrifuged at 500 g for 10 min at RT and SNs collected. Then, 200 μL of each samples' SN were added to 200 μL glacial acetic acid and 200 μL ninhydrin solution. The reactions were incubated at 96 °C for 1 h and subsequently cooled on ice to stop the reaction. To extract free proline, 1 mL of toluene was added to the mixture followed by vigorous vortexing (for 15-20 s) which created a fine emulsion. When a complete separation of the organic and water phases was achieved, the organic (upper) phase was carefully removed to new tubes and, using toluene as blank, the absorbances read at 520 nm. The free proline content was determined recurring to a standard curve constructed with known concentration of proline and the results were expressed in mg g⁻¹ F.W.

2.4 Bioinformatics characterisation of *Solanum lycopersicum* GS-encoding gene family (SIGs)

The relative expressions of SIGs were studied using Tomato eFP browser (bar.utoronto.ca.). All SIGs sequences (Supplemental Data 1) were aligned using MEGA 7 (Molecular Evolutionary Genetics Analysis) software, which allows to deduce overtime the molecular evolutionary relationships between genes, genomes and species (Supplemental Data 2) (Kumar et al., 2016).

2.5 Evaluation of expression of *Solanum lycopersicum* GS gene family

2.5.1 RNA extraction, quantification and assessment of its purity

Total RNA from plant tissues was extracted with NZYol (Nzytech®) according to the supplier's instructions. Shoots and roots (50-100 mg) were homogenized in 1 mL of NZYol followed by a centrifugation at 12,000 g for 10 min at 6 °C. The recovered SNs were incubated at RT for 5 min, and then 0.2 mL of chloroform was added followed by 15 s of vigorous shaking to efficiently denature proteins and other cell constituents. Samples were incubated for 2-3 min at RT and centrifuged at 12,000 g for 15 min at 6 °C and three distinct phases were obtained: a pale green phenol-chloroform phase; an interphase, consisting on cell debris and proteins; and an upper colourless aqueous phase, which contains the total RNA. The aqueous phase was carefully transferred to a new tube by pipetting and to precipitate the RNA, 0.5 mL of chilled isopropanol were added. The samples were incubated at RT for 10 min and centrifuged again at 12,000 g for 10 min at 6 °C. After discarding the SN, the pelleted RNA was washed with 75% ethanol, vortexed, and centrifuged at 7,500 g for 5 min at 6 °C. After ethanol evaporation, the RNA was dissolved in RNase free water.

RNA concentration was spectrophotometrically quantified at 260 nm, using a µDrop Plate (Thermo Fisher Scientific) and a Multiskan GO microplate spectrophotometer (Thermo Fisher Scientific). RNA purity was evaluated by the calculation of the ratios Abs_{260}/Abs_{280} and Abs_{260}/Abs_{230} , which should be at 2.0 ± 0.1 and between 2.0-2.4, respectively, for uncontaminated RNA preparations. Only RNA samples with Abs_{260}/Abs_{280} above 1.8 were used in subsequent assays.

The quality of RNA was evaluated by separating 300 ng of total RNA in a 0.8% (w/v) agarose gel electrophoresis, which allowed to observe possible RNA degradation and genomic DNA contamination. Possible genomic DNA contamination was removed by

DNase treatment with ezDNase enzyme (Invitrogen), according to the manufacturer's instructions. RNA preparations were then stored at -80 °C until future use.

2.5.2 Reverse Transcription (cDNA Synthesis)

All the cDNA synthesis reactions were performed with SuperScript™ IV VILLO™ Master Mix, following the instructions for reverse transcription (Invitrogen). The reactions were prepared in chilled, sterile and RNase-free 1.5 mL tubes. The reactions contained: 4 µL SuperScript™ IV VILLO™ Master Mix, 2.5 µg of total RNA and nuclease-free water to a final volume of 20 µL and the final reaction was mixed gently. Additionally, negative RT controls were prepared, where the SuperScript™ IV VILLO™ Master Mix was replaced by 4 µL SuperScript™ IV VILLO™ no RT Control and nuclease-free water to a final volume of 20 µL. Then, the tubes were incubated at 25 °C for 10 min for primer annealing (dNTPs, oligo-dT and random primers provided in the Master Mix) and the reverse transcription took place at 60 °C for 20 min. Finally, enzyme inactivation occurred at 85 °C for 5 min. At the end of the procedure, the cDNAs were stored at -20 °C until future use.

2.5.3 Primer design

A total of 5 GS-encoding cDNA sequences were selected from the NCBI platform and conserved primers were designed using the PrimerIdent tool (Pessoa et al., 2010), considering the following conditions: (based on (Thornton and Basu, 2011)): a) primer size: around 20 bp; b) Primer T_m: similar between each pair, 55-65 °C; c) % GC: 45-55; d) GC-clamp: check for maximum of 2-3 GC' in the last 5 oligonucleotides of primer 3' end ; e) Maximum self-complimentary and 3' self-complimentary: lowest possible; f) product size range: between 120-200 bp. After that, primers were checked with Primer 3 (<http://bioinfo.ut.ee/primer3-0.4.0/>). All primers were ordered at STAB VIDA (Portugal). All forward and reverse primers for *SIGSs*, as well as their specificities are listed in Table 3.

Table 3. Gene-specific primers, their T_m and respective expected amplicon sizes for the performed RT-PCR reactions.

Gene	Primer	Sequence (5'-3')	T_m (°C)	Amplicon size (bp)
GS2	Forward	TCTCTCACTCCTAACACAAC	68 °C	189 bp
	Reverse	GCGTGTCTTTTCTGCTTC	62 °C	
GS1.1	Forward	CGGAGAAAGGAAAGGGATAC	70 °C	178 bp
	Reverse	CATGTGAGGAAAGGCTGTTAAG	68 °C	
GS1.2	Forward	GGTTGCTGGAGTTGTTGTTTC	58 °C	191 bp
	Reverse	CGTTCATTGCCTTCACCATA	58 °C	
GS1.3	Forward	CTGGTGATGAAGTGTGGGTAG	64 °C	164 bp
	Reverse	TTTCATAGCCTCCGTCTTCC	60 °C	
GS1.4	Forward	GAGAGCCCATCCCAACAAA	58 °C	192 bp
	Reverse	GCACCAACACCACAGAAGTATG	66 °C	

In a series of initial experiments, all primers were checked for their product size by 0.8% (w/v) agarose gels electrophoresis prepared on sodium boric acid (SB) buffer and stained with Roti-Safe GelStain (Quanta Biotech), according to standard molecular biology procedures (Sambrook et al., 1989). All the obtained results were captured with GenoSmart2 (VWR®).

2.5.4 Gene Sequencing

To confirm if the primers were annealing and amplifying the right cDNA, the amplification products from each *S/GS*-encoding cDNA were sequenced. To perform that, each amplified fragment corresponding to each *S/GS*-encoding cDNA was separated in 0.8% (w/v) agarose gels (250 V, non-limiting amperage, 8 min). The gel bands were excised and purified with GenElute™ Gel Extraction Kit (Sigma). The gel bands were weighted and solubilized in 3 volumes (300 μ L:100 mg) of gel solubilization solution and incubated at 60 °C for 10 min, with brief vortex in between till all agarose have been dissolved. Later, 1 gel volume of 100% isopropanol was added, and, after binding column preparation (500 μ L of column preparation solution were added followed by centrifugation), the mixture was loaded and 700 μ L of wash solution was added to the binding column, followed by centrifugation (1 min at 12,300 g), discarding the flow-through. Then, the mixture was incubated for 5 min at RT. To remove the excess of ethanol, another centrifugation, like the previous one, was performed. The binding column was placed in a new tube and to recover the eluate, 25 μ L of elution solution was added to the column followed by two centrifugations. The purified DNA was quantified at 260 nm with a μ Drop Plate (Thermo Fisher Scientific) and a Multiskan GO microplate spectrophotometer (Thermo Fisher Scientific). The PCR products (2 ng μ L⁻¹ in a final

volume of 15 μ L), with the respective Forward Primer were sent to Eurofins laboratories to be sequenced. Finally, the DNA was stored at -20 °C for future testing.

2.5.5 Expression of *S/GS* genes by Semi-quantitative RT-PCR

The accumulation of mRNA transcripts of the *S/GS*1.2-4 genes was evaluated by semi-quantitative reverse-transcription PCR. All the RT-PCR reactions were prepared with: 1x Taq Master Mix (Bioron), 0.4 μ M of each forward and reverse primers (see table 1), 0.8 μ L cDNA obtained for each treatment and organ and sterile distilled water to a final volume of 10 μ L. The reactions were performed in a MJ Mini thermocycler (Bio-Rad®). The PCR conditions were as follows: an initial denaturation step at 94 °C for 2 min, followed by 30 cycles at 94 °C for 30 s, a temperature gradient at 54-62 °C for 30 s followed by 72 °C for 20 s, and a final extension at 72 °C for 5 min. The amplification products were loaded on 2% (w/v) agarose gels prepared on SB buffer and stained with Roti-Safe GelStain (Quanta Biotech) and the electrophoresis occurred at 250 V with non-limiting amperage for 8 min. To assure that the concentration of DNA loaded on the gel for each treatment was the same, the amount of all treatments' cDNA volume to load was determined using 18S as an internal control (Leclercq et al., 2002). To confirm the size of amplified fragments, the molecular weight marker GeneRuler 50 bp DNA Ladder (Thermo Fisher Scientific) was used. All images were captured with GenoSmart2 (VWR®).

2.5.6 Evaluation of *S/GS* gene expression by Real-time PCR (qPCR)

All the reactions for each organ, treatment and *S/GS*2- and *S/GS*1.1-encoding genes were performed in triplicate. The reaction mixes consisted in 10 μ L of 2x PowerUp™ SYBR™ Green Master Mix (Applied Biosystems), 1 μ L of 1/10 diluted cDNA, 0.5 μ M of both forward and reverse primers (see table 1) and distilled sterile water to a final volume of 20 μ L. Data normalization was achieved using actin and ubiquitin genes as reference genes (Løvdaal and Lillo, 2009). The PCR reactions were conducted in a CFX96 Real-time Detection System (Bio-Rad®) and the cycling parameters were: 2 min at 50 °C and 2 min at 95 °C, followed by 45 cycles alternating between 3 s at 95 °C and 30 s with a gradient temperature, according to melting temperatures of the primers (see table 1). Afterwards, a melting curve was carried out by increasing the temperature from 60 to 95 °C with 0.5 °C intervals to verify primer specificity and if only a single amplified product was detected for each gene (Supplemental data 4). The obtained results were analysed in CFX Manager Software (BioRad®, Portugal) and because the primer efficiency was

less than 90%, the quantification of mRNA levels was achieved according to the Pfaffl method (Pfaffl, 2001).

2.6 Evaluation of photosynthetic-related genes expression by qPCR

Additionally, photosynthesis-related gene expression was verified. To do so, the expression of two genes coding for photosystem II proteins (D1 and CP47) and two genes encoding RuBisCO units (*rbcL* and *rbcS*) was evaluated (Table 4). The PCR reactions as well as the reference genes used were the same as described at 5.7 section.

Table 4. Photosynthetic gene-specific primers and respective expected amplicon sizes.

Gene	Primer	Sequence (5'-3')	Amplicon size (bp)
<i>PSIIa</i>	Forward	TGGATGGTTTGGTGTGTTTGATG	191
	Reverse	CCGTAAAGTAGAGACCCTGAAAC	
<i>PSIIb</i>	Forward	CCTATTCCATCTTAGCGTCCG	142
	Reverse	TTGCCGAACCATAACACATAG	
<i>rbcL</i>	Forward	ATCTTGCTCGGGAAGGTAATG	81
	Reverse	TCTTTCCATACCTCACAAAGCAG	
<i>rbcS</i>	Forward	TGAGACTGAGCACGGATTTG	148
	Reverse	TTAGCCTCTTGAACCTCAGC	

The PCR reactions were conducted in a CFX96 Real-time Detection System (Bio-Rad®) and the cycling parameters were: 2 min at 50 °C and 2 min at 95 °C, followed by 40 cycles alternating between 3 s at 95 °C and 30 s at 60 °C. The melting curve analysis was conducted by the same method as above described (Supplemental data 5). The obtained data was analyzed in CFX Manager Software (BioRad®, Portugal) and the quantification of mRNA levels was achieved according to the $2^{-\Delta\Delta Ct}$ method of Livak and Schmittgen (Livak and Schmittgen, 2001).

2.7 Overexpression of GS2-encoding cDNA

2.7.1 Obtaining *S/GS2*-encoding cDNA sequence

2.7.1.1 Genomic DNA extraction

Initially, a strategy to obtain the full *S/GS2* gene (Supplemental data 6) was attempted. Genomic DNA was extracted with GeneJET Plant Genomic DNA Purification Mini Kit (Thermo Fisher Scientific). About 150 mg of leaf tissue were homogenised with a mortar and pestle in a 1.5 mL microcentrifuge tube, and 50 µL of lysis buffer B and 20 µL of RNase A were added and the mixture was incubated at 60 °C for 10 min, with occasional

vortexing. Then, 130 μ L of precipitation solution were added to the tube and it was inverted 2-3 times and placed on ice for 5 min. The samples were centrifuged at 20,000 g for 5 min, the SNs were collected to a new tube and 400 μ L of plant gDNA binding solution and 400 μ L of 96% ethanol were added and mixed. The mixture was transferred to a spin column and centrifuged at 6,000 g for 1 min. Afterwards, 500 μ L of wash buffer I were added to the column, followed by a centrifugation at 8,000 g for 1 min, the flow-through was discarded and 500 μ L of wash buffer II were added. A new centrifugation at maximum speed \geq 20,000 g for 3 min was performed, the flow-through was discarded and the column was centrifuged at maximum speed for 3 min. The column was placed in a new 1.5 mL microcentrifuge tube and the gDNA was eluted when 100 μ L of elution buffer were added to the centre of the column membrane, incubated at RT for 5 min and centrifuged at 8,000 g for 1 min. DNA concentration was spectrophotometrically quantified at 260 nm, using a μ Drop Plate (Thermo Fisher Scientific) and a Multiskan GO microplate spectrophotometer (Thermo Fisher Scientific).

2.7.1.2 Obtaining the *SGS2* gene

To obtain the *SGS2* gene, a PCR was performed. All the reactions were prepared with 1x Phusion Flash PCR Master Mix (Thermo Fisher Scientific), 0.5 μ M of forward (5' CTC TCA CTC CTC TCA ACA CAA C 3') and reverse (5' CAT TCG GAA AGA GCA CAC CA 3') primers, 5 ng of gDNA and sterile water to a final volume of 10 μ L. The reactions were performed in a MJ Mini thermocycler (Bio-Rad®). The PCR conditions were as follows: an initial denaturation step at 98 °C for 10 s, followed by 30 cycles at 98 °C for 1 s, 53.4 °C for 5 s followed by 72 °C for 1 min and 20 s, and a final extension at 72 °C for 1 min. Previously, a gradient PCR was performed to choose the best annealing temperature for the primer pair used.

2.7.1.3 Obtaining *SGS2*-encoding cDNA

The *SGS2*-encoding cDNA was obtained by the same method as described at 2.5.1 and 2.5.2 sections, and using specific primers for the *SGS2* gene, described at 2.7.1.2 section. A PCR was conducted with 2x Phusion Flash PCR Master Mix (Thermo Fisher Scientific), 0.5 μ L of each forward and reverse primers, 0.5 μ L cDNA and sterile distilled water to a final volume of 10 μ L. The reactions were performed in a MJ Mini thermocycler (Bio-Rad®). The PCR conditions were as follows: an initial denaturation step at 98 °C for 30 s, followed by 35 cycles at 98 °C for 10 s, 53.4 °C for 15 s followed by 72 °C for 45 s, and a final extension at 72 °C for 7.5 min. The amplification products were loaded on 0.8% (w/v) agarose gels prepared on SB buffer and stained with Roti-Safe GelStain

(Quanta Biotech) and the electrophoresis occurred at 250 V and non-limiting amperage for 8 min. After electrophoresis, the band of interest was cut, weighted and placed into an Eppendorf tube and then purified as previously described.

2.7.2 Bacterial strains and culture conditions

Escherichia coli DH5 α was streaked and incubated on L-agar (Luria-Bertani (LB) and agar) plates. A single bacterial colony was picked up and cultured in LB broth medium ON at 37 °C with agitation to reach saturation conditions. Then, 2 mL of the culture were grown in 200 mL of LB at 37 °C with agitation, until achieving between 0.35-0.45 optical density (OD) at 600 nm (in this OD interval, the bacteria reach the log growth phase). Once attained the mid log phase, the cultures were placed on ice and the thermal competency and electro competency induction were started.

2.7.3 Induction of chemical competency in *E. coli* DH5 α

The bacteria were distributed by 50 mL conic tubes, placed on ice during 20 min followed by a 10-min centrifugation at 2,500 g, in cold conditions. The SN was discarded, and the tubes were inverted 2 min to allow the remaining SN elimination. After that, each pellet was resuspended in 8 mL of ice-cold Inoue transformation buffer (1.51 g piperazine-N,N'-bis(2-ethanesulfonic acid) pH 6.7; 1.088 g MgCl₂·H₂O; 0.22 g CaCl₂·H₂O; 1.865 g KCl and distilled water to a final volume of 100 mL), previously filtered with a 0.45 μ m filter. The centrifugation and SN elimination processes were repeated, and the pellet was resuspended in 2 mL of Inoue transformation buffer, followed by the addition of 1.5 mL dimethyl sulfoxide (DMSO) and mixing. The bacteria were resuspended in 400 μ L 10% glycerol and the tube content was divided in aliquots of 50 μ L and stored at -80°C.

2.7.4 Induction of electro competency in *E. coli* DH5 α

Once the OD_{600nm} between 0.35-0.45 was reached, the bacteria were divided in 50 mL conic tubes and maintained on ice for 20 min. Then, they were centrifuged at 2,500 g for 10 min, in cold conditions and resuspended in 20 mL of sterile deionized water. The bacteria were centrifuged again and resuspended in 8 mL sterile 10% glycerol, followed by a new centrifugation. The bacteria were then resuspended in 400 μ L 10% glycerol, distributed in aliquots of 50 μ L and stored at -80 °C until future use.

2.7.5 Ligation to the pJET 1.2 plasmid

The obtained S/GS2-encoding cDNA was purified, quantified and inserted into a cloning vector. The chosen plasmid was pJET 1.2 and the ligation was performed with the

CloneJET PCR Cloning Kit (ThermoFisher Scientific), according to manufacturer's procedure, with few modifications. The reactions were performed on ice and contained 5 μL of Reaction Buffer, 40 ng of PCR product reaction, 0.5 μL of pJET vector, 1 μL of T4 DNA ligase and nuclease-free water to a final volume of 10 μL . The mixtures were incubated ON at RT. Then, the ligation reaction was used for *E. coli* DH5 α transformation.

2.7.6 Transformation of chemical competent *E. coli* DH5 α

About 25 ng DNA of pUC18 (positive control) or the total ligation volume were added to 50 μL competent cells and tubes were incubated on ice for 30 min, followed by 45-60 s at 42 $^{\circ}\text{C}$, without shaking. After that, the tubes were transferred to ice for 2 min. Then, 800 μL LB were added and the cells were incubated at 37 $^{\circ}\text{C}$ for 45 min, with gentle agitation. Afterwards, the bacteria were centrifuged at 1,500 g for 2 min, the SN was discarded, and the cells were resuspended in 100 μL LB. Finally, the bacteria were plated on L-agar with 50 $\mu\text{g mL}^{-1}$ ampicillin (AMP) and incubated ON at 37 $^{\circ}\text{C}$ in an inverted position.

2.7.7 Electro Transformation of *E. coli* DH5 α

Five ng of pUC18 (positive control) or 5-10 μL of the ligation reaction were added to defrosted electrocompetent *E. coli* cells and mixed gently. Then, the mixture was placed in a prechilled electroporation cuvette and the transformation occurred at 1.5 kV (Bio-Rad®). After transformation, 1 mL of LB was added, mixing gently and the cells were incubated at 37 $^{\circ}\text{C}$ for 30-45 min. Afterwards, 100-200 μL of *E. coli* cells were plated on L-agar plates containing 50 $\mu\text{g mL}^{-1}$ AMP. The plates were incubated at 37 $^{\circ}\text{C}$ ON in an inverted position.

2.7.8 Plasmid Isolation

Each colony resulting from the transformation procedure was inoculated on LB with 50 $\mu\text{g mL}^{-1}$ AMP and incubated ON at 37 $^{\circ}\text{C}$. About 1.5 mL of the culture were transferred to a 1.5 mL and centrifuged 20 s at maximum speed. The SN was aspirated, and the pellet was resuspended in 200 μL STET [8% (w/v) sucrose; 50 mM Tris-HCl pH 8.0; 50 mM EDTA; 0.1% Triton X-100] and the centrifugation was repeated. Then, 4 μL (50 mg mL^{-1}) lysozyme were added, the mixture was incubated at RT for 5 min and the tubes were heated at 95 $^{\circ}\text{C}$ on heating block for 45 s to inactivate the enzymes. The mixture was centrifuged for 10 min at maximum speed. The pellet was removed with a sterile toothpick and 200 μL isopropanol were added to the SN and the tubes vortexed to allow

DNA precipitation. The mixture was centrifuged 10 min at maximum speed, the SN was aspirated and 200 μL of 70% ethanol were added without homogenization and the mixture was centrifuged for 5 min at maximum speed. The SN was carefully aspirated, and the tubes were inverted and placed at RT for 5-10 min to allow pellet drying. The DNA was resuspended in 20 μL sterile water and stored at $-20\text{ }^{\circ}\text{C}$.

2.7.9 Plasmid DNA extraction using NZYMiniprep kit

Four mL of bacterial culture in LB medium with $50\text{ }\mu\text{g mL}^{-1}$ AMP were grown at 37°C ON with shaking. The whole culture was placed in a 1.5 mL tube, centrifuged at $12,000\text{ g}$ for 30 s and resuspended in 250 μL of buffer A1 by vortexing. Afterwards, 250 μL of buffer A2 were added and mixed gently by inverting the tube followed by an incubation at RT for 4 min. 300 μL of buffer A3 were then added and the tube was gently inverted 6-8 times, and centrifuged again for 10 min. The SN from the previous step was loaded into a NZYTech spin column, previously placed in a 2 mL collection tube, centrifuged for 1 min at $11,000\text{ g}$ and the flow-through discarded. After that, 500 μL of buffer AY were loaded into the column and centrifuged for 1 min at $12,000\text{ g}$ and the flow-through discarded. Then, 600 μL of buffer A4 were then added and the column centrifuged again for 1 min and the flow-through discarded. The column was then re-inserted in the empty collection tube and centrifuged for 2 min at $12,000\text{ g}$ to allow filter drying. The column was inserted in a sterile 1.5 mL tube and 50 μL of buffer AE were added to its centre. After a 1 min incubation at RT a centrifugation for 1 min at $12,000\text{ g}$ was performed. The flow-through was reloaded into the column and the centrifugation repeated. The minipreps were stored at -20°C .

2.7.10 Restriction Analysis

The obtained plasmids were cut and analysed for the presence of insert. To do that, two single restriction enzymes analysis were performed with *XhoI* and *NcoI* because both enzymes recognise one restriction site within the GS2-encoding cDNA and one in the pJET 1.2 vector (Supplemental Data 7), next to the insertion site of the PCR fragment, thus allowing not only the certification of the successful cloning, but also to know the insert's orientation. In each reaction were used: 4 μL of plasmid, 1 μL of the appropriate 10x restriction buffer, 0.5 μL of *XhoI* or *NcoI* (ThermoFisher Scientific) and sterile water to a final volume of 10 μL . To confirm the presence of GS2-encoding cDNA, a new restriction analysis was conducted using *SacI*, an enzyme that recognizes 3 restriction sites within the GS2-encoding cDNA sequence. The reactions contained: 8.5 μL of

plasmid, 1 μL of the 10x restriction buffer, 0.5 μL of *SacI* (ThermoFisher Scientific) and sterile water to a final volume of 10 μL .

The tubes containing the restrictions with *XhoI* and *NcoI* were incubated ON at 37 °C, while the tubes containing the restriction with *SacI* were incubated for 1 h at 37 °C. The results were visualized on an 0.8% (w/v) agarose gel prepared on SB buffer and stained with Xpert Green DNA Stain (Grisp). The electrophoresis occurred at 250 V and non-limiting amperage for 8 min. All images were captured with GenoSmart2 (VWR®).

2.8 Statistical Analysis

All experiments were carried out, at least, in three biological replicates ($n \geq 3$) for each parameter and the results expressed as mean \pm standard deviation. Significant differences were detected by one-way ANOVA followed by Dunnett's *post-hoc* test for comparison between the means of control and each treatment. The statistical analysis was performed using the software GraphPad Prism 7.00 (GraphPad Software Inc., USA) and differences at $p < 0.05$ were considered significant.

3. Results

3.1 Cr accumulation on tomato plants' shoots and roots

The accumulation of Cr in tomato plants' tissues was studied and the results are shown in Figure 6. The uptake of this HM increased in a concentration-dependent manner, in both organs, being roots the organ with higher Cr amounts in both Cr (VI) treatments.

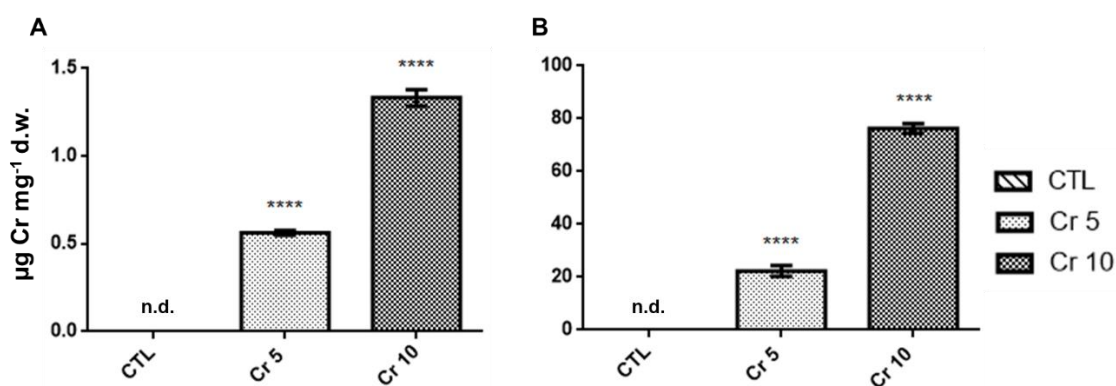


Figure 6. Chromium accumulation levels in shoots (A) and roots (B) of tomato plants. CTL: Control; Cr 5: 5 µM Chromium (VI); Cr 10: 10 µM Chromium (VI); n.d.: non-detected. Values presented are mean plus SD. **** above bars indicate significant statistical differences from control at $p \leq 0.0001$

The content of Cr in shoots increased 0.5- and 1.3- fold, with the lowest and the highest Cr (VI) concentration, respectively, while in roots, the observed increase was 22- and 76-fold, respectively.

3.2 Effects of Cr (VI) and DCF on nitrogen assimilation

3.2.1 GS and GDH activity

To assess the influence of these two contaminants on N assimilation, the activity of GS and GDH was measured in shoots and roots of tomato plants. GS activity (Figure 7) of plants treated with Cr (VI), exhibited significant differential responses. The lowest concentration of Cr (VI) positively affected shoot GS activity (about 0.7-fold) while it decreased about 0.3-fold in roots. However, the 10 µM Cr (VI) exposure decreased GS activity by 0.5-fold in shoots and 0.4-fold in roots. Regarding the 0.5 mg L⁻¹ DCF treatment, a differential response in shoots and roots was observed. GS activity decreased 0.2-fold in shoots and increased 0.8-fold in roots when plants were exposed to 0.5 mg L⁻¹ DCF. The highest concentration of DCF negatively affected GS activity in both shoots (0.5-fold) and roots (0.4-fold).

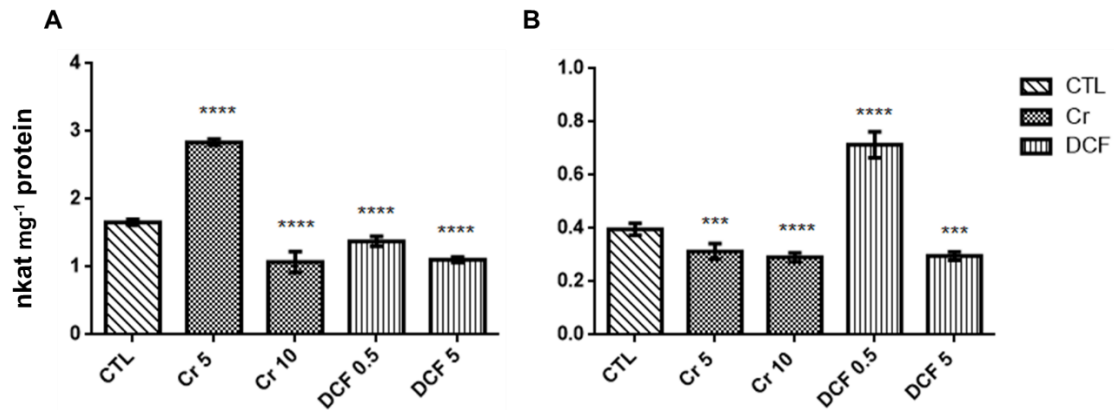


Figure 7. GS activity in shoots (A) and roots (B) of tomato plants exposed to Cr (VI) and DCF expressed as nkat mg⁻¹ protein. CTL: Control; Cr 5: 5 μ M Chromium (VI); Cr 10: 10 μ M Chromium (VI); DCF 0.5: 0.5 mg L⁻¹ Diclofenac; DCF 5: 5 mg L⁻¹ Diclofenac. Values presented are mean \pm SD. *** and **** above bars indicate significant statistical differences from control at $p \leq 0.001$ and $p \leq 0.0001$, respectively.

GDH activity was analysed by non-denaturing polyacrylamide gel electrophoresis (Figure 8). In shoots (Figure 8A), a total of three bands could be observed. The two bands appearing in the control situation revealed an increased intensity with the Cr (VI) treatments, where the appearance of a third band was also noticed. Concerning the DCF treatments, the bands' intensities common to the control increased and, once again, a third band appeared, but only with the highest DCF concentration used.

In roots (Figure 8B), 5 bands were observed in all treatments. Overall, all bands increased their intensity with both Cr (VI) treatments. In plants treated with DCF, only bands 2, 3 and 5 showed an increase in their intensity, particularly the band 3.

Furthermore, the bands intensity increased in a concentration-dependent manner for both contaminants.

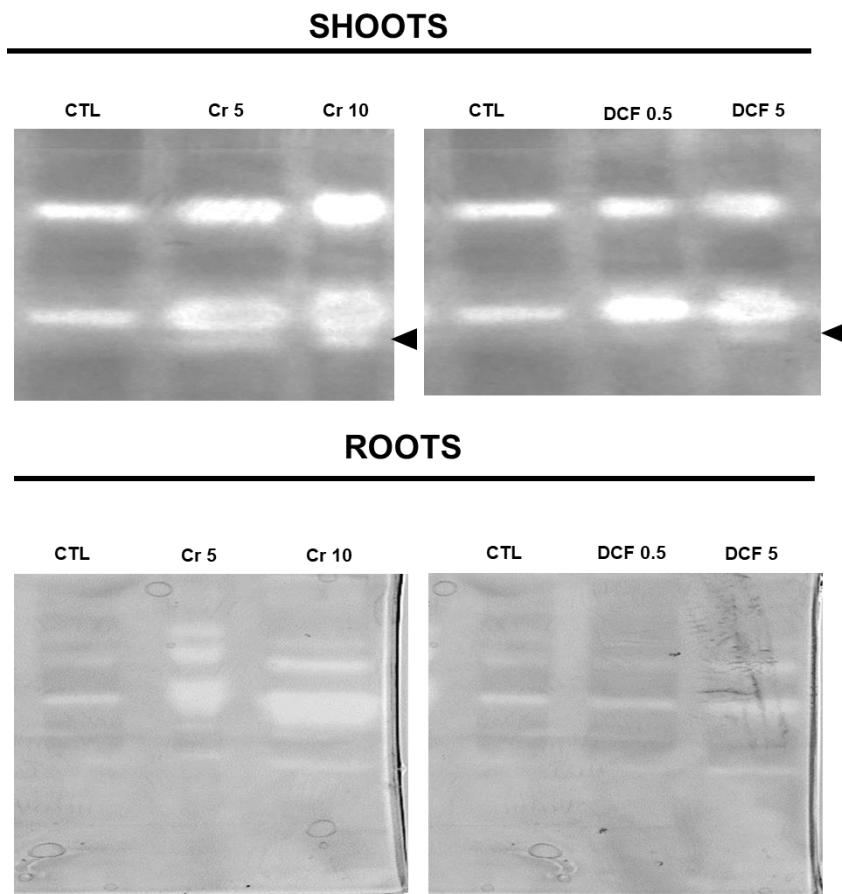


Figure 8. Typical GDH activity results for shoots and roots by native PAGE analysis. CTL: Control; Cr 5: 5 μM Chromium (VI); Cr 10: 10 μM Chromium (VI); DCF 0.5: 0.5 mg L^{-1} Diclofenac; DCF 5: 5 mg L^{-1} Diclofenac.

3.2.2 Western Blotting Analysis

To assess the impact of both contaminants on N metabolism at the protein accumulation, a western blotting analysis was conducted. Specific antibodies were used for GS (Figure 9) and GDH (Figure 10).

The shoot GS western blot (Figure 9A) revealed two bands, corresponding to the two main GS isoenzymes: the cytosolic (41 kDa) and the plastidic (45 kDa), while in roots (Figure 9B) only one band, which corresponds to the cytosolic form was noticed. The GS content markedly increased with the lowest concentration of Cr (VI) in shoots and no differences were detected with 10 μM Cr (VI). No differences in GS content were also observed for both DCF treatments in shoots. In roots (Figure 9B) and in both Cr (VI) concentrations no band was detected, depicting a large decrease in the accumulation of GS1 in response to Cr (VI), while with both DCF treatments a slight decrease in GS content was observed.

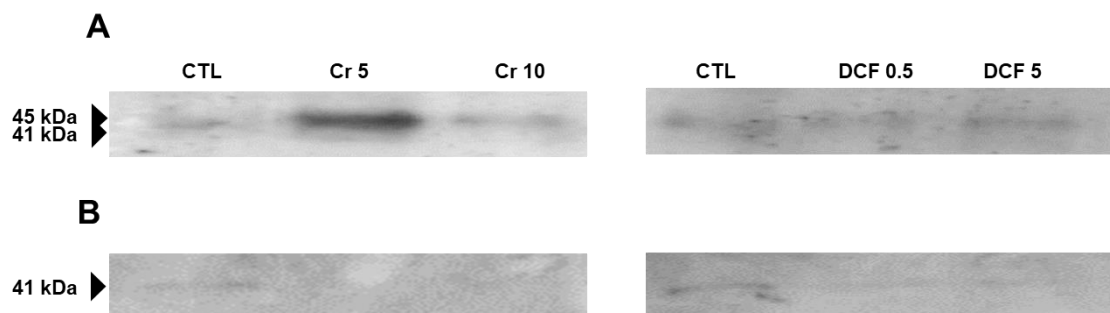


Figure 9. One-dimensional western blotting analysis of shoot (A) and root (B) tomato GS using GS antibodies raised to *Pinus* cytosolic GS. CTL: Control; Cr 5: 5 μ M Chromium (VI); Cr 10: 10 μ M Chromium (VI); DCF 0.5: 0.5 mg L⁻¹ Diclofenac; DCF 5: 5 mg L⁻¹ Diclofenac.

Regarding GDH protein content (Figure 10), it was more abundant in roots than in shoots. In both organs, only a single band with about 43 kDa was detected.

GDH gradually decreased with the increasing Cr (VI) treatments in shoots (Figure 10A), with no band being detected with 10 μ M Cr (VI). In roots (Figure 10B), there was a decrease with 5 μ M Cr (VI), but GDH polypeptide content increased with the highest concentration of Cr (VI). DCF treatments decreased the GDH content in both shoots and roots, in a concentration-dependent manner.

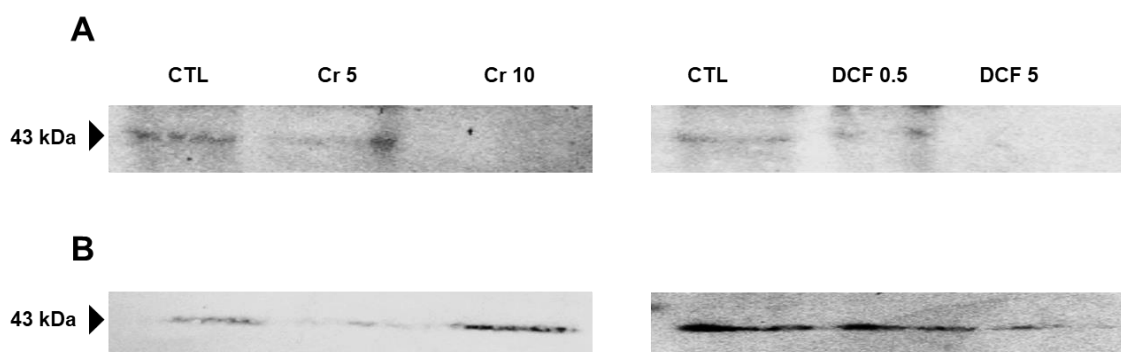


Figure 10. One-dimensional western blotting analysis of shoot (A) and root (B) tomato NAD-GDH using antibodies raised to *Vitis vinifera* NAD-GDH. CTL: Control; Cr 5: 5 μ M Chromium (VI); Cr 10: 10 μ M Chromium (VI); DCF 0.5: 0.5 mg L⁻¹ Diclofenac; DCF 5: 5 mg L⁻¹ Diclofenac.

3.3 Soluble polypeptide accumulation analysis after Cr (VI) and DCF exposure

PAGE analysis was performed to check if the tomato plants exposure to these two contaminants altered their shoot's and root's soluble polypeptide profiles (Figure 11). The exposure to both Cr (VI) and DCF led to a qualitative and quantitative alteration of the electrophoretic profile of the soluble polypeptides. Additionally, for both

contaminants' treatments the disappearance of a band with 250 kDa in shoots (Figure 11A) was observed.

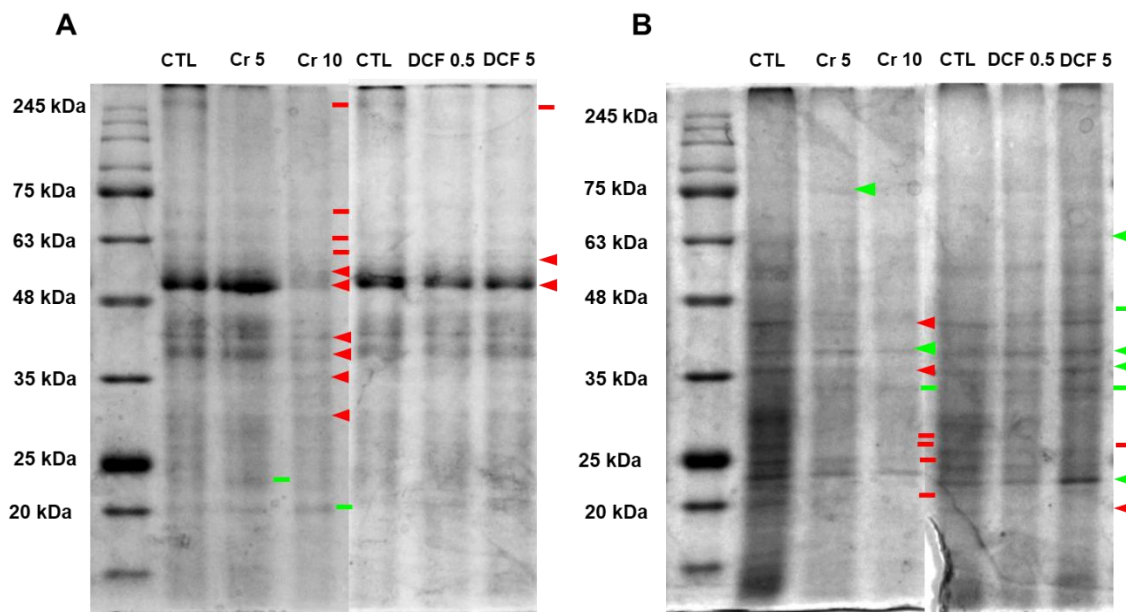


Figure 11. Typical SDS-PAGE analysis of soluble proteins on shoots (A) and roots (B) of *S. lycopersicum*. CTL: Control; Cr 5: 5 μM Chromium (VI); Cr 10: 10 μM Chromium (VI); DCF 0.5: 0.5 mg L^{-1} Diclofenac; DCF 5: 5 mg L^{-1} Diclofenac. Arrows indicate common bands that suffered a decreased (red) or an increased accumulation; - indicates qualitative changes: red – disappearance; green – *de novo* polypeptide. The used ladder was BLUE Wide Range CSL-BBL Prestained Protein Ladder (Cleaver Scientific Ltd).

Concerning Cr (VI) treatments, the large RuBisCO subunit (near 50 kDa) increased its intensity with the lowest Cr (VI) concentration and almost disappeared with 10 μM Cr (VI). Also, it was observed a disappearance of the bands around 70, 58 and 50 kDa in shoots, and with 27 and 26 kDa in roots (Figure 11B). The highest concentration of Cr (VI) was more severe, with a disappearance of bands with 25 and 20 kDa in roots, and a decrease in bands with 42, 40, 37 and 33 kDa in shoots. The bands with 20 kDa in shoots and 32 kDa in roots appeared with both Cr (VI) treatments. The 5 μM Cr (VI) treatment induced the appearance of new bands with 22 and 75 kDa in shoots and in roots, respectively. Finally, it was also observed a decrease in staining intensity of bands with 42 and 35 kDa bands with both treatments and an increase in 37 kDa band with the lowest concentration of Cr (VI) in roots.

DCF treatments were less severe to the shoot's soluble polypeptide population than Cr (VI) treatments', being this scenario even more evident in roots. In shoots, there was a decrease in the intensity of a 55 kDa band and in the large subunit of RuBisCO band. In roots, only a band with 27 kDa disappeared with the highest concentration of this drug and a decrease in 20 kDa band was observed for both treatments. Two new bands with 46 and 33 kDa appeared with both treatments and an increase in bands with 63, 40 and

36 kDa was observed. Moreover, with the 5 mg L⁻¹ DCF treatment, an increase in staining intensity in 22 kDa band was observed.

3.4 Evaluation of Cr (VI) and DCF impact on physiological parameters associated with nitrogen metabolism

Knowing the role of GS and GDH on proline biosynthesis, as well as the function of proline in stressful conditions, it is important to understand the effects of these two contaminants on this amino acid levels. As seen in Figure 12, in comparison to the control situation no differences in the levels of proline were detected in shoots, for the lowest concentration of Cr (VI). Yet, with this treatment, the proline levels in roots increased 1.0-fold. With the 10 μM Cr (VI) treatment, proline levels increased in both shoots and roots by 0.6- and 0.7-fold, respectively.

Although there was a significant increase of proline levels with the highest DCF concentration in shoots and roots (about 0.6- and 2.3-fold), the lowest concentration of this contaminant lead to no statistical differences for both organs, in relation to the control situation.

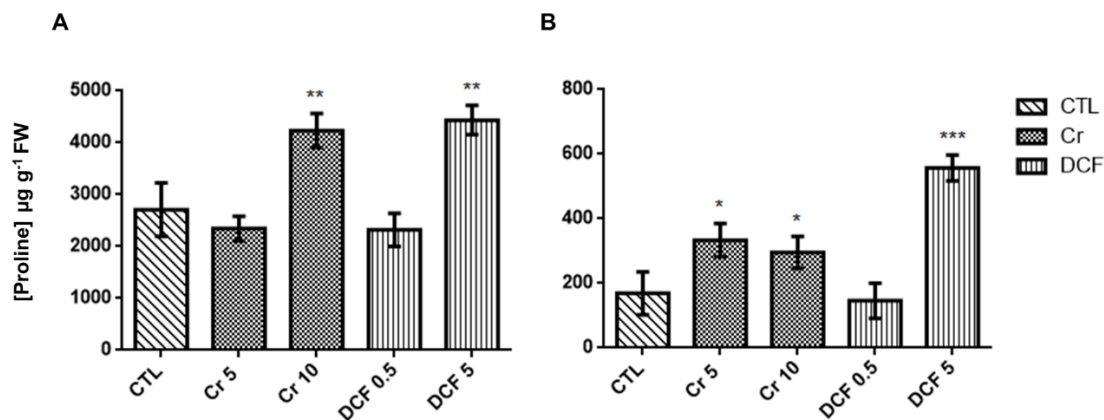


Figure 12. Proline levels in shoots (A) and roots (B) of tomato plants exposed to Cr (VI) and DCF. CTL: Control; Cr 5: 5 μM Chromium (VI); Cr 10: 10 μM Chromium (VI); DCF 0.5: 0.5 mg L⁻¹ Diclofenac; DCF 5: 5 mg L⁻¹ Diclofenac. Values presented are mean ± SD. *, ** and *** above bars indicate significant statistical differences from control at $p \leq 0.05$, $p \leq 0.01$ and $p \leq 0.001$, respectively.

3.5 Assessment of the Cr (VI) and DCF effects on several photosynthetic endpoints

To gain an insight on the impact of these two contaminants on the C metabolism, some physiological parameters like photosynthetic pigments content, gas exchange and starch

accumulation were measured. Besides all these biochemical techniques, a molecular approach was conducted, where the expression of some photosynthetic-related genes under both treatments was evaluated.

3.5.1 Photosynthetic pigments

Overall, both contaminants had a positive influence on photosynthetic pigments content in tomato leaves (Figure 13). Concerning the chlorophyll content levels (Figure 13A), no statistical differences were found with 5 μM Cr (VI) treatment, although there was a significant increase of 0.7-fold with the 10 μM Cr (VI) treatment. Regarding DCF exposure, there was a significant increase of 1.4- and 1.6-fold with the lowest and highest concentrations, respectively. The carotenoid content (Figure 13B) did not alter with the lowest Cr (VI) exposure but increased 0.7-fold with the 10 μM Cr (VI) concentration. The 0.5 mg L^{-1} DCF treatment significantly stimulated the carotenoid content by 0.9-fold. Interestingly, no differences in the content of these pigments were observed with the highest DCF concentration.

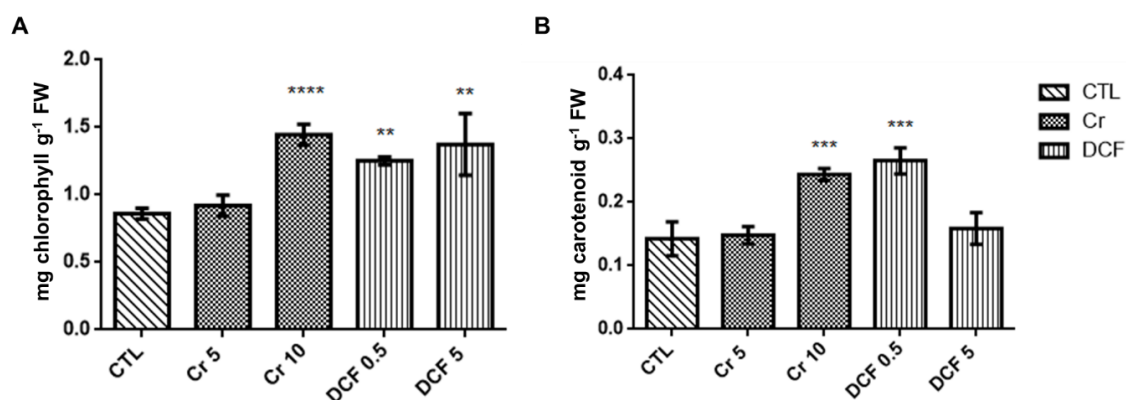


Figure 13. Total chlorophylls (A) and carotenoids (B) levels of tomato plants exposed to Cr (VI) and DCF. CTL: Control; Cr 5: 5 μM Chromium; Cr 10: 10 μM Chromium; DCF 0.5: 0.5 mg L^{-1} Diclofenac; DCF 5: 5 mg L^{-1} Diclofenac. Values presented are mean \pm SD. **, *** and **** above bars indicate significant statistical differences from control at $p \leq 0.01$, $p \leq 0.001$ and $p \leq 0.0001$, respectively.

3.5.2 Photosynthetic apparatus

The parameters stomatal conductance (G_s) and transpiration rate (E) significantly increased with the 10 μM Cr (VI) treatment in 0.8- and 2.1-fold, respectively. Moreover, the G_s decreased 1.4-fold with the lowest Cr (VI) concentration. The remain parameters, net photosynthetic rate (A), the water use efficiency (WUE) and the ratio of internal and external CO_2 remained stable in all growth conditions (Table 5).

Table 5. Gas exchange measurement of plants exposed to Cr (VI) and DCF, considering the following parameters: A, CO₂ uptake (μmol m⁻² s⁻¹); E, transpiration rate (mmol m⁻² s⁻¹); G_s, stomatal conductance (mmol m⁻² s⁻¹); WUE, water use efficiency (nmol mol⁻¹); Ci/Ca, internal and environmental CO₂ ratio. CTL: Control; Cr 5: 5 μM Chromium (VI); Cr 10: 10 μM Cr (VI); DCF 0.5: 0.5 mg L⁻¹ Diclofenac; DCF 5: 5 mg L⁻¹ Diclofenac. Values presented are mean ± SD. ** above bars indicate significant statistical differences from control at p ≤ 0.01

Treatment	A μmol m ⁻² s ⁻¹	G _s mmol m ⁻² s ⁻¹	E mmol m ⁻² s ⁻¹	WUE mmol mol ⁻¹	Ci/Ca
CTL	8.451 ± 0.330	0.123 ± 0.018	0.539 ± 0.139	7.935 ± 0.634	0.691 ± 0.030
5 μM Cr (VI)	3.936 ± 0.531	0.052 ± 0.003 **	0.497 ± 0.023	9.386 ± 2.212	0.617 ± 0.085
10 μM Cr (VI)	7.282 ± 1.256	0.223 ± 0.009 **	1.664 ± 0.045 **	6.640 ± 1.364	0.770 ± 0.044
0.5 mg L ⁻¹ DCF	6.186 ± 0.151	0.094 ± 0.008	0.839 ± 0.005	7.368 ± 0.132	0.725 ± 0.003
5 mg L ⁻¹ DCF	6.185 ± 2.339	0.084 ± 0.008	0.829 ± 0.154	7.187 ± 1.486	0.687 ± 0.090

3.5.3 Photosynthesis-related gene expression

To understand the influence of Cr (VI) and DCF on tomato plants' photosynthesis, the transcript accumulation of some photosynthetic-related genes by qPCR was verified: two genes coding the protein subunits of PSII: D1 protein (*PSIIa*) and CP47 (*PSIIb*), respectively, and two genes coding the small and large subunits of RuBisCO, *rbcS* and *rbcL*, respectively (Figures 14 and 15).

According to Figure 14, it was possible to observe a significant up-regulation of *PSIIa* with the lowest concentration of Cr (VI) (1.6-fold) and a down-regulation of *PSIIb*, under the same treatment condition (0.25-fold). Concerning the 10 μM Cr (VI) treatment, *PSIIa* transcript remained constant and the *PSIIb* transcripts levels decreased (0.20-fold). On the other hand, the transcript levels of both PSII genes increased with both DCF treatments (0.4-fold). In particular, the levels of *PSIIa* transcripts increased with the rise in the DCF concentration (0.5- and 1.5-fold, respectively).

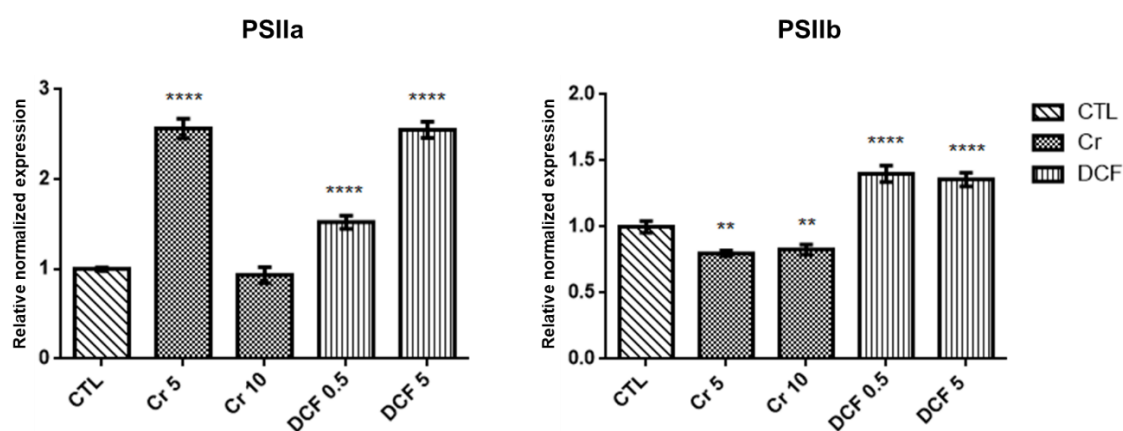


Figure 14. Expression profile of two genes coding for protein subunits of PSII, D1 protein (*PSIIa*) and CP47 (*PSIIb*), respectively, of tomato leaves exposed to Cr (VI) and DCF. CTL: Control; Cr 5: 5 μM Chromium; Cr 10: 10 μM Cr (VI);

DCF 0.5: 0.5 mg L⁻¹ Diclofenac; DCF 5: 5 mg L⁻¹ Diclofenac. Values presented are mean ± SD. ** and **** above bars indicate significant statistical differences from control at $p \leq 0.01$ and $p \leq 0.0001$, respectively.

The transcript levels of *rbcS* and *rbcL* significantly decreased with both Cr (VI) treatments (3.3-, 0.4-, 1.3- and 1.6-fold, respectively), however the observed decrease in *rbcS* transcript levels was more pronounced with the lowest Cr (VI) concentration (3.3-fold). Moreover, it was possible to observe a down-regulation of both *rbcS* and *rbcL* transcript levels with the two DCF treatments (0.1-, 0.6-, 0.8 and 0.3-fold, respectively), occurring the decrease in *rbcS* levels in a concentration-dependent mode.

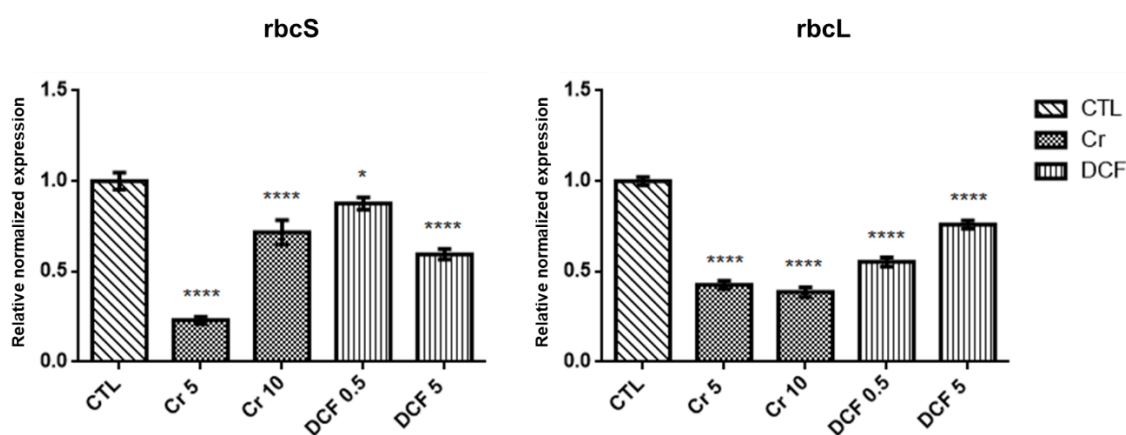


Figure 15. Expression profile of the small and large subunits of RuBisCO, *rbcS* and *rbcL*, respectively, of tomato leaves exposed to Cr (VI) and DCF. CTL: Control; Cr 5: 5 μM Chromium; Cr 10: 10 μM Cr (VI); DCF 0.5: 0.5 mg L⁻¹ Diclofenac; DCF 5: 5 mg L⁻¹ Diclofenac. Values presented are mean ± SD. * and **** above bars indicate significant statistical differences from control at $p \leq 0.05$ and $p \leq 0.0001$, respectively.

Overall, the PSII genes presented an up-regulation while, the RuBisCO genes suffered a down regulation under Cr (VI) and DCF exposure (Table 6).

Table 6. Effects of Cr (VI) treatments on photosynthetic-related genes expression. It was considered up regulated or down regulated if expression increased, or decreased (respectively) with $p < 0.05$, and no change if $p > 0.05$; CTL: Control; Cr 5: 5 μM Chromium (VI); Cr 10: 10 μM Chromium (VI); DCF 0.5: 0.5 mg L⁻¹ Diclofenac; DCF 5: 5 mg L⁻¹ Diclofenac.

TREATMENT	PHOTOSYNTHETIC-RELATED GENES			
	PSIIa	PSIIb	<i>rbcS</i>	<i>rbcL</i>
Cr 5	↑	↓	↓	↓
Cr 10	No change	↓	↓	↓
DCF 0.5	↑	↑	↓	↓
DCF 5	↑	↑	↓	↓

3.5.4 Starch accumulation

A histochemical coloration of starch grains was conducted to observe starch accumulation on tomato leaves (Figure 16). The intensity of the blue colour is indicative of a higher starch content. As it can be observed, the control leaves exhibited the highest starch levels, which was negatively affected by both Cr (VI) and DCF, in a concentration-

dependent manner. Furthermore, it seemed clear from the images that Cr (VI) exerted a much more pronounced effect than DCF.

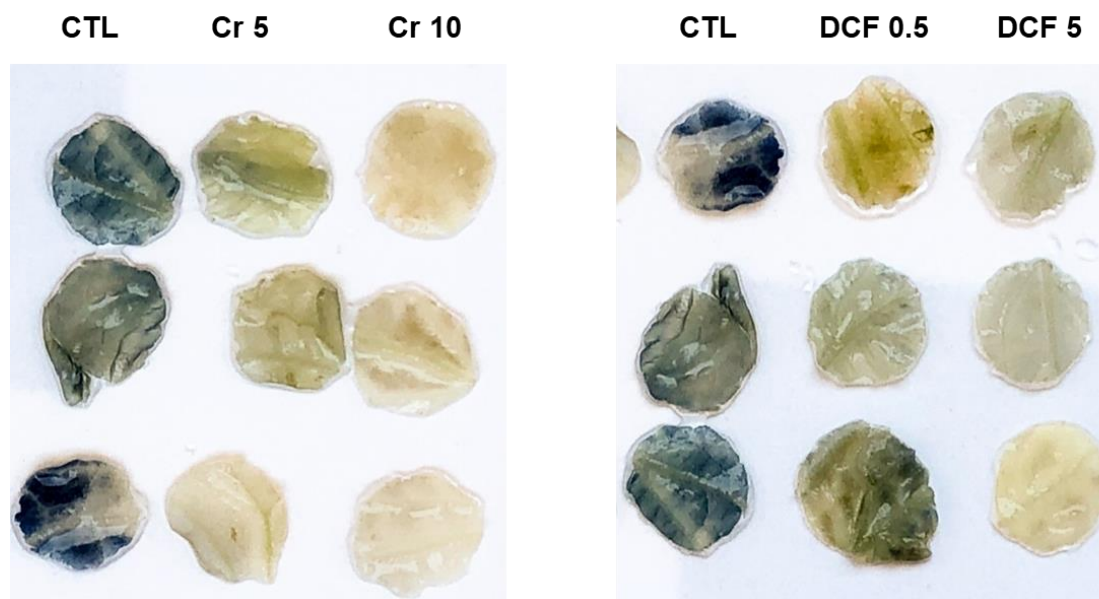


Figure 16. Lugol staining of starch in tomato leaves exposed to Cr (VI) and DCF. CTL: Control; Cr 5: 5 μM Chromium (VI); Cr 10: 10 μM Chromium (VI); DCF 0.5: 0.5 mg L^{-1} Diclofenac; DCF 5: 5 mg L^{-1} Diclofenac.

3.6 Bioinformatics characterisation of *Solanum lycopersicum* L.'s GS-encoding gene family

The tomato GS-encoding genes used in this work were selected based on an exploration performed at the NCBI platform (<https://www.ncbi.nlm.nih.gov/>) and SOL Genomics Network (SGN) database (<https://solgenomics.net/>), having 5 different cDNA sequences related to tomato GS been retrieved and then analysed as described.

This explorative work allowed the identification of 1 gene encoding the plastidic isoenzyme (*SIGS2*), and 4 coding for cytosolic isoenzymes: *SIGS1.1*; *SIGS1.2*; *SIGS1.3* and *SIGS1.4*.

3.6.1 Phylogenetic analysis of *S. lycopersicum* cDNAs coding for GS (SIGSs)

To understand the evolutionary relationships between the retrieved *SIGSs* genes, a phylogenetic tree was constructed using *MEGA* software (Figure 17). The tomato GS-encoding cDNA nucleotide and deduced protein sequences and respective accession data are assembled in the supplemental data (Supplemental data 1); their respective accession number can be visualised in Table 7.

The phylogenetic analysis showed that *SIGS1.1* and *SIGS 1.2* cDNA sequences are the most closely related, followed by *SIGS 1.3* and then by *SIGS 1.4*. *SIGS2* is phylogenetically the farthest GS-encoding sequence of all *SIGS*s.

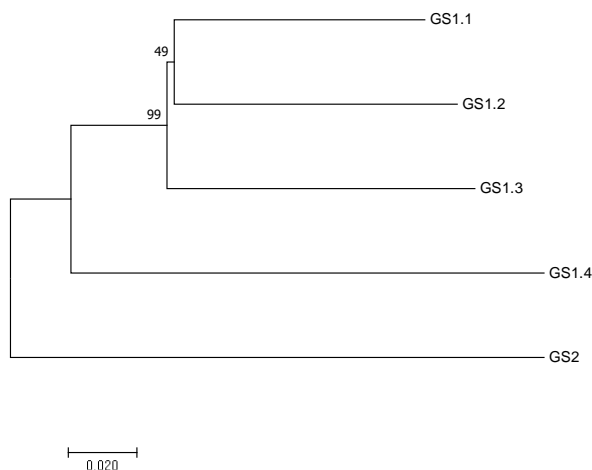


Figure 17. Phylogenetic tree constructed with all *S. lycopersicum* GS cDNA sequences recovered from the databases referred in the text. The bootstrap consensus tree was generated using the Neighbour-Joining method with MEGA7, with 1000 bootstrap replicates. The percentage of replicate trees in which the associated taxa clustered together in the bootstrap test are shown next to the branches. Bar represents the scale length.

3.6.2 *SIGS*s relative expression analysis using the eFP browser

The retrieved *SIGS* genes were analysed with the Tomato eFP browser to determine in which plant organs, and at what levels they would be expressed. The obtained data for leaves and roots is listed in Table 7.

Table 7. Relative expression levels of the tomato GS-encoding genes on leaves and roots.

Gene name	Accession number	Relative Expression	
		Leaves	Roots
<i>GS2</i>	Solyc01g080280.2	829.65	58.16
<i>GS1.1</i>	Solyc04g014510.2	29.25	819.92
<i>GS1.2</i>	Solyc05g051250.2	1.33	20.53
<i>GS1.3</i>	Solyc11g011380.1	136.6	981.3
<i>GS1.4</i>	Solyc12g041870.1	0	0

The tomato GS genes displayed different levels of expression on an organ-dependent manner. According to Tomato eFP Browser, *SIGS2* presented the highest levels of expression in leaves (829.65). Moreover, that was the only GS gene presenting high values in leaves. *SIGS1.1*, 2 and 3 expression levels are higher in roots when compared

to leaves, being *SIGS1.3* that with the highest value of expression (981.3) in roots, followed by *SIGS1.1*. *SIGS1.2* gene presented relatively low levels of expression in both organs when compared to *SIGS2*, *SIGS1.1* and *SIGS1.3*. *SIGS1.4* gene showed no levels of expression in either organ considered in this tool.

3.6.3 *SIGS* gene family relative expression analysis by RT-PCR

The cDNA sequences coding for the 5 GS isoenzymes were firstly aligned using Clustal Omega and the retrieved alignment was submitted in its Fasta format to PrimerIdent for cDNA-specific primer design.

In a series of initial experiments, the product sizes of the designed primers were checked, the PCR conditions were optimized and the differential expression of the several GS genes in tomato plants was inferred. To do so, gDNA, as well as cDNAs synthesised from mRNA extracted from shoots and roots of tomato plants grown under optimal conditions, were used. A series of gradient PCRs, using gDNA as template, was first conducted to determine the optimum annealing temperatures for each primer pair to be used in subsequent PCRs.

Having the optimum annealing temperatures been selected, it was possible to observe that all the primers annealed to the gDNA and resulted in amplicons after the PCR (Figure 18). Most of the amplified fragments presented bigger sizes than those theoretically expected if cDNAs were used as template in the PCR, indicating the presence of introns (Table 8). According to Figure 18, the biggest amplicon (about 1400 bp) is that of GS2 and the lowest amplicon (about 200 bp) was observed for GS1.1. GS1.3 and GS1.4 presented an amplicon of about 600 bp while GS1.2 presented an amplicon of about 550 bp. Therefore, all fragments, except for GS1.1, presented a size higher than the expected, indicating the presence of introns. Taking this particular result into consideration, future RT-PCR reactions for GS1.1 were prepared together with a negative control (where RNA was used instead of cDNA) to discard eventual gDNA contaminations and therefore, any false positive result.

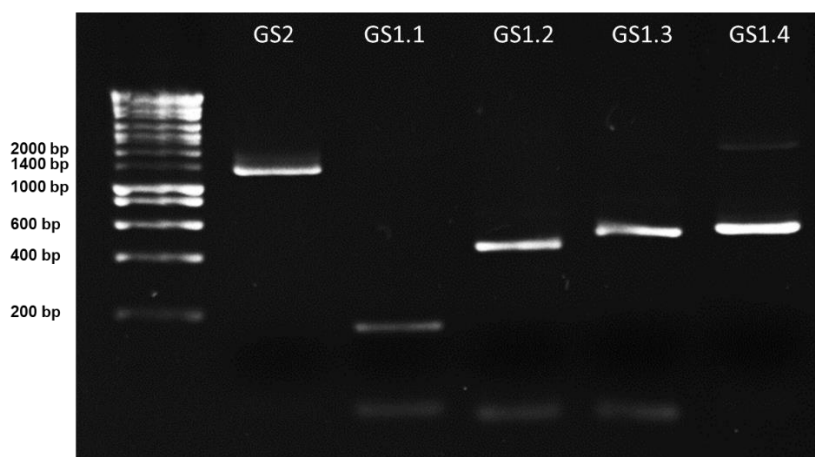


Figure 18. Agarose gel (0.8% (w/v)) electrophoresis evidencing the PCR products of GS2, GS1.1, GS1.2, GS1.3 and GS1.4 of *S. lycopersicum* when gDNA was used as template. The used ladder was NZYDNA Ladder III (Nzytech®, Portugal).

Table 8. Summary of chosen temperatures, expected sizes and intron presence of all *S/GS*-encoding genes.

Gene name	Chosen temperature (°C)	Expected size (cDNA)	Intron presence
GS2	55 °C	189 bp	+
GS1.1	62 °C	178 bp	-
GS1.2	54 °C	191 bp	+
GS1.3	56 °C	164 bp	+
GS1.4	54 °C	192 bp	+

Most primers detected their corresponding cDNAs in both shoots and roots. It is possible to observe that GS2, GS1.2 and GS1.3 presented higher mRNA accumulations in shoots than in roots, GS2 corresponding to that with the highest gene expression (Figure 19). GS1.1 expression was equally detected on both shoots and roots, being the most expressed gene on roots. GS1.4 presented no expression in both organs. All PCR products had their expected sizes. Moreover, no amplicons were detected in the negative control reactions for GS1.1 in either shoots or roots, indicating that the cDNA reactions used were not contaminated by gDNA.

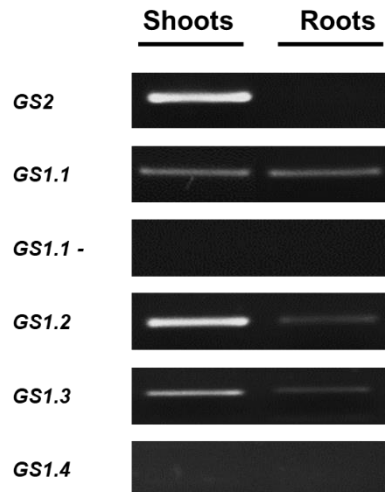


Figure 19. Results for GS2, GS1.1, GS1.2, GS1.3 and GS1.4 RT-PCR analysis by 0.8 % (w/v) agarose gel electrophoresis in both shoots and roots; Expected sizes: 189 bp; 178 bp, 191 bp; 164 bp; 192 bp, respectively. GS1.1- corresponds to the negative control reaction for GS1.1.

3.7 Study of Cr (VI) and DCF impact on S/GS gene family expression

3.7.1 Changes in transcript levels of tomato GS genes under Cr (VI)- and DCF-induced stress

To examine the effect of the exposure to Cr (VI) and DCF in the transcript amount of the tomato GS gene family members, a qPCR for GS2 and GS1.1 genes and a semi-quantitative RT-PCR for the remaining GS genes were performed using both actin and ubiquitin, and 18S genes as reference genes, respectively. For both reactions, total RNA extracted from leaves and roots of the control and treated plants was quantified and its quality was checked by agarose gel electrophoresis (Figure 20).

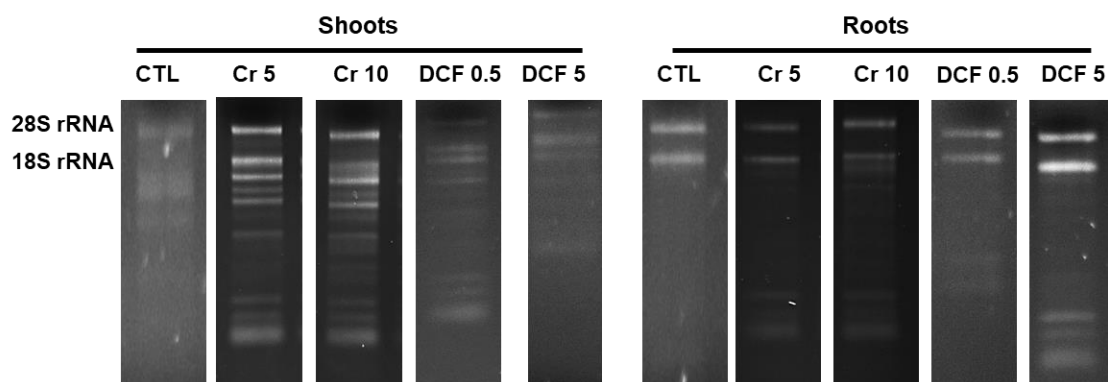


Figure 20. Total RNA extracted from shoots and roots of tomato plants exposed to Cr (VI) and DCF. For quality assessment of total RNA, it was separated on agarose gel at 0.8 % (w/v). CTL: Control; Cr 5: 5 μ M Chromium (VI); Cr 10: 10 μ M Chromium; DCF 0.5: 0.5 mg L⁻¹ Diclofenac; DCF 5: 5 mg L⁻¹ Diclofenac.

The analysis of the total RNA preparations revealed that these appeared not to be contaminated by gDNA, as no bands were visible near the wells where the samples were loaded. Furthermore, the visualization of well-defined rRNA bands showed that it was possible to proceed to the RT-PCR analysis.

The levels of transcripts of *GS2* (Figure 21), which were investigated by qPCR, in shoots did not present significant differences with the exposure to either Cr (VI) concentration used. In roots, their levels decreased 0.4-fold in the lowest Cr (VI) concentration and did not alter with 10 μ M Cr (VI). DCF exposure led to a down-regulation of the *GS2* transcript levels by 4.1- and 6.7-fold in shoots in a concentration-dependent manner. In roots, only the lowest concentration of this contaminant significantly decreased them (0.6-fold), while the highest DCF concentration did not present any significant differences.

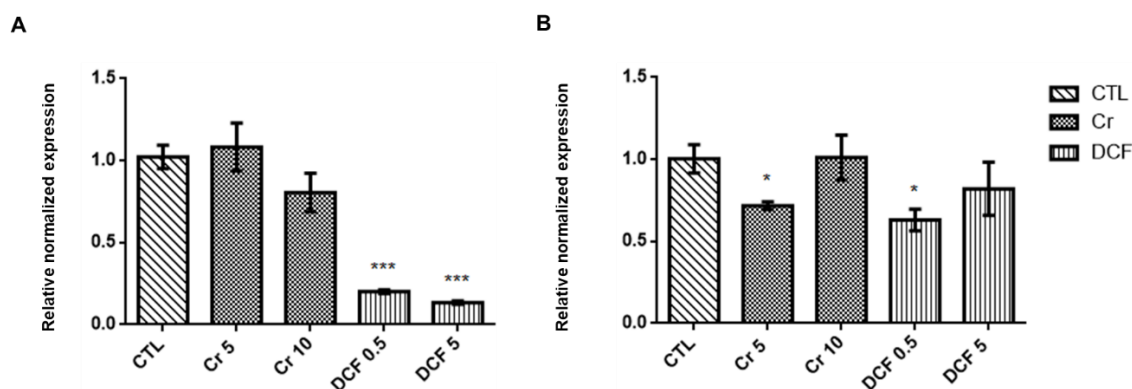


Figure 21. Expression profile of *GS2* gene in shoots (A) and roots (B), of tomato leaves exposed to Cr (VI) and DCF. CTL: Control; Cr 5: 5 μ M Chromium (VI); Cr 10: 10 μ M Chromium (VI); DCF 0.5: 0.5 mg L⁻¹ Diclofenac; DCF 5: 5 mg L⁻¹ Diclofenac. Values presented are mean \pm SD. * and *** above bars indicate significant statistical differences from control at $p \leq 0.05$ and $p \leq 0.001$, respectively.

The qPCR analysis showed that shoots' *GS1.1* transcript levels (Figure 22) decreased with both Cr (VI) treatments by 2.0- and 1.5-fold, with the lowest and highest concentrations, respectively, while they only decreased with the lowest Cr (VI) concentration in roots (2.7-fold). Also, no differences were observed for the highest concentration of the contaminant. The 0.5 mg L⁻¹ DCF treatment altered *GS1.1* expression in an organ-specific manner: *GS1.1* transcript levels decreased 0.2-fold in shoots, while in roots, the expression of this gene increased 1.2-fold. The highest DCF concentration induced an up-regulation of the *GS1.1* gene expression by 0.6- and 3.7-fold in shoots and roots, respectively.

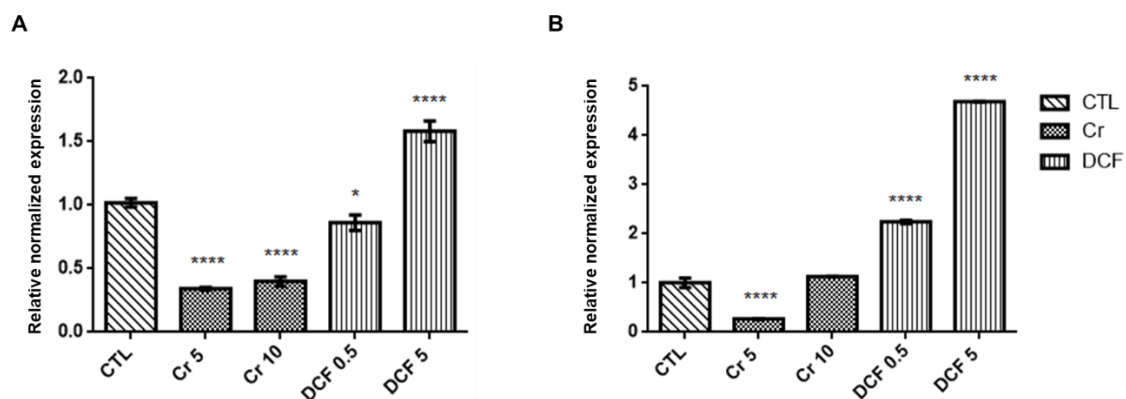


Figure 22. Expression profile of *GS1.1* gene in shoots (A) and roots (B), of tomato leaves exposed to Cr (VI) and DCF. CTL: Control; Cr 5: 5 μ M Chromium (VI); Cr 10: 10 μ M Chromium (VI); DCF 0.5: 0.5 mg L⁻¹ Diclofenac; DCF 5: 5 mg L⁻¹ Diclofenac. Values presented are mean \pm SD. * and **** above bars indicate significant statistical differences from control at $p \leq 0.05$ and $p \leq 0.0001$, respectively.

The continuous exposure to the higher levels of Cr (VI) stimulated the transcription of *SIGS1.3* in both organs. Curiously, the increasing Cr (VI) concentrations used seemed to stimulate the transcription of *SIGS1.2* in shoots, but in roots the expression of this gene was somewhat repressed, revealing that this gene presented a differential expression in shoots and roots in response to the Cr (VI) treatments (Figure 23).

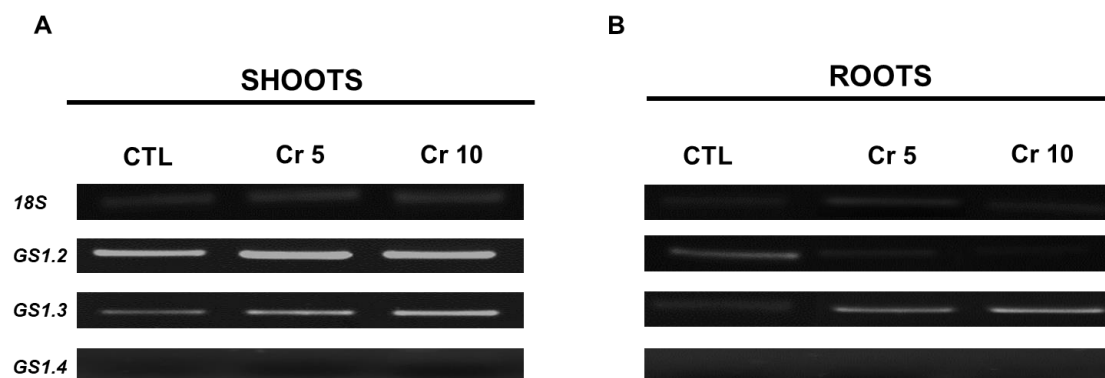


Figure 23. Typical results for *GS1.2*, *GS1.3* and *GS1.4* semi-quantitative RT-PCR analysis by 2 % (w/v) agarose gel electrophoresis in both shoots (A) and roots (B) of tomato plants exposed to increasing concentrations of Cr (VI); Expected sizes: 191 bp; 164 bp; 192 bp, respectively. CTL: Control; T1: 5 μ M Cr (VI); T2: 10 μ M Cr (VI).

Both DCF treatments stimulated the transcription of *SIGS1.2* in shoots, and *SIGS1.2* and 3 in roots. Indeed, *SIGS1.2* showed the highest expression in treated plants in both shoots and roots (Figure 24).

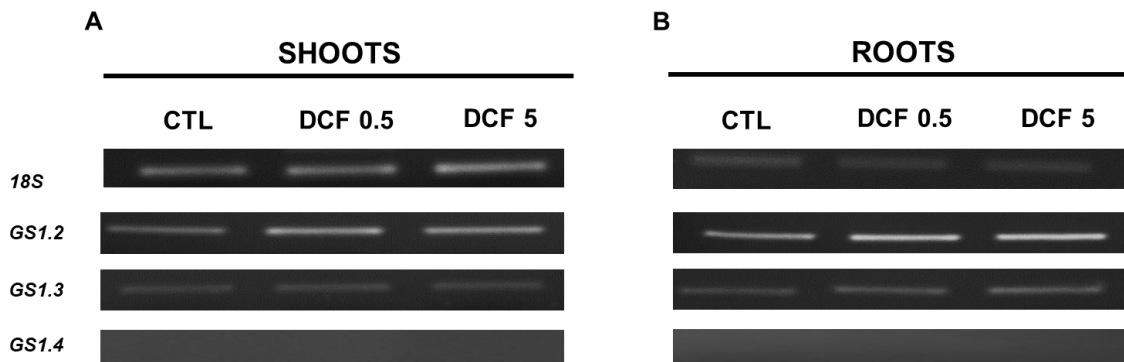


Figure 24. Typical results for *GS1.2*, *GS1.3* and *GS1.4* semi quantitative RT-PCR analysis by 2 % (w/v) agarose gel electrophoresis in both shoots (A) and roots (B) of tomato plants exposed to increasing concentrations of DCF; Expected sizes: 191 bp; 164 bp; 192 bp, respectively. CTL: Control; T1: 0.5 mg L⁻¹ DCF; T2: 5 mg L⁻¹ DCF.

S/GS1.4 presented no expression in shoots and roots, in all situations (CTL, Cr (VI)- and DCF-treated plants). The effects of Cr (VI) and DCF exposure on the transcript accumulation levels of the GS gene members are summarised in Table 9 (see discussion).

3.8 Cloning of the *S/GS2*-encoding cDNA

Before this procedure, the product size of the designed primers was checked, and the PCR conditions were optimized using gDNA as template to obtain the full *S/GS2* gene. A series of gradient PCR's were performed and the optimum annealing temperature was selected. Three annealing temperatures (54.7, 53.4 and 51 °C, respectively) were tested and the selected temperature for future amplifications was 53.4 °C (Figure 25).

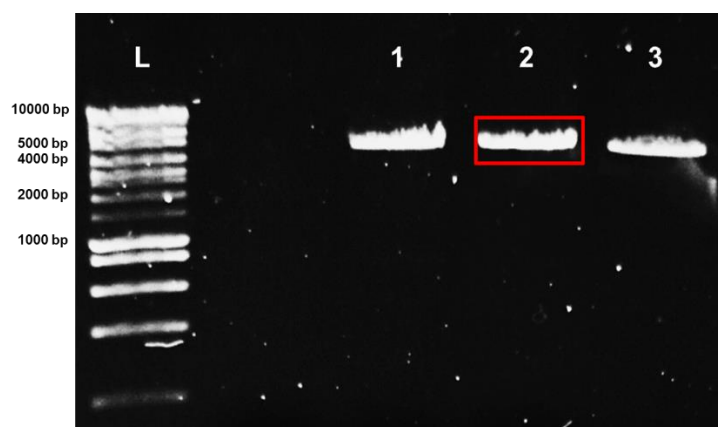


Figure 25. Agarose gel (0.8% (w/v)) electrophoresis evidencing the PCR products of *GS2* of *S. lycopersicum* when gDNA was used as template, using 54.7, 53.4 and 51 °C as annealing temperatures (lanes 1 to 3, respectively). The chosen temperature is highlighted. The ladder used was NZYDNA Ladder III (Nzytech®, Portugal).

Afterwards, the *S/GS2*-encoding cDNA was obtained and purified, and it was cloned into the pJET 1.2 vector. Then, the *E. coli* were transformed, and the putative positive (recombinant) colonies were screened for the presence of insert. To choose the

appropriated restriction enzymes, a virtual cut of the *SIGS2*-encoding cDNA was performed using the Serial Cloner tool (Figure 26).

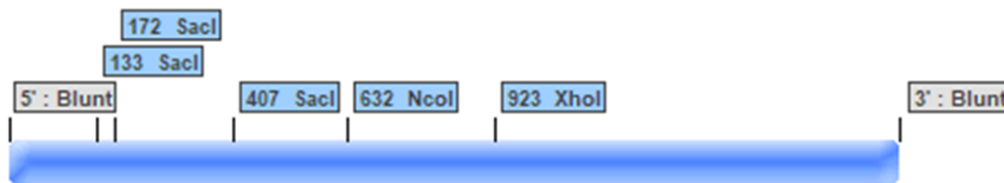


Figure 26. Schematic representation of the GS2 cDNA insert depicting the sites for the restriction enzymes *SacI*, *NcoI* and *XhoI*. The cDNA size is 1684 bp.

Through Figure 23, it can be observed three distinct recognition sites for *SacI* and one for both *NcoI* and *XhoI*.

After transformation, three distinct colonies (1, 2 and 3) were identified, the screening was conducted by simple restriction digestions for two restriction enzymes - *XhoI* and *NcoI*, and the results are shown in Figure 27.

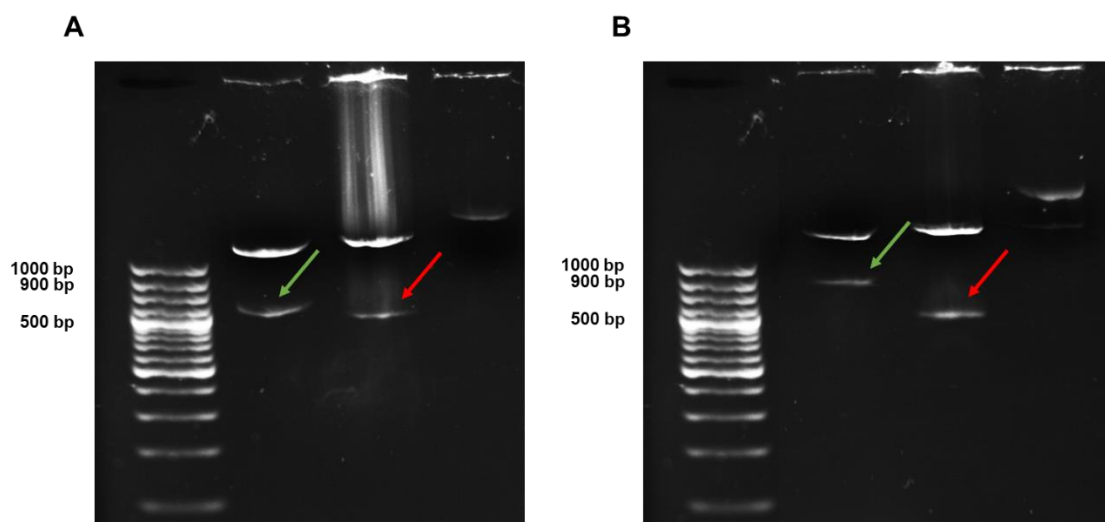


Figure 27. Agarose gel (0.8 % (w/v)) electrophoresis evidencing three distinct colonies digested with *XhoI* (A) and *NcoI* (B). The green and red arrows highlight the *SIGS2*-encoding cDNA in the sense and antisense orientations, respectively. 1, 2 and 3 represent the three distinct colonies. The ladder used was GeneRuler 100 bp Plus DNA ladder, ready-to-use (ThermoFisher Scientific).

Both *XhoI* and *NcoI* presented different fragment sizes, which had the expected sizes. The fragment size of colony 1 when restricted with *XhoI* was 932 bp and when restricted with *NcoI* was 1094 bp. Colony 2 presented a smaller size than colony 1, with both restriction enzymes. After that, a new restriction analysis was performed with *SacI* (Figure 28) in colonies 1 and 2.

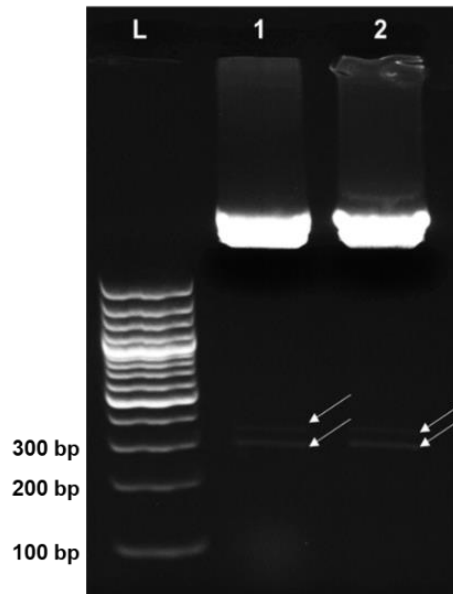


Figure 28. Agarose gel (0.8 % (w/v)) electrophoresis evidencing two distinct colonies digested with *SacI*. 1 and 2 represent colonies 1 and 2, respectively. The arrows evidence two bands resulting from the restriction. The used ladder was GeneRuler 100 bp Plus DNA ladder, ready-to-use (ThermoFisher Scientific).

It was possible to obtain equal banding patterns, composed of three bands for both colonies 1 and 2 (Lanes 1 and 2, respectively). The larger and brighter band was higher than 3,000 bp, as expected. The other two bands presented 235 bp and 274 bp, respectively.

4. Discussion

4.1 The accumulation of Cr occurs predominately in roots

In any study, the quantification of the contaminant (sometimes more than one) levels on plants' tissues is the first step to evaluate the phytotoxicity of these substances (Kummerová et al., 2016)

Tomato plants have the capacity to accumulate HMs, being Cr one of them (Jacob and Kakulu, 2012), and in many crops, this metal is more accumulated under the hexavalent form rather than in its trivalent state (Zayed et al., 1998). For these reasons, the content of Cr in tomato plants' organs was investigated. The amount of Cr was much higher in roots than in shoots, being as greater as the Cr (VI) concentration applied to the plants. Indeed, similar studies had proven that this metal is more accumulated in roots in various species, including tomato (Singh and Sinha, 2005). Cr preferential accumulation in roots is suggested as a strategy that plants possess to protect the aboveground parts from Cr-induced toxicity, particularly the photosynthetic apparatus in leaves (Brune et al., 1995). The low mobility of this metal to the aerial parts of plants also explains the low content of Cr in tomato plants' shoots. In fact, Cr has proven to be the least mobile HM from the roots to the shoots (Shukla et al., 2007).

Up to now, numerous studies have been conducted regarding DCF uptake and accumulation by plants (Bartha et al., 2014; Kummerová et al., 2016; García et al., 2018; Pierattini et al., 2018). The bibliography showed that this drug, similarly to HMs, tends to be more accumulated in roots and is poorly translocated to the aerial parts of the plants, due to DCF hydrophobicity. The time limitations and some technical issues hampered the determination of the DCF content in tomato plants' organs for this study. However, the quantification of DCF on tomato plants' shoots and roots will be further undertaken.

4.2 GS – from gene to protein

Given the importance of N for plant growth and development, coupled with the role of GS in N metabolism and in stress responses, the characterisation of this enzyme, either at the gene or at the protein level in tomato plants is an important issue.

The search for tomato GS-encoding genes identified 5 genes. Among that, one encoded the plastidic isozyme and the remaining encoded cytosolic isoenzymes. The results obtained in this work are in accordance with those observed by Liu et al. (2016). The results from the phylogenetic analysis suggest that the cytosolic and chloroplastic GS

isoenzymes form two separated groups, with *GS2* being the farthest *GS* gene of all *SIGS*s. Indeed, this separation happened before the monocots and dicots diverged, about 300 million years ago, and resulted from gene duplication followed by the alteration of regulatory regions within the promoters of duplicated genes (Biesiadka and Legocki, 1997).

Some of the results from the *in silico* analysis of *SIGS* expression are consistent with the ones obtained in this study from RT-PCR in shoots and roots of tomato plants grown under optimal conditions, while others are the opposite. For instance, the *SIG2* presented the highest values of expression in shoots, being this pattern confirmed by RT-PCR analysis. This result is no surprise since most of the physiological functions of the protein encoded by this gene remain in green organs (Swarbreck et al., 2010). Comparing the *in silico* analysis to those obtained by RT-PCR, the results for *SIGS1.1 - 3* are not consistent. Through the qPCR approach, Liu et al. (2016) reported that *SIGS1.2 and 3* showed higher expression in the shoots than in the roots, being these results in accordance to what was observed in this work (Figure 18; Table 9).

The same authors demonstrated that *SIGS1.1* had higher expression levels in roots than in shoots, contrary to what was found in this work. However, considering its highest expression in roots in the RT-PCR analysis when compared to the *SIGS1*-encoding genes, the *GS1.1* was considered the main *GS1* gene in this organ, in the present study.

From these results, the evaluation of the *SIGS* gene family expression was performed, using qPCR for the considered main *GS* genes in shoots and roots (*GS2* and *GS1.1*, respectively), due to its high sensitivity and specificity (Bustin et al., 2009), and a semi-quantitative RT-PCR was used for the remaining and less representative genes.

4.3 Cr (VI) and DCF differentially influenced N metabolism at gene expression, enzyme activity and polypeptide levels

It is well established that exposure to either HMs or PPCP's has negative effects on plant growth and development. Knowing the role of N on plant growth and productivity, two enzymes involved in N assimilation were studied in this work: glutamine synthetase, which is responsible to convert the produced/absorbed NH_4^+ into amino acids, and glutamate dehydrogenase, which is involved in the formation of glutamate under high NH_4^+ concentrations. Several authors reported the negative influence of HMs, particularly

Cr (VI), on N metabolism, however, the information about the effects of PPCP's like DCF on this metabolism remains scarce.

This study is the first depicting the effects of Cr (VI) and DCF exposure on the specific transcript accumulation levels for each tomato GS gene member. The gathered results from the accumulation of GS2 transcripts with the Cr (VI) treatments revealed that this gene presented a differential expression in shoots and in roots. The transcript levels of this gene tended to increase in shoots and significantly decreased in roots under 5 μ M Cr (VI) exposure. With the highest Cr (VI) concentration, the levels of the transcripts tended to decrease in shoots and remained constant in roots. Previously, a semi-quantitative RT-PCR for the *SIGS1.1* gene was conducted as well as for the corresponding negative controls. As no bands were detected in the negative controls (data not shown), no gDNA contamination of the RNA preparations was assumed. Therefore, this gene expression was assessed by qPCR without the negative controls. In this context, the cytosolic GS genes had different expression profiles in response to the exposure to both contaminants. Regarding *GS1.1*, its transcript levels decreased with both Cr (VI) treatments in shoots and had no changes in roots, despite the slight decrease observed in the lowest Cr (VI) concentration. Contrarily, both *SIGS1.2* and 3 showed an increase in their transcript accumulation in shoots with both Cr (VI) treatments. In roots the levels of *SIGS1.2* markedly decreased under Cr (VI) exposure, while the *SIGS1.3* expression in roots also increased with both treatments.

Overall, Cr (VI)-induced stress lead to a decrease in GS activity in shoots and in roots. Previous studies showed a relation between the decrease in the activity of this enzyme and oxidative modifications of GS proteins caused by HM-induced stress (Balestrasse et al., 2006). Moreover, the decrease in GS activity in shoots and in roots under Cr (VI) exposure was already reported by Gangwar and Singh (2011) and Kumar and Joshi (2008) in *Pisum sativum* and *Sorghum bicolor* plants, respectively. However, a positive response in shoots was evidenced with the lowest concentration of Cr (VI). This result is supported by the observed upregulation of the GS2 gene and the increase in the GS protein content in response to this concentration. Observing the performance of GS in the levels of transcription, activity and polypeptide, it is possible to state that 5 μ M Cr (VI) was not adverse to tomato shoot GS. Because Cr (VI) is preferentially accumulated in roots and poorly translocated to shoots (Lopez-Luna et al., 2009), the activity of GS on roots was negatively affected by this contaminant accumulation in these organ. The negative effects of Cr (VI) on this enzyme at the root level activity are supported by the transcript levels, since *GS1.1* and *GS1.2* genes expressions decreased in the roots of

the Cr (VI)-treated plants. The GS polypeptide content was barely detectable, thus corroborating the GS gene expressions and activity results.

The DCF exposure resulted in a strong decrease in GS2 transcript levels in shoots in both concentrations of this contaminant. In roots, despite no changes were observed for the highest concentration of DCF due to the high standard deviation, a down-regulation of GS2 transcript levels was observed with 0.5 mg L⁻¹ DCF. The lowest DCF concentration induced a differential and organ-specific expression of GS1.1, since the levels of transcript of this gene decreased in shoots and were up-regulated in roots. Additionally, a differential and organ-specific response was also observed for GS1.3 transcript accumulation in treated plants for both conditions: this gene had no changes in shoots but increased in roots. As observed with Cr (VI) treatments, GS1.2 transcript accumulation increased upon DCF exposure, in both organs. Curiously, a shift between GS2 and GS1.1 accumulation profiles with the DCF treatments for both organs was analysed: as GS2 transcript levels decrease, the GS1.1 mRNA suffer an increase in their accumulation.

Table 9. Summary of the effects of Cr (VI) and DCF exposure on the mRNA accumulation of the tomato GS-encoding genes. (=) means no changes, (-) means decreased accumulation and (+) means increased accumulation relative to the control. (x) means no mRNA accumulation.

GS gene	5 µM Cr (VI)	10 µM Cr (VI)	0.5 mg L ⁻¹ DCF	5 mg L ⁻¹ DCF	Organ
2	=	=	-	-	Shoots
	-	=	-	=	Roots
1.1	-	-	-	+	Shoots
	-	=	+	+	Roots
1.2	+	+	+	+	Shoots
	-	-	+	+	Roots
1.3	+	+	=	=	Shoots
	+	+	+	+	Roots
1.4	x	x	x	x	Both

Regarding DCF results, it was noticed that this contaminant negatively affected GS activity in shoots, in a concentration-dependent manner. The results observed for GS2 gene expression also confirmed that DCF strongly injured shoot GS activity. Yet, no differences were detected in GS polypeptide content in response to both concentrations. It was also observed that despite the increase of GS1.1 transcripts in shoots, it was not enough to prevent the decrease in total GS activity, implying that the activity of this enzyme in the aerial parts is mainly due to GS2. Similar results were obtained for *Solanum nigrum* L. shoots after the exposure to acetophenone, where a reduction in GS2-related transcripts was accompanied by increased GS1a- and GS1b-related

transcripts, although resulting in a decrease of shoot GS activity (Moreira et al., 2018). In roots, the lowest concentration of DCF increased the GS activity. This result agrees with the observed increase for *GS1.1* and *GS1.2* transcripts in roots from the 0.5 mg L⁻¹ DCF exposure. The xenobiotic acetophenone also led to an upregulation of the *GS1*-encoding genes in roots of *S. nigrum* L. plants, along with an increased root GS activity (Moreira et al., 2018). Interestingly, the highest concentration caused a decrease in the enzyme activity and the GS polypeptide content, contrary to what was found at *GS1.1* gene expression. Taking into account this particular result, two assumptions are possible to have occurred: 1) Despite 5 mg L⁻¹ did not impair *GS1.1* transcript accumulation, the translated protein possibly suffered post-translational modifications that affected the enzyme's activity. Indeed, some authors reported the regulation of GS activity by several possible post-translational modifications, including phosphorylation (Finnemann and Schjoerring, 2000; Man and Kaiser, 2001; Riedel et al., 2001; Lima et al., 2006); 2) It was discovered that DCF compromised the uptake of NO₃⁻ by decreasing the activity of NR in roots of *Medicago sativa* L. (Christou et al., 2016). Because the NR is the first enzyme involved on NO₃⁻ assimilation and being its activity impaired, it is expected that the activity of the following N-assimilatory enzymes decreases, including GS. Besides DCF, acetaminophen, another pharmaceutical, decreased both NR and GS activities in roots of *Hordeum vulgare* L. (Soares et al., 2018), thus supporting this hypothesis and corroborating the results observed for the GS activity in this work.

Any of these two assumptions (or both of them) is valid for these results. The root GS polypeptide content slightly decreased with both DCF concentrations, confirming the negative effects of this contaminant at the protein level. Furthermore, it was observed that the highest concentration of DCF was the most damaging for tomato GS. Additionally, the inconsistency of results between the GS activity and gene expression might be related to the existence of several GS forms that have non-redundant functions or accumulate at different tissues in different physiological conditions, thus the measurement of GS activity may mask isozyme-specific differences (James et al., 2018).

Contrary to what was observed for GS activity, the GDH activity increased with the exposure to both contaminants in both organs analysed. By observing the differences in the number of bands in shoots and roots in control and treated plants, it can be assumed that the major diversity of GDH isoenzymes is present in the non-green organs. In fact, Liu et al. (2016) found that roots were the preferential organ for the expression of two of the four *SIGDH* genes, when compared to the shoot GDH gene family expression.

In shoots of plants treated with both Cr (VI) concentrations and with 5 mg L⁻¹ DCF, a third band appeared, that did not exist in the control. The appearance of this band may indicate that this specific isoenzyme functions under stressful conditions, thus suggesting a role of GDH in response to abiotic stresses. However, the GDH polypeptide content detected by western blotting in this organ decreased with the increasing Cr (VI) concentrations. In roots, five bands were observed and, with Cr (VI) treatments, all of them increased their intensity in a concentration-dependent manner. The GDH polypeptide content in roots slightly decreased with the lowest Cr (VI) concentration but increased with 10 µM Cr (VI), accounting for the increased GDH activity registered. Yet, similar to what was observed in this study, previous other studies showed that under HM-induced stress, the activity of GDH increased in shoots and roots of triticale, rice and tomato plants (Chiraz et al., 2003; Jha and Dubey, 2004; Gajewska and Skłodowska, 2009). The increase in GDH activity was also observed under salinity by Kwinta and Cal (2005) and Purnell et al. (2005). Also, the 2nd, 3rd and 5th bands increased their intensity in DCF-treated plants, being the intensity as higher as the concentration of this contaminant. On the contrary, the GDH protein content did not change with the 0.5 mg L⁻¹ DCF but decreased under the highest concentration of DCF. By these reasons, it can be assumed that the increase in GDH activity under stress conditions is transversal to many types of abiotic stresses, thus explaining the kinetics of this enzyme under DCF exposure (Chiraz et al., 2003; Jha and Dubey, 2004; Kwinta and Cal, 2005; Purnell et al., 2005; Gajewska and Skłodowska, 2009).

Considering the GS and GDH activities towards Cr (VI) and DCF treatments, it is possible to affirm that due to the negative effects of both contaminants on GS activity, the reassimilation of ammonium is compromised, thus leading to an excess of the NH₄⁺ ions. This way, GDH represents an alternative pathway to perform the assimilation of these ions (El-Shora and Abo-Kassem, 2001).

4.4 Proline accumulation is positively affected by both contaminants

It is known that the amino acid proline plays various roles in plant responses to many types of biotic and abiotic stresses (Szepesi and Szöllősi, 2018).

The results in the present study showed that the lowest Cr (VI) concentration did not affect the accumulation of proline, whereas the treatment with 10 µM of Cr (VI) induced a great increase in aerial part. The accumulation of this amino acid in roots was induced by both Cr (VI) treatments. A relation between HM-induced stress and proline

accumulation was established many years ago (Saradhi, 1991). Indeed, several studies reported that plants exposure to different HMs, including Cr (VI), induced the proline accumulation (Bassi and Sharma, 1993; Gallardo et al., 1994; Rai et al., 2004; Singh and Sinha, 2005), thus supporting the results of this work. The proline functions under HM-induced stress are diversified and fundamental to mitigate the effects provoked by HMs on plants. This amino acid acts as an osmoprotectant, a HM chelator and it is also important to suppress reactive oxygen species (ROS). Moreover, the formation of phytochelatin, which is responsible for the chelation of HMs, is induced by proline (Farago and Mullen, 1979; de Knecht et al., 1994; Xu et al., 2009).

Concerning the DCF treatments, a similar pattern to that of Cr (VI) was observed for both shoots and roots: the lowest concentration did not alter the proline accumulation while a huge increase was observed for the 5 mg L⁻¹ DCF treatment. From these results, it can be assumed that under low DCF concentrations, tomato plants did not have the need to accumulate proline in both organs, suggesting that this concentration was not stressful for these plants. Soares et al. (2018) reported an increase in levels of proline towards acetaminophen exposure in shoots and in roots of *Hordeum vulgare* L. Furthermore, it was noticed that the plants exposure to acetophenone increased the proline levels in shoots and in roots of *Solanum nigrum* L. (Moreira et al., 2018). All these data support that the response of proline accumulation is transversal to distinct types of abiotic stresses. However, contrary to these results, the levels of proline were negatively influenced by DCF in *Medicago sativa* L in shoots and in roots (Christou et al., 2016). Such differences may derive from the amount of exposure to this contaminant, as well as plant species used.

4.4.1 GDH - An alternative pathway that allow proline accumulation under stressful conditions

Under stressful circumstances, the accumulation of proline by plants is highly dependent on the production of its main precursor, glutamate (Lutts et al., 1999). Indeed, when plants are exposed to unfavourable growth conditions, the main source of glutamate for proline production was thought to be the GS/GOGAT cycle in the phloem (Brugière et al., 1999). However, other studies demonstrated the importance of GDH as an alternative route to glutamate formation (Wang et al., 2007; Gajewska and Skłodowska, 2009). The data of the present study showed that the levels of proline increased under Cr (VI) and DCF exposure as well as GDH activity, while the GS activity decreased. This way, these findings suggest that, under Cr (VI)- and DCF-induced stresses, GDH represents an alternative and predominant pathway not only for NH₄⁺ re-assimilation, but also for

glutamate biosynthesis, providing glutamate for proline biosynthesis and accumulation (Figure 29).

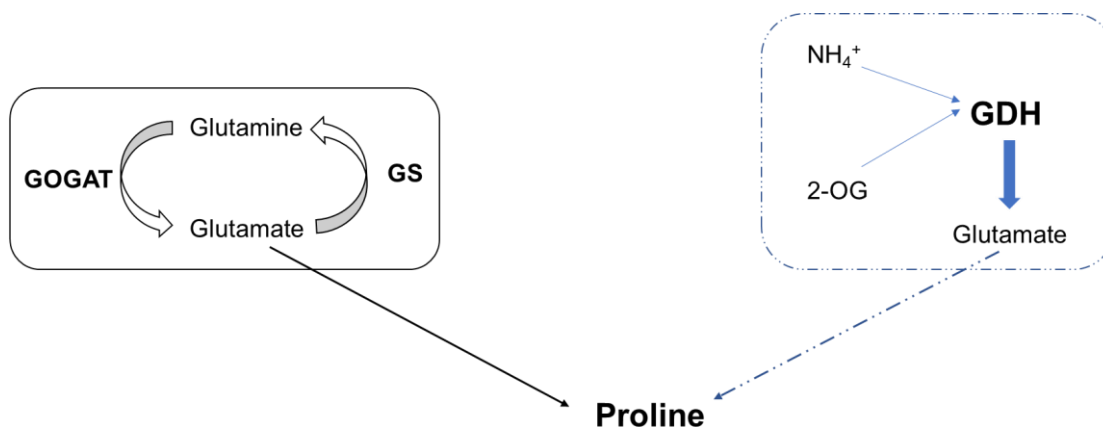


Figure 29. Two pathways that provide the glutamate for proline production and accumulation, under stressful conditions. The dashed arrow corresponds to the GDH pathway, which is an alternative route for amino acid's production, while the GS/GOGAT cycle corresponds to the principal pathway of glutamate, and thus, proline production.

4.5 The exposure of tomato plants to Cr (VI) and DCF did not impair photosynthetic activity

It is well-known that HMs induce negative effects on photosynthesis in many ways (Shahid et al., 2017) and the performed studies on the impact of pharmaceuticals on photosynthesis are not consensual regarding the possible effects these contaminants exert on this primary metabolism, either in plants or in algae (Michelini et al., 2013; Kummerová et al., 2016; Majewska et al., 2018; Pierattini et al., 2018). This study focused not only on the physiological effects of both Cr (VI) and DCF on several photosynthetic endpoints, but the genetic response of some photosynthetic-related genes was also investigated. Furthermore, the changes in starch content under both contaminants' exposure were histochemically visualized.

The chloroplast is the primary target of biotic and abiotic stresses. This way, the first indication of organelle damage is the decrease in pigments content (Mostowska, 1997). Contrary to what was expected, while no changes were observed in pigments content (both total chlorophylls and carotenoids) with the lowest Cr (VI) treatment, a positive influence was observed with 10 μM Cr (VI). Indeed, Cr, along with other HMs, can interfere with photosynthetic pigments biosynthesis by degrading the ALAD, that is the responsible enzyme for chlorophyll biosynthesis (Dey and Mondal, 2016) and by competing with Fe and Mg ions (Vernay et al., 2007). Furthermore, this metal can also replace the Mg ions

from their active sites in many enzymes, therefore emptying the chlorophyll content (Vajpayee et al., 2000). Although several studies reported negative effects of Cr (VI) in photosynthetic pigments, some authors observed a positive response under Cr (VI) exposure in different plant species. An increase in chlorophyll and carotenoids contents of mustard plants exposed to different Cr (VI) concentrations was observed by Pandey et al. (2005). Additionally, Dixit et al. (2002) reported an increase in chlorophylls a and b in *Pisum sativum* L. under Cr (VI)- induced stress. The generation of ROS, specifically oxygen radical and singlet oxygen, in response to Cr (VI) exposure during the illuminated period of the day, is prevented by carotenoids. In fact, the interaction of carotenoids with these ROS may prevent some damaging processes such as lipid peroxidation (Pandey et al., 2005). This way, this type of pigments plays an important role in chlorophyll protection, thus explaining the enhancement of carotenoids content detected in this study. Rodriguez et al. (2012) observed that pea plants exposed to Cr (VI) increased their Mg and Fe levels in shoots thereby suggesting that these increases influenced the rise in chlorophyll content, due to the crucial roles of Mg and Fe on chlorophyll biosynthesis. A similar conclusion can be assumed for the results observed in this study.

The negative influence of Cr on gas exchange parameters has been observed in several species (Vernay et al., 2007; Subrahmanyam, 2008; Rodriguez et al., 2012). Despite the increase in pigments content, some gas exchange parameters, such as A, WUE and Ci/Ca did not alter with Cr (VI) treatments. However, and curiously, all parameters, except for WUE, presented the same pattern under Cr (VI) exposure: it was observed a decrease under the lowest Cr (VI) concentration followed by an increase of these parameters with the highest Cr (VI) concentration. The significantly increase in stomatal conductance was accompanied by an increase in transpiration rate with the 10 μ M Cr (VI) treatment. These results are in accordance with the enhancement of pigments content, since an increase in leaf transpiration results in a rise in water loss and a decreased leaf water content. This way, the pigments concentration would increase as was observed.

PSII has been suggested to be the main target of Cr-induced stress on photosynthesis (Davies Jr et al., 2002). Therefore, it is important to study the impact of this HM in these photosystem genes. The transcript levels of the two PSII-encoding genes demonstrated the negative influence of this HM on PSII, except for *PSIIa* under the lowest Cr (VI) treatment. The impact of HMs on PSII is related to the inhibition of the photosynthetic carbon reduction cycle enzymes, changes in ATP levels or through the plastoquinone pool (Rai et al., 2016).

Carbon metabolism in both C₃ and C₄ plants photosynthesis is primarily catalysed by RuBisCO and phosphoenol-pyruvate carboxylase (PEPC; EC 4.1.1.31), which are considered the most sensitive targets of HM-induced stress (Rai et al., 2016). Despite the RuBisCO-encoding genes had been severely affected by Cr (VI), the lowest Cr (VI) concentration had a positive response on the RuBisCO content. A study performed in 2010 by Bah et al., found that the exposure of *Typha angustifolia* to Cr induced the expression of the RuBisCO's small unit. In this work, the increase in the content of this enzyme could be a strategy to protect plants against Cr-induced stress. On the other hand, the RuBisCO content was strongly repressed by the 10 µM Cr (VI) treatment. Similar injuries provoked by Cr (VI) on RuBisCO have also been reported by others (Dhir et al., 2009; Rodriguez et al., 2012). According to these authors, some metal ions, such as Cr may substitute the Mg²⁺ in the active site of RuBisCO subunits, thereby causing oxidative damages to this enzyme (Sinha et al., 2018). The low impact of Cr (VI) in photosynthetic activity can also be due to the low content of this metal on the aerial parts of tomato plants, since translocation root-to-shoot is, as already reported, very limited (Shukla et al., 2007).

Understanding the impact of Cr on the changes of the soluble sugars and starch accumulation is an essential task to better characterise the Cr-induced phytotoxicity (Sinha et al., 2018). Cr (VI)-induced stress was very pronounced on starch accumulation, where it highly decreased with both Cr (VI) treatments. Even when compared to the damages provoked by DCF treatments, Cr (VI) was much more severe. Similar results were found in *Phyllanthus amarus* (Rai and Mehrotra, 2008) and *Pisum sativum* L. (Tiwari et al., 2009) exposed to Cr (VI). It has been suggested that the decrease in starch content is due to the decrease in the photosynthetic rate under Cr (VI)-induced stress, which is in accordance with the results obtained in the present study.

The DCF treatments induced an increase in chlorophylls' contents and the lowest DCF concentration also had a positive effect on carotenoids content. The authors are not consensual concerning the effects of pharmaceuticals, including DCF, on these photosynthesis-related parameters, since some reported no differences in pigments content, while others showed that these contaminants affected the chlorophylls and carotenoids (Michelini et al., 2013; Kummerová et al., 2016; Pierattini et al., 2018; Soares et al., 2018). In some studies, it was noticed that while the chlorophyll content decreased, the carotenoid remained constant or vice-versa, indicating differences between the content within the pigment type (Carter et al., 2015; Di Baccio et al., 2017). The increase in carotenoids content under DCF exposure was also observed by Majewska et al.

(2018) using the model green algae *Chlamydomonas reinhardtii*, confirming once again the protective effect of this pigment towards chlorophylls under stress conditions. All the gas exchange parameters did not alter with the DCF exposure, despite the observed slight decrease in A and Gs with both DCF treatments. As the decrease of these parameters was not significant and in the absence of studies reporting the effects of this drug on the photosynthetic apparatus, it can be assumed that, at least with these concentrations used in the present work, DCF did not impair the photosynthetic activity. Moreover, at the gene level, the encoding genes for PSII increased their levels in a concentration-dependent manner, thus supporting this theory. In fact, no differences on the photosynthetic apparatus were observed in *Lemna gibba* plants treated with ibuprofen, another NSAID that is commonly detected in surface waters (Di Baccio et al., 2017). However, the RuBisCO enzyme was particularly damaged by DCF both at the gene and polypeptide content levels, thus contributing for a decrease in starch accumulation, an effect that was more evident with the highest DCF concentration used.

4.6 Both Cr (VI) and DCF induced changes in soluble polypeptide content and profile

The content of soluble proteins was strongly repressed by Cr (VI) treatments in shoots of tomato plants, being this effect more pronounced with the 10 μ M Cr (VI) concentration. Yet, two bands appeared only in shoots of Cr (VI)-treated plants. In roots, distinct results were observed: an increase and a decrease in some bands intensity; a total suppression of three bands, and an appearance of one band. A relation between HMs and the induction of a variety of low-molecular weight protein metallochaperones or chelators such as heat-shock proteins was previously established (Emamverdian et al., 2015). This way, the increasing low molecular weight polypeptides observed in this study might be one of these proteins.

The effects of DCF on polypeptide content both in shoot and roots were less severe than those provoked by Cr (VI). Indeed, in shoots, only one band was repressed and two bands, being one of them the RuBisCO, decreased their intensity. Interestingly, both Cr (VI) and DCF treatments decreased the intensity of a band with the same size (250 kDa). In the future, a proteomic approach could shed some light on this issue by attempting to uncover the identity of this polypeptide.

In roots, the impact of DCF on polypeptide content was, overall, positive. The appearance of some polypeptides that were not shown in control plants was due to DCF exposure, and it was also detected the increase in other polypeptides' intensities. These

bands may correspond to stress-related proteins, thus increasing their intensity towards DCF-exposure, particularly that with 22 kDa, whose intensity was higher with the increase in DCF concentration. However, the polypeptide that presented the lowest size decreased its intensity with DCF treatments.

4.7 Development of new tools that will allow the overexpression of *S/GS2*-encoding cDNA

The importance of GS in crucial features of NUE and yield in crops, as well as its potential application for sustainable agriculture, was already evidenced in different plants through genetic, molecular and physiological approaches. Indeed, the authors that attempted to modulate the *in planta* levels of the GS enzymes were based on two premises: i) improving GS activity should increase N uptake, therefore increasing plants growth; ii) enhancing GS activity should be crucial for the remobilization of N from vegetative parts to the seeds, during senescence or under low N conditions (Fuentes et al., 2001; Habash et al., 2001; Thomsen et al., 2014; James et al., 2018). Bearing this in mind, one of the objectives of this work was to overexpress the *S/GS2*-encoding cDNA in an attempt to increase GS2 activity, and, therefore, increase the plants' tolerance to stress. So far, this is the first study reporting the overexpression of a GS gene in tomato plants. However, due to time constrictions, this work only reports the final steps of the procedure that led to the cloning of the GS2-encoding cDNA into pJET.

To obtain the highest amount of insert, an optimal annealing temperature was first chosen. According to Figure 22, all the three bands had the expected size. Yet, the band that had the best appearance was the one obtained when the annealing temperature corresponded to 53.4 °C, and therefore, this was the temperature selected to amplify the GS2-encoding cDNA.

Considering bacteria transformation, two approaches were conducted: the electro transformation and the heat-shock transformation. Due to the lack of positive colonies with the electro transformation, this technique was discarded, and the work continued with the heat-shock transformation, where three positive colonies were obtained.

Confronting the results obtained with the restriction enzyme analysis performed with those obtained with the *in silico* visualization for the *NcoI*, *SacI* and *XhoI* restriction sites, it is correct to state that at least minipreps 1 and 2 (Figures 23 and 24) contained the GS2 cDNA (see below). The band that resulted from the restriction of miniprep 3, as each enzyme had a size well over 3,000 bp, indicates that the plasmid had an insert, since the size of the pJET plasmid is 2,974 bp. However, the insert did not correspond

to the GS2 cDNA because no additional bands were observed, as it was expected to occur when using either of these enzymes. Consequently, this miniprep was eliminated from the following procedures.

Regarding colonies 1 and 2, the obtained bands after restriction are according to the virtually supposed. Since both *NcoI* and *XhoI* cut the insert and vector once, two bands in each lane were expected. The different sizes of the bands from miniprep 1 to miniprep 2, obtained with each enzyme, can be interpreted by each having the same insert, but in opposite orientations.

Due to the lack of recognition sites from *SacI* in the vector, and the fact that the insert had three of these sites, the recombinant plasmids were cut in three pieces: 2 from the GS2 cDNA and another bearing the rest of the cDNA plus the pJET vector (Figure 25). As the smaller piece (39 bp) is too small, it did not appear in the gel. The other band that derived from the DNA insert should have 235 bp. However, in this gel two bands appeared around that size instead of one. Such can be explained by an incomplete restriction: considering the larger (fainter) band, *SacI* only cut twice and so the 39 bp band was not excised, creating a band with 274 bp ($235 + 39 = 274$ bp). The largest and brightest band contains the rest of the insert, as well as the pJET vector. Because all these restriction patterns are in accordance to what was virtually expected, these results proved that the GS2 cDNA-encoding sequence was cloned successfully into pJET, and that colonies 1 and 2 possess the insert in the sense and anti-sense orientations, respectively. Furthermore, the existence of two recombinant plasmids bearing opposite orientations of the insert is profitable because it increases the restriction enzyme combinations possible to be used in downstream subcloning procedures, aimed at producing the gene construction to be delivered into the tomato plant genome in the future.

5. Concluding remarks

From the collected results by this work, the following conclusions were acquired:

- The exposure to Cr (VI) and DCF imposed some physiological challenges to tomato plants, with Cr (VI) being more damaging than DCF;
- Cr (VI) content was higher in roots than in shoots, revealing a protective role for roots;
- Both contaminants affected the GS gene expression, activity and polypeptide levels:
 - The coordinated decrease in the levels of GS genes' transcripts, activity and polypeptide content in response to Cr (VI) reflects a common down-regulation mechanism.
 - DCF induced some posttranslational changes in GS enzymes.
- The increased GDH activity in response to both contaminants evidences an alternative route that tomato plants used to overcome the Cr (VI)- and DCF-induced injuries in the N assimilatory metabolism;
- A positive correlation between proline accumulation and GDH activity suggest the involvement of this enzyme in an alternative pathway for providing glutamate for proline biosynthesis;
- The increase in proline levels, along with the *de novo* appearance of distinct polypeptides indicate that tomato plants triggered several defence mechanisms to overcome Cr (VI) and DCF phytotoxicity;
- Despite transcript levels of photosynthetic-related genes were altered, the photosynthetic activity was not greatly affected either by Cr (VI) or DCF;
- The *SGS2*-encoding cDNA was cloned in opposite orientations, which is quite promising since it will facilitate the ensuing procedures to overexpress this cDNA.

6. Future Perspectives

This work provided important insights on the influence of Cr (VI) and DCF in tomato plants' physiology, particularly on the primary N and C metabolisms. Actually, up to now, this work presents the first report on the influence of DCF on the primary metabolism of tomato plants. Also, results presented in this dissertation constitute the first step to achieve the first tomato plants overexpressing the *SIGS2*-encoding cDNA. In the future, it is important to fulfil the gaps of this work by performing the following:

- Quantification of DCF levels in the nutrient solution and in shoots and roots of tomato plants and quantify both Cr (VI) and DCF contents in tomato fruits, since these are the edible parts of the plant as it will provide a better understanding of the impact of these contaminants on human health;
- Evaluation of several photosynthetic-related endpoints, such as chlorophyll fluorescence analysis, to better understand the effects of both contaminants on the photosynthesis light-dependent reactions;
- Study the expression profile of *SIGS1.4* gene across different plant organs other than those analysed in this study to verify whether this is really a pseudo-gene;
- Investigate possible changes in GDH gene expression in response to Cr (VI) and DCF exposure, to reinforce the hypothesis of this enzyme being an alternative role for NH_4^+ assimilation and proline accumulation;
- Overexpress tomato plants with *SIGS2* increased (abiotic) stress tolerance. This would be complemented with biometric data and Cr (VI)- and DCF-induced stress response analysis as presented in this work, to evaluate tolerance and fitness of such genetically modified plants.

7. References

- Ahmed F, Hossain M, Abdullah AT, Akbor M, Ahsan M** (2016) Public health risk assessment of chromium intake from vegetable grown in the wastewater irrigated site in Bangladesh. *Pollution* **2**: 425-432
- Al-Farsi RS, Ahmed M, Al-Busaidi A, Choudri B** (2018) Translocation of pharmaceuticals and personal care products (PPCPs) into plant tissues: A review. *Emerging Contaminants*
- Aoki K, Yano K, Suzuki A, Kawamura S, Sakurai N, Suda K, Kurabayashi A, Suzuki T, Tsugane T, Watanabe M** (2010) Large-scale analysis of full-length cDNAs from the tomato (*Solanum lycopersicum*) cultivar Micro-Tom, a reference system for the Solanaceae genomics. *BMC genomics* **11**: 210
- Ashraf A, Bibi I, Niazi NK, Ok YS, Murtaza G, Shahid M, Kunhikrishnan A, Li D, Mahmood T** (2017) Chromium (VI) sorption efficiency of acid-activated banana peel over organo-montmorillonite in aqueous solutions. *International journal of phytoremediation* **19**: 605-613
- aus der Beek T, Weber FA, Bergmann A, Hickmann S, Ebert I, Hein A, Küster A** (2016) Pharmaceuticals in the environment—Global occurrences and perspectives. *Environmental toxicology and chemistry* **35**: 823-835
- Bah AM, Sun H, Chen F, Zhou J, Dai H, Zhang G, Wu F** (2010) Comparative proteomic analysis of *Typha angustifolia* leaf under chromium, cadmium and lead stress. *Journal of Hazardous Materials* **184**: 191-203
- Balakrishna K, Rath A, Praveenkumarreddy Y, Guruge KS, Subedi B** (2017) A review of the occurrence of pharmaceuticals and personal care products in Indian water bodies. *Ecotoxicology and environmental safety* **137**: 113-120
- Balestrasse K, Gallego S, Tomaro M** (2006) Oxidation of the enzymes involved in nitrogen assimilation plays an important role in the cadmium-induced toxicity in soybean plants. *Plant and soil* **284**: 187-194
- Bartha B, Huber C, Schröder P** (2014) Uptake and metabolism of diclofenac in *Typha latifolia*—How plants cope with human pharmaceutical pollution. *Plant Science* **227**: 12-20
- Bartrons M, Peñuelas J** (2017) Pharmaceuticals and personal-care products in plants. *Trends in plant science* **22**: 194-203
- Bassi R, Sharma SS** (1993) Proline accumulation in wheat seedlings exposed to zinc and copper. *Phytochemistry* **33**: 1339-1342
- Bates L, Waldren R, Teare I** (1973) Rapid determination of free proline for water-stress studies. *Plant and soil* **39**: 205-207

- Benotti MJ, Trenholm RA, Vanderford BJ, Holady JC, Stanford BD, Snyder SA** (2008) Pharmaceuticals and endocrine disrupting compounds in US drinking water. *Environmental science & technology* **43**: 597-603
- Bergougnoux V** (2014) The history of tomato: from domestication to biopharming. *Biotechnology advances* **32**: 170-189
- Bernard SM, Habash DZ** (2009) The importance of cytosolic glutamine synthetase in nitrogen assimilation and recycling. *New Phytologist* **182**: 608-620
- Biesiadka J, Legocki AB** (1997) Evolution of the glutamine synthetase gene in plants. *Plant Science* **128**: 51-58
- Bradford MM** (1976) A rapid and sensitive method for the quantitation of microgram quantities of protein utilizing the principle of protein-dye binding. *Analytical biochemistry* **72**: 248-254
- Brauer EK, Shelp BJ** (2010) Nitrogen use efficiency: re-consideration of the bioengineering approach. *Botany* **88**: 103-109
- Broadway A, Cave MR, Wragg J, Fordyce FM, Bewley RJ, Graham MC, Ngwenya BT, Farmer JG** (2010) Determination of the bioaccessibility of chromium in Glasgow soil and the implications for human health risk assessment. *Science of the total environment* **409**: 267-277
- Brugière N, Dubois F, Limami AM, Lelandais M, Roux Y, Sangwan RS, Hirel B** (1999) Glutamine synthetase in the phloem plays a major role in controlling proline production. *The Plant Cell* **11**: 1995-2011
- Brune A, Urbach W, Dietz K-J** (1995) Differential toxicity of heavy metals is partly related to a loss of preferential extraplasmic compartmentation: a comparison of Cd-, Mo-, Ni- and Zn-stress. *New Phytologist* **129**: 403-409
- Burakov AE, Galunin EV, Burakova IV, Kucherova AE, Agarwal S, Tkachev AG, Gupta VK** (2018) Adsorption of heavy metals on conventional and nanostructured materials for wastewater treatment purposes: A review. *Ecotoxicology and environmental safety* **148**: 702-712
- Buser H-R, Poiger T, Müller MD** (1998) Occurrence and fate of the pharmaceutical drug diclofenac in surface waters: rapid photodegradation in a lake. *Environmental Science & Technology* **32**: 3449-3456
- Bustin SA, Benes V, Garson JA, Hellemans J, Huggett J, Kubista M, Mueller R, Nolan T, Pfaffl MW, Shipley GL** (2009) The MIQE guidelines: minimum information for publication of quantitative real-time PCR experiments. *Clinical chemistry* **55**: 611-622

- Campos ML, Carvalho RF, Benedito VA, Peres LEP** (2010) Small and remarkable: the Micro-Tom model system as a tool to discover novel hormonal functions and interactions. *Plant signaling & behavior* **5**: 267-270
- Cancer IAfRo** (1987) Overall evaluations of carcinogenicity: an updating of IARC Monographs volumes 1 to 42. *IARC Monogr Eval Carcinog Risks Hum Suppl* **7**: 1-440
- Canton FR, Garcia-Gutierrez A, Crespillo R, Cánovas FM** (1996) High-level expression of *Pinus sylvestris* glutamine synthetase in *Escherichia coli*. *FEBS letters* **393**: 205-210
- Carter LJ, Williams M, Böttcher C, Kookana RS** (2015) Uptake of pharmaceuticals influences plant development and affects nutrient and hormone homeostases. *Environmental science & technology* **49**: 12509-12518
- Chapman PM** (2007) Determining when contamination is pollution—weight of evidence determinations for sediments and effluents. *Environment International* **33**: 492-501
- Chiraz C, Houda G, Habib GM** (2003) Nitrogen metabolism in tomato plants under cadmium stress. *Journal of plant nutrition* **26**: 1617-1634
- Christou A, Agüera A, Bayona JM, Cytryn E, Fotopoulos V, Lambropoulou D, Manaia CM, Michael C, Revitt M, Schröder P** (2017) The potential implications of reclaimed wastewater reuse for irrigation on the agricultural environment: The knowns and unknowns of the fate of antibiotics and antibiotic resistant bacteria and resistance genes—A review. *Water research* **123**: 448-467
- Christou A, Antoniou C, Christodoulou C, Hapeshi E, Stavrou I, Michael C, Fatta-Kassinou D, Fotopoulos V** (2016) Stress-related phenomena and detoxification mechanisms induced by common pharmaceuticals in alfalfa (*Medicago sativa* L.) plants. *Science of the Total Environment* **557**: 652-664
- Cren M, Hirel B** (1999) Glutamine synthetase in higher plants regulation of gene and protein expression from the organ to the cell. *Plant and Cell Physiology* **40**: 1187-1193
- Cristaldi A, Conti GO, Jho EH, Zuccarello P, Grasso A, Copat C, Ferrante M** (2017) Phytoremediation of contaminated soils by heavy metals and PAHs. A brief review. *Environmental Technology & Innovation* **8**: 309-326
- Cullimore JV, Sims AP** (1980) An association between photorespiration and protein catabolism: studies with *Chlamydomonas*. *Planta* **150**: 392-396
- Davies Jr F, Puryear J, Newton R, Egilla J, Saraiva Grossi J** (2002) Mycorrhizal fungi increase chromium uptake by sunflower plants: influence on tissue mineral

- concentration, growth, and gas exchange. *Journal of Plant Nutrition* **25**: 2389-2407
- Davies NM, Anderson KE** (1997) Clinical pharmacokinetics of diclofenac. *Clinical pharmacokinetics* **33**: 184-213
- de Knecht JA, van Dillen M, Koevoets PL, Schat H, Verkleij JA, Ernst WH** (1994) Phytochelatins in cadmium-sensitive and cadmium-tolerant *Silene vulgaris* (chain length distribution and sulfide incorporation). *Plant Physiology* **104**: 255-261
- de Oliveira LM, Gress J, De J, Rathinasabapathi B, Marchi G, Chen Y, Ma LQ** (2016) Sulfate and chromate increased each other's uptake and translocation in As-hyperaccumulator *Pteris vittata*. *Chemosphere* **147**: 36-43
- de Oliveira LM, Ma LQ, Santos JA, Guilherme LR, Lessl JT** (2014) Effects of arsenate, chromate, and sulfate on arsenic and chromium uptake and translocation by arsenic hyperaccumulator *Pteris vittata* L. *Environmental pollution* **184**: 187-192
- Dey U, Mondal NK** (2016) Ultrastructural deformation of plant cell under heavy metal stress in Gram seedlings. *Cogent Environmental Science* **2**: 1196472
- Dhir B, Sharmila P, Saradhi PP, Nasim SA** (2009) Physiological and antioxidant responses of *Salvinia natans* exposed to chromium-rich wastewater. *Ecotoxicology and Environmental Safety* **72**: 1790-1797
- Di Baccio D, Pietrini F, Bertolotto P, Pérez S, Barcelò D, Zacchini M, Donati E** (2017) Response of *Lemna gibba* L. to high and environmentally relevant concentrations of ibuprofen: Removal, metabolism and morpho-physiological traits for biomonitoring of emerging contaminants. *Science of The Total Environment* **584**: 363-373
- Díaz P, Betti M, Sánchez DH, Udvardi MK, Monza J, Márquez AJ** (2010) Deficiency in plastidic glutamine synthetase alters proline metabolism and transcriptomic response in *Lotus japonicus* under drought stress. *New Phytologist* **188**: 1001-1013
- Dixit V, Pandey V, Shyam R** (2002) Chromium ions inactivate electron transport and enhance superoxide generation in vivo in pea (*Pisum sativum* L. cv. Azad) root mitochondria. *Plant, Cell & Environment* **25**: 687-693
- Doskočilová A, Plíhal O, Volc J, Chumová J, Kourová H, Halada P, Petrovská B, Binarová P** (2011) A nodulin/glutamine synthetase-like fusion protein is implicated in the regulation of root morphogenesis and in signalling triggered by flagellin. *Planta* **234**: 459-476
- Dubey S, Rai L** (1987) Effect of chromium and tin on survival, growth, carbon fixation, heterocyst differentiation, nitrogenase, nitrate reductase and glutamine

- synthetase activities of *Anabaena doliolum*. Journal of plant physiology **130**: 165-172
- Dubois F, Tercé-Laforgue T, Gonzalez-Moro M-B, Estavillo J-M, Sangwan R, Gallais A, Hirel B** (2003) Glutamate dehydrogenase in plants: is there a new story for an old enzyme? Plant Physiology and Biochemistry **41**: 565-576
- Eggen T, Asp TN, Grave K, Hormazabal V** (2011) Uptake and translocation of metformin, ciprofloxacin and narasin in forage-and crop plants. Chemosphere **85**: 26-33
- El-Shora H, Abo-Kassem E** (2001) Kinetic characterization of glutamate dehydrogenase of marrow cotyledons. Plant Science **161**: 1047-1053
- Emamverdian A, Ding Y, Mokhberdoran F, Xie Y** (2015) Heavy metal stress and some mechanisms of plant defense response. The Scientific World Journal **2015**
- Food and Agriculture Organization of the United Nations, 2014**. FAOSTAT Statistics Database. FAOSTAT, 2014. www.faostat.org.
- Farago M, Mullen W** (1979) Plants which accumulate metals. Part IV. A possible copper-proline complex from the roots of *Armeria maritima*. Inorganica Chimica Acta **32**: L93-L94
- Fatta-Kassinos D, Meric S, Nikolaou A** (2011) Pharmaceutical residues in environmental waters and wastewater: current state of knowledge and future research. Analytical and bioanalytical chemistry **399**: 251-275
- Feito R, Valcárcel Y, Catalá M** (2012) Biomarker assessment of toxicity with miniaturised bioassays: diclofenac as a case study. Ecotoxicology **21**: 289-296
- Ferraro G, Bortolotti S, Mortera P, Schlereth A, Stitt M, Carrari F, Kamenetzky L, Valle EM** (2012) Novel glutamate dehydrogenase genes show increased transcript and protein abundances in mature tomato fruits. Journal of plant physiology **169**: 899-907
- Finnemann J, Schjoerring JK** (2000) Post-translational regulation of cytosolic glutamine synthetase by reversible phosphorylation and 14-3-3 protein interaction. The Plant Journal **24**: 171-181
- Fontaine J-X, Tercé-Laforgue T, Armengaud P, Clément G, Renou J-P, Pelletier S, Catterou M, Azzopardi M, Gibon Y, Lea PJ** (2012) Characterization of a NADH-dependent glutamate dehydrogenase mutant of Arabidopsis demonstrates the key role of this enzyme in root carbon and nitrogen metabolism. The Plant Cell: tpc. 112.103689
- Forde BG, Lea PJ** (2007) Glutamate in plants: metabolism, regulation, and signalling. Journal of experimental botany **58**: 2339-2358

- Fu Q, Ye Q, Zhang J, Richards J, Borchardt D, Gan J** (2017) Diclofenac in Arabidopsis cells: Rapid formation of conjugates. *Environmental pollution* **222**: 383-392
- Fuentes SI, Allen DJ, Ortiz-Lopez A, Hernández G** (2001) Over-expression of cytosolic glutamine synthetase increases photosynthesis and growth at low nitrogen concentrations. *Journal of Experimental Botany* **52**: 1071-1081
- Gajewska E, Skłodowska M** (2009) Nickel-induced changes in nitrogen metabolism in wheat shoots. *Journal of plant physiology* **166**: 1034-1044
- Gallardo F, Fu J, Cantón FR, García-Gutiérrez A, Cánovas FM, Kirby EG** (1999) Expression of a conifer glutamine synthetase gene in transgenic poplar. *Planta* **210**: 19-26
- Gallardo M, Turner N, Ludwig C** (1994) Water relations, gas exchange and abscisic acid content of *Lupinus cosentinii* leaves in response to drying different proportions of the root system. *Journal of Experimental Botany* **45**: 909-918
- Ganesh KS, Baskaran L, Rajasekaran S, Sumathi K, Chidambaram A, Sundaramoorthy P** (2008) Chromium stress induced alterations in biochemical and enzyme metabolism in aquatic and terrestrial plants. *Colloids and Surfaces B: Biointerfaces* **63**: 159-163
- Gangwar S, Singh VP** (2011) Indole acetic acid differently changes growth and nitrogen metabolism in *Pisum sativum* L. seedlings under chromium (VI) phytotoxicity: implication of oxidative stress. *Scientia horticultrae* **129**: 321-328
- García MG, Fernández-López C, Pedrero-Salcedo F, Alarcón JJ** (2018) Absorption of carbamazepine and diclofenac in hydroponically cultivated lettuces and human health risk assessment. *Agricultural Water Management* **206**: 42-47
- Gardea-Torresdey J, Peralta-Videa J, Montes M, De la Rosa G, Corral-Diaz B** (2004) Bioaccumulation of cadmium, chromium and copper by *Convolvulus arvensis* L.: impact on plant growth and uptake of nutritional elements. *Bioresource technology* **92**: 229-235
- Gerszberg A, Hnatuszko-Konka K** (2017) Tomato tolerance to abiotic stress: a review of most often engineered target sequences. *Plant Growth Regulation* **83**: 175-198
- González-Naranjo V, Boltes K, de Bustamante I, Palacios-Diaz P** (2015) Environmental risk of combined emerging pollutants in terrestrial environments: chlorophyll a fluorescence analysis. *Environmental Science and Pollution Research* **22**: 6920-6931
- Gorito AM, Ribeiro AR, Almeida CMR, Silva AM** (2017) A review on the application of constructed wetlands for the removal of priority substances and contaminants of

emerging concern listed in recently launched EU legislation. Environmental pollution **227**: 428-443

Habash D, Massiah A, Rong H, Wallsgrove R, Leigh R (2001) The role of cytosolic glutamine synthetase in wheat. *Annals of Applied Biology* **138**: 83-89

Hare P, Cress W (1997) Metabolic implications of stress-induced proline accumulation in plants. *Plant growth regulation* **21**: 79-102

He B-s, Wang J, Liu J, Hu X-m (2017) Eco-pharmacovigilance of non-steroidal anti-inflammatory drugs: Necessity and opportunities. *Chemosphere* **181**: 178-189

Hellmann H, Funck D, Rentsch D, Frommer WB (2000) Hypersensitivity of an Arabidopsis sugar signaling mutant toward exogenous proline application. *Plant Physiology* **122**: 357-368

Hillis DG, Fletcher J, Solomon KR, Sibley PK (2011) Effects of ten antibiotics on seed germination and root elongation in three plant species. *Archives of environmental contamination and toxicology* **60**: 220-232

Hodges M (2002) Enzyme redundancy and the importance of 2-oxoglutarate in plant ammonium assimilation. *Journal of Experimental Botany* **53**: 905-916

Hoffman BM, Lukoyanov D, Yang Z-Y, Dean DR, Seefeldt LC (2014) Mechanism of nitrogen fixation by nitrogenase: the next stage. *Chemical reviews* **114**: 4041-4062

Hoshida H, Tanaka Y, Hibino T, Hayashi Y, Tanaka A, Takabe T, Takabe T (2000) Enhanced tolerance to salt stress in transgenic rice that overexpresses chloroplast glutamine synthetase. *Plant molecular biology* **43**: 103-111

Huber C, Bartha B, Schröder P (2012) Metabolism of diclofenac in plants—Hydroxylation is followed by glucose conjugation. *Journal of hazardous materials* **243**: 250-256

Huber C, Preis M, Harvey PJ, Grosse S, Letzel T, Schröder P (2016) Emerging pollutants and plants—Metabolic activation of diclofenac by peroxidases. *Chemosphere* **146**: 435-441

Jacob JO, Kakulu SE (2012) Assessment of heavy metal bioaccumulation in spinach, jute mallow and tomato in farms within Kaduna Metropolis, Nigeria. *American Journal of Chemistry* **2**: 13-16

James D, Borphukan B, Fartyal D, Achary V, Reddy M (2018) Transgenic Manipulation of Glutamine Synthetase: A Target with Untapped Potential in Various Aspects of Crop Improvement. *In Biotechnologies of Crop Improvement*, Volume 2. Springer, pp 367-416

- Jha AB, Dubey RS** (2004) Arsenic exposure alters activity behaviour of key nitrogen assimilatory enzymes in growing rice plants. *Plant growth regulation* **43**: 259-268
- Kim SD, Cho J, Kim IS, Vanderford BJ, Snyder SA** (2007) Occurrence and removal of pharmaceuticals and endocrine disruptors in South Korean surface, drinking, and waste waters. *Water research* **41**: 1013-1021
- Kumada Y, Benson D, Hillemann D, Hosted T, Rochefort D, Thompson C, Wohlleben W, Tateno Y** (1993) Evolution of the glutamine synthetase gene, one of the oldest existing and functioning genes. *Proceedings of the National Academy of Sciences* **90**: 3009-3013
- Kumar M, Puri A** (2012) A review of permissible limits of drinking water. *Indian journal of occupational and environmental medicine* **16**: 40
- Kumar S, Joshi U** (2008) Nitrogen metabolism as affected by hexavalent chromium in sorghum (*Sorghum bicolor* L.). *Environmental and Experimental Botany* **64**: 135-144
- Kumar S, Stecher G, Tamura K** (2016) MEGA7: molecular evolutionary genetics analysis version 7.0 for bigger datasets. *Molecular biology and evolution* **33**: 1870-1874
- Kummerová M, Zezulka Š, Babula P, Tříška J** (2016) Possible ecological risk of two pharmaceuticals diclofenac and paracetamol demonstrated on a model plant *Lemna minor*. *Journal of hazardous materials* **302**: 351-361
- Kwinta J, Cal K** (2005) Effects of Salinity Stress on the Activity of Glutamine Synthetase and Glutamate Dehydrogenase in Triticale Seedlings. *Polish Journal of Environmental Studies* **14**
- Laemmli UK** (1970) Cleavage of structural proteins during the assembly of the head of bacteriophage T4. *nature* **227**: 680
- Lajayer BA, Ghorbanpour M, Nikabadi S** (2017) Heavy metals in contaminated environment: Destiny of secondary metabolite biosynthesis, oxidative status and phytoextraction in medicinal plants. *Ecotoxicology and environmental safety* **145**: 377-390
- Lam H-M, Coschigano K, Oliveira I, Melo-Oliveira R, Coruzzi G** (1996) The molecular-genetics of nitrogen assimilation into amino acids in higher plants. *Annual review of plant biology* **47**: 569-593
- Lapworth D, Baran N, Stuart M, Ward R** (2012) Emerging organic contaminants in groundwater: a review of sources, fate and occurrence. *Environmental pollution* **163**: 287-303

- Larher F, Aziz A, Deleu C, Lemesle P, Ghaffar A, Bouchard F, Plasman M** (1998) Suppression of the osmoinduced proline response of rapeseed leaf discs by polyamines. *Physiologia Plantarum* **102**: 139-147
- Lea PJ, Mifflin BJ** (2003) Glutamate synthase and the synthesis of glutamate in plants. *Plant Physiology and Biochemistry* **41**: 555-564
- Leclercq J, Adams-Phillips LC, Zegzouti H, Jones B, Latché A, Giovannoni JJ, Pech J-C, Bouzayen M** (2002) *LeCTR1*, a tomato CTR1-like gene, demonstrates ethylene signaling ability in Arabidopsis and novel expression patterns in tomato. *Plant Physiology* **130**: 1132-1142
- Lehmann T, Ratajczak L** (2008) The pivotal role of glutamate dehydrogenase (GDH) in the mobilization of N and C from storage material to asparagine in germinating seeds of yellow lupine. *Journal of plant physiology* **165**: 149-158
- Lichtenthaler HK** (1987) [34] Chlorophylls and carotenoids: pigments of photosynthetic biomembranes. *In Methods in enzymology*, Vol 148. Elsevier, pp 350-382
- Lightfoot DA, Green NK, Cullimore JV** (1988) The chloroplast-located glutamine synthetase of *Phaseolus vulgaris* L.: nucleotide sequence, expression in different organs and uptake into isolated chloroplasts. *Plant molecular biology* **11**: 191-202
- Lima L, Seabra A, Melo P, Cullimore J, Carvalho H** (2006) Post-translational regulation of cytosolic glutamine synthetase of *Medicago truncatula*. *Journal of Experimental Botany* **57**: 2751-2761
- Liu D, Zou J, Wang M, Jiang W** (2008) Hexavalent chromium uptake and its effects on mineral uptake, antioxidant defence system and photosynthesis in *Amaranthus viridis* L. *Bioresource Technology* **99**: 2628-2636
- Liu F, Ying G-G, Tao R, Zhao J-L, Yang J-F, Zhao L-F** (2009) Effects of six selected antibiotics on plant growth and soil microbial and enzymatic activities. *Environmental Pollution* **157**: 1636-1642
- Liu L, Wang J, Han Z, Sun X, Li H, Zhang J, Lu Y** (2016) Molecular analyses of tomato GS, GOGAT and GDH gene families and their response to abiotic stresses. *Acta physiologiae plantarum* **38**: 229
- Livak KJ, Schmittgen TD** (2001) Analysis of relative gene expression data using real-time quantitative PCR and the $2^{-\Delta\Delta CT}$ method. *Methods* **25**: 402-408
- Lonappan L, Brar SK, Das RK, Verma M, Surampalli RY** (2016) Diclofenac and its transformation products: Environmental occurrence and toxicity-A review. *Environment international* **96**: 127-138

- Lopez-Luna J, Gonzalez-Chavez M, Esparza-Garcia F, Rodriguez-Vazquez R** (2009) Toxicity assessment of soil amended with tannery sludge, trivalent chromium and hexavalent chromium, using wheat, oat and sorghum plants. *Journal of Hazardous Materials* **163**: 829-834
- Loulakakis C, Roubelakis-Angelakis K** (1990) Immunocharacterization of NADH-glutamate dehydrogenase from *Vitis vinifera* L. *Plant physiology* **94**: 109-113
- Loulakakis KA, Roubelakis-Angelakis KA** (1991) Plant NAD (H)-glutamate dehydrogenase consists of two subunit polypeptides and their participation in the seven isoenzymes occurs in an ordered ratio. *Plant physiology* **97**: 104-111
- Løvdal T, Lillo C** (2009) Reference gene selection for quantitative real-time PCR normalization in tomato subjected to nitrogen, cold, and light stress. *Analytical biochemistry* **387**: 238-242
- Lutts S, Majerus V, Kinet JM** (1999) NaCl effects on proline metabolism in rice (*Oryza sativa*) seedlings. *Physiologia Plantarum* **105**: 450-458
- Ma H-w, Hung M-L, Chen P-C** (2007) A systemic health risk assessment for the chromium cycle in Taiwan. *Environment international* **33**: 206-218
- Madikizela LM, Ncube S, Chimuka L** (2018) Uptake of pharmaceuticals by plants grown under hydroponic conditions and natural occurring plant species: A review. *Science of the Total Environment* **636**: 477-486
- Majewska M, Harshkova D, Guściora M, Aksmann A** (2018) Phytotoxic activity of diclofenac: Evaluation using a model green alga *Chlamydomonas reinhardtii* with atrazine as a reference substance. *Chemosphere* **209**: 989-997
- Man HM, Kaiser WM** (2001) Increased glutamine synthetase activity and changes in amino acid pools in leaves treated with 5-aminoimidazole-4-carboxamide ribonucleoside (AICAR). *Physiologia Plantarum* **111**: 291-296
- Martí E, Gisbert C, Bishop GJ, Dixon MS, García-Martínez JL** (2006) Genetic and physiological characterization of tomato cv. Micro-Tom. *Journal of Experimental Botany* **57**: 2037-2047
- Masclaux-Daubresse C, Daniel-Vedele F, Dechorgnat J, Chardon F, Gaufichon L, Suzuki A** (2010) Nitrogen uptake, assimilation and remobilization in plants: challenges for sustainable and productive agriculture. *Annals of botany* **105**: 1141-1157
- Meissner R, Jacobson Y, Melamed S, Levyatuv S, Shalev G, Ashri A, Elkind Y, Levy A** (1997) A new model system for tomato genetics. *The Plant Journal* **12**: 1465-1472

- Melo-Oliveira R, Oliveira IC, Coruzzi GM** (1996) Arabidopsis mutant analysis and gene regulation define a nonredundant role for glutamate dehydrogenase in nitrogen assimilation. *Proceedings of the National Academy of Sciences* **93**: 4718-4723
- Metcalfe CD, Miao XS, Koenig BG, Struger J** (2003) Distribution of acidic and neutral drugs in surface waters near sewage treatment plants in the lower Great Lakes, Canada. *Environmental Toxicology and Chemistry: An International Journal* **22**: 2881-2889
- Michelini L, La Rocca N, Rascio N, Ghisi R** (2013) Structural and functional alterations induced by two sulfonamide antibiotics on barley plants. *Plant physiology and biochemistry* **67**: 55-62
- Michelini L, Reichel R, Werner W, Ghisi R, Thiele-Bruhn S** (2012) Sulfadiazine uptake and effects on *Salix fragilis* L. and *Zea mays* L. plants. *Water, Air, & Soil Pollution* **223**: 5243-5257
- Mifflin BJ, Habash DZ** (2002) The role of glutamine synthetase and glutamate dehydrogenase in nitrogen assimilation and possibilities for improvement in the nitrogen utilization of crops. *Journal of experimental botany* **53**: 979-987
- Migge A, Carrayol E, Hirel B, Becker TW** (2000) Leaf-specific overexpression of plastidic glutamine synthetase stimulates the growth of transgenic tobacco seedlings. *Planta* **210**: 252-260
- Miyashita Y, Good AG** (2008) NAD (H)-dependent glutamate dehydrogenase is essential for the survival of *Arabidopsis thaliana* during dark-induced carbon starvation. *Journal of Experimental Botany* **59**: 667-680
- Mohan D, Pittman Jr CU** (2006) Activated carbons and low cost adsorbents for remediation of tri-and hexavalent chromium from water. *Journal of hazardous materials* **137**: 762-811
- Moreira JT, Moreira TM, Cunha JB, Azenha M, Fidalgo F, Teixeira J** (2018) Differential effects of acetophenone on shoots' and roots' metabolism of *Solanum nigrum* L. plants and implications in its phytoremediation. *Plant Physiology and Biochemistry* **130**: 391-398
- Mostowska A** (1997) Environmental factors affecting chloroplasts. *Handbook of Photosynthesis* **28**: 407-426
- Nagajyoti P, Lee K, Sreekanth T** (2010) Heavy metals, occurrence and toxicity for plants: a review. *Environmental chemistry letters* **8**: 199-216
- Naidu R, Espana VAA, Liu Y, Jit J** (2016) Emerging contaminants in the environment: risk-based analysis for better management. *Chemosphere* **154**: 350-357

- Nguyen GN, Kant S** (2018) Improving nitrogen use efficiency in plants: effective phenotyping in conjunction with agronomic and genetic approaches. *Functional Plant Biology* **45**: 606-619
- Nieva F, Castellanos E, Figueroa M, Gil F** (1999) Gas exchange and chlorophyll fluorescence of C₃ and C₄ saltmarsh species. *Photosynthetica* **36**: 397-406
- Norpoth K, Nehr Korn A, Kirschner M, Holsen H, Teipel H** (1973) Studies on the problem of solubility and stability of steroid ovulation inhibitors in water waste water and activated sludge. *Zentralblatt fuer Bakteriologie (Orig. B)* **156**: 500-511
- Oaks JL, Gilbert M, Virani MZ, Watson RT, Meteyer CU, Rideout BA, Shivaprasad H, Ahmed S, Chaudhry MJI, Arshad M** (2004) Diclofenac residues as the cause of vulture population decline in Pakistan. *Nature* **427**: 630
- Obiadalla-Ali H, Fernie AR, Kossmann J, Lloyd JR** (2004) Developmental analysis of carbohydrate metabolism in tomato (*Lycopersicon esculentum* cv. Micro-Tom) fruits. *Physiologia Plantarum* **120**: 196-204
- Odendaal C, Seaman MT, Kemp G, Patterton HE, Patterton H-G** (2015) An LC-MS/MS based survey of contaminants of emerging concern in drinking water in South Africa. *South African Journal of Science* **111**: 01-06
- Oh YJ, Song H, Shin WS, Choi SJ, Kim Y-H** (2007) Effect of amorphous silica and silica sand on removal of chromium (VI) by zero-valent iron. *Chemosphere* **66**: 858-865
- Okabe Y, Asamizu E, Ariizumi T, Shirasawa K, Tabata S, Ezura H** (2012) Availability of Micro-Tom mutant library combined with TILLING in molecular breeding of tomato fruit shelf-life. *Breeding science* **62**: 202-208
- Oliveira H** (2012) Chromium as an environmental pollutant: insights on induced plant toxicity. *Journal of Botany* **2012**
- Öllers S, Singer HP, Fässler P, Müller SR** (2001) Simultaneous quantification of neutral and acidic pharmaceuticals and pesticides at the low-ng/l level in surface and waste water. *Journal of chromatography A* **911**: 225-234
- Panda S, Choudhury S** (2005) Chromium stress in plants. *Brazilian journal of plant physiology* **17**: 95-102
- Pandey V, Dixit V, Shyam R** (2005) Antioxidative responses in relation to growth of mustard (*Brassica juncea* cv. Pusa Jaikisan) plants exposed to hexavalent chromium. *Chemosphere* **61**: 40-47
- Park E-J, Lee S-D, Chung E-J, Lee M-H, Um H-Y, Murugaiyan S, Moon B-J, Lee S-W** (2007) MicroTom - A model plant system to study bacterial wilt by *Ralstonia solanacearum*. *The Plant Pathology Journal* **23**: 239-244

- Pascual MB, Jing ZP, Kirby EG, Cánovas FM, Gallardo F** (2008) Response of transgenic poplar overexpressing cytosolic glutamine synthetase to phosphinothricin. *Phytochemistry* **69**: 382-389
- Pathak RR, Ahmad A, Lochab S, Raghuram N** (2008) Molecular physiology of plant nitrogen use efficiency and biotechnological options for its enhancement. *Current Science*: 1394-1403
- Pesole G, Bozzetti M, Lanave C, Preparata G, Saccone C** (1991) Glutamine synthetase gene evolution: a good molecular clock. *Proceedings of the National Academy of Sciences* **88**: 522-526
- Pessoa AM, Pereira S, Teixeira J** (2010) PrimerIdent: a web based tool for conserved primer design. *Bioinformatics* **5**: 52
- Pfaffl MW** (2001) A new mathematical model for relative quantification in real-time RT-PCR. *Nucleic acids research* **29**: e45-e45
- Pierattini EC, Francini A, Huber C, Sebastiani L, Schröder P** (2018) Poplar and diclofenac pollution: A focus on physiology, oxidative stress and uptake in plant organs. *Science of The Total Environment* **636**: 944-952
- Purnell MP, Botella JR** (2007) Tobacco isoenzyme 1 of NAD (H)-dependent glutamate dehydrogenase catabolizes glutamate in vivo. *Plant Physiology* **143**: 530-539
- Purnell MP, Skopelitis DS, Roubelakis-Angelakis KA, Botella JR** (2005) Modulation of higher-plant NAD (H)-dependent glutamate dehydrogenase activity in transgenic tobacco via alteration of beta subunit levels. *Planta* **222**: 167-180
- Rabiet M, Togola A, Brissaud F, Seidel J-L, Budzinski H, Elbaz-Poulichet F** (2006) Consequences of treated water recycling as regards pharmaceuticals and drugs in surface and ground waters of a medium-sized Mediterranean catchment. *Environmental science & technology* **40**: 5282-5288
- Rai R, Agrawal M, Agrawal S** (2016) Impact of heavy metals on physiological processes of plants: with special reference to photosynthetic system. *In Plant Responses to Xenobiotics*. Springer, pp 127-140
- Rai V, Mehrotra S** (2008) Chromium-induced changes in ultramorphology and secondary metabolites of *Phyllanthus amarus* Schum & Thonn.–an hepatoprotective plant. *Environmental monitoring and assessment* **147**: 307-315
- Rai V, Vajpayee P, Singh SN, Mehrotra S** (2004) Effect of chromium accumulation on photosynthetic pigments, oxidative stress defense system, nitrate reduction, proline level and eugenol content of *Ocimum tenuiflorum* L. *Plant science* **167**: 1159-1169

- Ribeiro C, Ribeiro AR, Tiritan ME** (2016) Priority substances and emerging organic pollutants in Portuguese aquatic environment: a review. *In* Reviews of Environmental Contamination and Toxicology Volume 238. Springer, pp 1-44
- Riedel J, Tischner R, Mäck G** (2001) The chloroplastic glutamine synthetase (GS-2) of tobacco is phosphorylated and associated with 14-3-3 proteins inside the chloroplast. *Planta* **213**: 396-401
- Rodriguez E, Azevedo R, Fernandes P, Santos Cao** (2011) Cr (VI) induces DNA damage, cell cycle arrest and polyploidization: a flow cytometric and comet assay study in *Pisum sativum*. *Chemical research in toxicology* **24**: 1040-1047
- Rodriguez E, Santos C, Azevedo R, Moutinho-Pereira J, Correia C, Dias MC** (2012) Chromium (VI) induces toxicity at different photosynthetic levels in pea. *Plant Physiology and Biochemistry* **53**: 94-100
- Sambrook J, Fritsch EF, Maniatis T** (1989) *Molecular cloning: a laboratory manual*. Cold spring harbor laboratory press
- Santos C, Rodriguez E** (2012) Review on some emerging endpoints of chromium (VI) and lead phytotoxicity. *In* Botany. InTech
- Saradhi PP** (1991) Proline accumulation under heavy metal stress. *Journal of Plant Physiology* **138**: 554-558
- Scarpeci TE, Marro ML, Bortolotti S, Boggio SB, Valle EM** (2007) Plant nutritional status modulates glutamine synthetase levels in ripe tomatoes (*Solanum lycopersicum* cv. Micro-Tom). *Journal of plant physiology* **164**: 137-145
- Seabra AR, Carvalho H, Pereira PJB** (2009) Crystallization and preliminary crystallographic characterization of glutamine synthetase from *Medicago truncatula*. *Acta Crystallographica Section F: Structural Biology and Crystallization Communications* **65**: 1309-1312
- Sela M, Garty J, Tel-Or E** (1989) The accumulation and the effect of heavy metals on the water fern *Azolla filiculoides*. *New Phytologist* **112**: 7-12
- Shahid M, Shamshad S, Rafiq M, Khalid S, Bibi I, Niazi NK, Dumat C, Rashid MI** (2017) Chromium speciation, bioavailability, uptake, toxicity and detoxification in soil-plant system: A review. *Chemosphere* **178**: 513-533
- Shanker AK, Cervantes C, Loza-Tavera H, Avudainayagam S** (2005) Chromium toxicity in plants. *Environment international* **31**: 739-753
- Shibata D** (2005) Genome sequencing and functional genomics approaches in tomato. *Journal of General Plant Pathology* **71**: 1-7

- Shukla O, Dubey S, Rai U** (2007) Preferential accumulation of cadmium and chromium: toxicity in *Bacopa monnieri* L. under mixed metal treatments. Bulletin of environmental contamination and toxicology **78**: 252-257
- Silva LS, Seabra AR, Leitão JN, Carvalho HG** (2015) Possible role of glutamine synthetase of the prokaryotic type (GSI-like) in nitrogen signaling in *Medicago truncatula*. Plant Science **240**: 98-108
- Singh HP, Mahajan P, Kaur S, Batish DR, Kohli RK** (2013) Chromium toxicity and tolerance in plants. Environmental Chemistry Letters **11**: 229-254
- Singh S, Sinha S** (2005) Accumulation of metals and its effects in *Brassica juncea* (L.) Czern.(cv. Rohini) grown on various amendments of tannery waste. Ecotoxicology and Environmental Safety **62**: 118-127
- Sinha V, Pakshirajan K, Chaturvedi R** (2018) Chromium tolerance, bioaccumulation and localization in plants: An overview. Journal of environmental management **206**: 715-730
- Skopelitis DS, Paranychianakis NV, Kouvarakis A, Spyros A, Stephanou EG, Roubelakis-Angelakis KA** (2007) The isoenzyme 7 of tobacco NAD (H)-dependent glutamate dehydrogenase exhibits high deaminating and low aminating activities in vivo. Plant physiology **145**: 1726-1734
- Soares C, Branco-Neves S, de Sousa A, Teixeira J, Pereira R, Fidalgo F** (2018) Can nano-SiO₂ reduce the phytotoxicity of acetaminophen?—a physiological, biochemical and molecular approach. Environmental Pollution
- Sorrequieta A, Ferraro G, Boggio SB, Valle EM** (2010) Free amino acid production during tomato fruit ripening: a focus on L-glutamate. Amino acids **38**: 1523-1532
- Subrahmanyam D** (2008) Effects of chromium toxicity on leaf photosynthetic characteristics and oxidative changes in wheat (*Triticum aestivum* L.). Photosynthetica **46**: 339
- Swarbreck SM, Defoin-Platel M, Hindle M, Saqi M, Habash DZ** (2010) New perspectives on glutamine synthetase in grasses. Journal of Experimental Botany **62**: 1511-1522
- Szabados L, Savoure A** (2010) Proline: a multifunctional amino acid. Trends in plant science **15**: 89-97
- Szepesi Á, Szöllősi R** (2018) Mechanism of Proline Biosynthesis and Role of Proline Metabolism Enzymes Under Environmental Stress in Plants. In Plant Metabolites and Regulation Under Environmental Stress. Elsevier, pp 337-353

- Tabak HH, Bunch R** (1970) Steroid hormones as water pollutants. I. Metabolism of natural and synthetic ovulation-inhibiting hormones by microorganisms of activated sludge and primary settled sewage. *Dev. Ind. Microbiol* **11**: 367-376
- Taiz L, Zeiger E, Møller IM, Murphy AS** (2015) *Plant physiology and development*, Sixth ed. Sinauer Associates, Inc., Sunderland, U.S.A.
- Takabe T, Tanaka Y, Hibino T, Araki E, Ishikawa H, Tanaka A, Takabe T** (2001) Overexpression of chloroplast glutamine synthetase conferred salt tolerance in rice. *Science Access* **3**
- Thomsen HC, Eriksson D, Møller IS, Schjoerring JK** (2014) Cytosolic glutamine synthetase: a target for improvement of crop nitrogen use efficiency? *Trends in Plant Science* **19**: 656-663
- Thornton B, Basu C** (2011) Real-time PCR (qPCR) primer design using free online software. *Biochemistry and Molecular Biology Education* **39**: 145-154
- Tiwari JK, Plett D, Garnett T, Chakrabarti SK, Singh RK** (2018) Integrated genomics, physiology and breeding approaches for improving nitrogen use efficiency in potato: translating knowledge from other crops. *Functional Plant Biology* **45**: 587-605
- Tiwari K, Dwivedi S, Singh N, Rai U, Tripathi R** (2009) Chromium (VI) induced phytotoxicity and oxidative stress in pea (*Pisum sativum* L.): biochemical changes and translocation of essential nutrients. *J Environ Biol* **30**: 389-394
- Torreira E, Seabra AR, Marriott H, Zhou M, Llorca Ó, Robinson CV, Carvalho HG, Fernández-Tornero C, Pereira PJB** (2014) The structures of cytosolic and plastid-located glutamine synthetases from *Medicago truncatula* reveal a common and dynamic architecture. *Acta Crystallographica Section D: Biological Crystallography* **70**: 981-993
- Turano FJ, Thakkar SS, Fang T, Weisemann JM** (1997) Characterization and expression of NAD (H)-dependent glutamate dehydrogenase genes in Arabidopsis. *Plant Physiology* **113**: 1329-1341
- Unno H, Uchida T, Sugawara H, Kurisu G, Sugiyama T, Yamaya T, Sakakibara H, Hase T, Kusunoki M** (2006) Atomic Structure of Plant Glutamine Synthetase a key enzyme for plant productivity. *Journal of Biological Chemistry* **281**: 29287-29296
- Vajpayee P, Tripathi R, Rai U, Ali M, Singh S** (2000) Chromium (VI) accumulation reduces chlorophyll biosynthesis, nitrate reductase activity and protein content in *Nymphaea alba* L. *Chemosphere* **41**: 1075-1082

- van Rooyen JM, Abratt VR, Belrhali H, Sewell T** (2011) Crystal structure of type III glutamine synthetase: surprising reversal of the inter-ring interface. *Structure* **19**: 471-483
- Verbruggen N, Hermans C** (2008) Proline accumulation in plants: a review. *Amino acids* **35**: 753-759
- Vernay P, Gauthier-Moussard C, Hitmi A** (2007) Interaction of bioaccumulation of heavy metal chromium with water relation, mineral nutrition and photosynthesis in developed leaves of *Lolium perenne* L. *Chemosphere* **68**: 1563-1575
- Vieno N, Sillanpää M** (2014) Fate of diclofenac in municipal wastewater treatment plant—a review. *Environment international* **69**: 28-39
- Vincent R, Fraisier V, Chaillou S, Limami MA, Deleens E, Phillipson B, Douat C, Boutin J-P, Hirel B** (1997) Overexpression of a soybean gene encoding cytosolic glutamine synthetase in shoots of transgenic *Lotus corniculatus* L. plants triggers changes in ammonium assimilation and plant development. *Planta* **201**: 424-433
- Von Caemmerer Sv, Farquhar GD** (1981) Some relationships between the biochemistry of photosynthesis and the gas exchange of leaves. *Planta* **153**: 376-387
- Wang Y, Fu B, Pan L, Chen L, Fu X, Li K** (2013) Overexpression of Arabidopsis Dof1, GS1 and GS2 enhanced nitrogen assimilation in transgenic tobacco grown under low-nitrogen conditions. *Plant Molecular Biology Reporter* **31**: 886-900
- Wang Z-Q, Yuan Y-Z, Ou J-Q, Lin Q-H, Zhang C-F** (2007) Glutamine synthetase and glutamate dehydrogenase contribute differentially to proline accumulation in leaves of wheat (*Triticum aestivum*) seedlings exposed to different salinity. *Journal of Plant Physiology* **164**: 695-701
- Xu J, Yin H, Li X** (2009) Protective effects of proline against cadmium toxicity in micropropagated hyperaccumulator, *Solanum nigrum* L. *Plant cell reports* **28**: 325-333
- Yang Y, Ok YS, Kim K-H, Kwon EE, Tsang YF** (2017) Occurrences and removal of pharmaceuticals and personal care products (PPCPs) in drinking water and water/sewage treatment plants: A review. *Science of the Total Environment* **596**: 303-320
- Zayed A, Lytle CM, Qian J-H, Terry N** (1998) Chromium accumulation, translocation and chemical speciation in vegetable crops. *Planta* **206**: 293-299

Zhang Y, Geißen S-U, Gal C (2008) Carbamazepine and diclofenac: removal in wastewater treatment plants and occurrence in water bodies. *Chemosphere* **73**: 1151-1161

Zhuang P, McBride MB, Xia H, Li N, Li Z (2009) Health risk from heavy metals via consumption of food crops in the vicinity of Dabaoshan mine, South China. *Science of the total environment* **407**: 1551-1561

Supplemental Data

Supplemental data 1. Tomato GS-cDNAs, the forward and reverse primers, the deduced amino acid sequences and accession numbers for each sequence.

GS2 (Solyc01g080280.2.1)

>S1GS2Fwd

|

A CCC ATC TTC ATC TTC TTC TCT CAC TCC TCT CAA CAC AAC ATT ATT TTC TGC ATT GTC CAC TTA GTT GGT < 70

TAG GAG GTG AAC ATG GCT CAG ATC CTG GCT CCG TCT GCA CAA TGG CAG ATG AGA ATG ACA AAG AGC TCA A < 140

M A Q I L A P S A Q W Q M R M T K S S T

<S1GS2Rev

|

CC GAT GCT AGT CCC TTG ACT TCA AAG ATG TGG AGC TCT GTG GTG CTG AAG CAG AAC AAA AGA CAC GCT CT < 210

D A S P L T S K M W S S V V L K Q N K R H A L

T AAA AGC TCT GCC AAA TTT AGA GTT TTT GCC CTA CAG TCT GAC AAT GGC ACC GTG AAC AGA GTG GAA CAG < 280

K S S A K F R V F A L Q S D N G T V N R V E Q

CTG CTA AAC TTG GAC GTA ACT CCA TAC ACT GAT AAG ATC ATT GCT GAA TAT ATT TGG ATC GGA GGG ACT G < 350

L L N L D V T P Y T D K I I A E Y I W I G G T G

GA ATT GAC ATG CGC AGT AAA TCA AGG ACT ATT TCG AAA CCA GTC AAG GAT GCT TCT GAG CTC CCA AAG TG < 420

I D M R S K S R T I S K P V K D A S E L P K W

G AAC TAC GAT GGA TCA AGT ACT GGA CAA GCA CCT GGA GAA GAC AGT GAA GTC ATT CTA TAT CCT CAG GCA < 490

N Y D G S S T G Q A P G E D S E V I L Y P Q A

ATA TTC AAA GAC CCT TTC CGT GGT GGT AAC AAC ATC TTG GTT ATC TGT GAT GCC TAC ACA CCA GCT GGA G < 560

I F K D P F R G G N N I L V I C D A Y T P A G E

AG CCA ATT CCT ACA AAC AAA CGC CAT AAA GCT GCT CAA ATT TTT AGC GAC CCA AAA GTT GCA GCT CAA GT < 630

P I P T N K R H K A A Q I F S D P K V A A Q V

T CCA TGG TTT GGA ATA GAA CAA GAG TAC ACC TTA CTC CAG CCA AAT GTA AAC TGG CCC TTA GGT TGG CCT < 700

P W F G I E Q E Y T L L Q P N V N W P L G W P

GTT GGA GGC TAC CCC GGA CCT CAG GGT CCT TAC TAC TGT GGT GCT GGA GCG GAA AAG TCA TTT GGC AGA G < 770
V G G Y P G P Q G P Y Y C G A G A E K S F G R D

AT ATA TCA GAT GCT CAC TAC AAG GCT TGC CTG TAT GCT GGA ATT AAC ATT AGT GGT ACT AAT GGA GAG GT < 840
I S D A H Y K A C L Y A G I N I S G T N G E V

T ATG CCA GGA CAG TGG GAA TTT CAA GTA GGT CCT AGT GTT GGA ATT GAA GGT GGA GAT CAT ATC TGG TGT < 910
M P G Q W E F Q V G P S V G I E G G D H I W C

GCT AGA TAC CTC CTC GAG AGA ATT ACT GAA CAA GCA GGA GTT GTC CTC TCA CTC GAT CCA AAA CCA ATT G < 980
A R Y L L E R I T E Q A G V V L S L D P K P I E

AG GGT GAC TGG AAC GGT GCA GGA TGC CAC ACT AAC TAC AGT ACA CTG AGT ATG AGA GAA GAG GGA GGT TT < 1050
G D W N G A G C H T N Y S T L S M R E E G G F

T GAA GTT ATA AAG AAA GCA ATT CTG AAT CTA TCC CTT CGC CAC AAG GAA CAT ATA AGT GCT TAT GGA GAA < 1120
E V I K K A I L N L S L R H K E H I S A Y G E

GGA AAT GAG AGA AGG TTG ACC GGA AAG CAT GAA ACT GCT AGT ATT GAC CAA TTT TCA TGG GGA GTT GCT A < 1190
G N E R R L T G K H E T A S I D Q F S W G V A N

AC CGT GGT TGC TCA ATC CGT GTG GGG CGT GAC ACT GAG AAG GAA GGC AAG GGT TAT TTG GAA GAC CGC CG < 1260
R G C S I R V G R D T E K E G K G Y L E D R R

C CCA GCT TCA AAC ATG GAC CCC TAT GTT GTG ACT GGA TTA CTT GCT GAA ACT ACT ATA CTG TGG GAG CCA < 1330
P A S N M D P Y V V T G L L A E T T I L W E P

ACC CTT GAG GCT GAA GCT CTT GCT GCC CAA AAG ATC TCA TTG AAG GTT TAG AGT ATA TGA GGG GAA ATT G < 1400
T L E A E A L A A Q K I S L K V *

TT TTC ATA ATA ATC CTC TTA GAA TTT ATG AGA TAA GTT CTG AAG CTT GTA CCT TGT TGA GGT TCC CTT AT < 1470

T TGG GAA AAT CTT GTA AAG GAA CCA AAA TTT ACC AGT TCA TCC TAG AAA ATA GGT TTC TTA AGA CAT GAG < 1540

ACT ACT TTG GAG TTG AGG TGT AAT TGT TGG ACT ACT TTG AAC ATC TTT ACC TTT CTT TTC TCC AGA TGA A < 1610

<SLGS2_3'

I

TC CAT TTC TCT GAA ATT CCA ATT GGT GTG CTC TTT CCG AAT GAA ATC TTT GAA CAT ATA ATC AGT CAT GT < 1680

A CAT < 1684

GS1.1 (Solyc04g014510.2.1)

CAA ATT AAT TAA ATT CTC TCA TTC AAT AAA TTC AAA CTT TGA ATT TAT TAT TGT TAT TAT TTT CAC ATA A < 70

M

TG GCT CAT CTT TCA GAT CTT GTC AAT CTT AAT CTC TCT GAT TCC TCT GAG AAA ATC ATT GCT GAA TAC AT < 140

A H L S D L V N L N L S D S S E K I I A E Y I

A TGG ATT GGT GGA TCA GGA ATG GAT GTA AGG AGC AAA GCC AGG ACT CTA TCT GGT CCT GTT GAT GAT CCT < 210

W I G G S G M D V R S K A R T L S G P V D D P

TCA AAG CTT CCC AAA TGG AAT TAT GAT GGT TCT AGC ACA GGT CAA GCT CCT GGA GAA GAC AGT GAA GTG A < 280

S K L P K W N Y D G S S T G Q A P G E D S E V I

TC CTA TAT CCT CAA GCA ATT TTC AAG GAT CCA TTC AGG AGG GGC AAC AAT ATC TTG GTC ATC TGT GAT TG < 350

L Y P Q A I F K D P F R R G N N I L V I C D C

T TAC ACC CCA GCT GGT GAA CCA ATT CCA ACA AAC AAG AGG CAC AAT GCT GCT AAA ATA TTT AGC AAC CCT < 420

Y T P A G E P I P T N K R H N A A K I F S N P

AAT GTT GTT GTT GAG GAA CCA TGG TAT GGT CTT GAG CAA GAA TAC ACC TTG CTA CAA AAG GAA ATT AAT T < 490

N V V V E E P W Y G L E Q E Y T L L Q K E I N W

GG CCT CTT GGA TGG CCT ATT GGT GGC TTT CCT GGA CCA CAG GGA CCA TAC TAC TGT GGA ATT GGA TGC GG < 560

P L G W P I G G F P G P Q G P Y Y C G I G C G

A AAG GCT TTT GGA CGC GAT ATT GTT GAT GCT CAT TAC AAG GCA TGT ATC TAT GCC GGG ATT AAC ATT AGT < 630

K A F G R D I V D A H Y K A C I Y A G I N I S

GGT ATC AAC GGA GAA GTG ATG CCT GGA CAG TGG GAA TTT CAA GTT GGA CCT TCA GTT GGC ATT GCA TCA G < 700

G I N G E V M P G Q W E F Q V G P S V G I A S G

GT GAC GAG TTG TGG GCA GCT CGT TAC ATT CTC GAG AGG ATT ACA GAG ATT GCT GGA GTT GTT GTG TCA TT < 770

D E L W A A R Y I L E R I T E I A G V V V S F

C GAC CCT AAA CCT ATT CCG GGT GAC TGG AAT GGT GCA GGA GCG CAT ACA AAT TAC AGT ACT AAG TCT ATG < 840
D P K P I P G D W N G A G A H T N Y S T K S M

AGA AAT GAG GGA GGG TAT GAA GTT ATC AAA AAG GCT ATT GAG AAG CTT GGA CTT AGG CAC AAG GAG CAC A < 910
R N E G G Y E V I K K A I E K L G L R H K E H I

TT GCA GCA TAT GGT GAA GGC AAT GAA CGT CGT CTC ACT GGA AGA CAC GAA ACA GCT GAC ATC AAC ACA TT < 980
A A Y G E G N E R R L T G R H E T A D I N T F

>SlGS1.1Fwd

|

C AAA TGG GGT GTT GCA AAT CGT GGT GCA TCT ATT CGT GTG GGA AGA GAC ACG GAG AAG GAA GGA AAG GGA < 1050
K W G V A N R G A S I R V G R D T E K E G K G

TAC TTT GAG GAC AGG AGG CCT GCA TCG AAC ATG GAT CCA TAT GTT GTG ACC TCT ATG ATC GCG GAG ACT A < 1120
Y F E D R R P A S N M D P Y V V T S M I A E T T

CC ATC CTG TGG AAC CCT TGA ACG CGT ATT GGA TGA ATG TGC AAC ATA TGG AGA AAG AAT TGA ATT TCT TA < 1190
I L W N P *

<SlGS1.1Rev

|

A CAG CCC TTT CCT CAC ATG ACC TAA AAA AGA GAG TTA TGT AGC TAG TCA TTT TGA TAT ATT ATG TTG TTT < 1260

TCT AAG TTT CAA TTT GTA TTG TAC TCA GCA AGG CTG AGT TCA TTG CCA TAA TGA TTT GGC AAT GTT GTT A < 1330

AA AAA TAA GAG TTT TAA TCT TAT TAA TAA CAA TAT GGA AGG GTT AAC TTT TCA GAA ATG CAT ATG TTA TG < 1400

T TTT ATT AGC TGT GAT TGT TTG TAA AGT TCT TTC GCA TCG ATA GTC AGG TGC ACG AAG TTG CCA CTC TTG < 1470

TGG CTT AAG CAG TTG TTG GCA CTG TGT AAG TTC TTA CGT < 1509

GS1.2 (Solyc05g051250.2.1)

AA AGG GAA TAA GTC ACT CTG AAT CAA TAA TAA TTT TTT CAT ACG CAA AAA CTT TGA AGA TTT TTC ATT AT < 70

G TCT ATG ATT TCA GAT CTC ATC AAT CTT AAT TTA TCT GAA TGC ACT AAG AAA ATT ATT GCC GAA TAC ATA < 140

TGG ATT GGT GGA TCA GGC ACT GAT CTC AGG AGC AAA GCC AGG ACT CTT TCA GGT CCT GTT AAG GAT CCT T < 210

AG AGC TTC CAA AAT GGA ACT ATG TCT ATG ATT TCA GAT CTC ATC AAT CTT AAT TTA TCT GAA TGC ACT AA < 280

M S M I S D L I N L N L S E C T K

G AAA ATT ATT GCC GAA TAC ATA TGG ATT GGT GGA TCA GGC ACT GAT CTC AGG AGC AAA GCC AGG ACT CTT < 350

K I I A E Y I W I G G S G T D L R S K A R T L

TCA GGT CCT GTT AAG GAT CCT TCA GAG CTT CCA AAA TGG AAC TAT GAC GGA TCT AGC ACA GGG CAA GCT T < 420

S G P V K D P S E L P K W N Y D G S S T G Q A S

CT GGA GAA GAC AGT GAA GTG ATC CTA TAT CCT CAA GCA ATT TTC AAG GAT CCA TTC AGG AGA GGT GAT AA < 490

G E D S E V I L Y P Q A I F K D P F R R G D N

T ATT TTG GTC ATG TGT GAT GCT TAC ACT CCA GCT GGT AAT CCC ATT CCA ACA AAC AAG AGG CAC AAT GCA < 560

I L V M C D A Y T P A G N P I P T N K R H N A

GCC AAG ATT TTC AGC AAC CCT GTT GTT GCT GCT GAA GAA CCA TGG TAT GGT ATC GAG CAA GAG TAC ACG T < 630

A K I F S N P V V A A E E P W Y G I E Q E Y T L

TG TTG CAG AAA GAG GTT AAC TGG CCT CTC GGA TGG CCT ATT GGA GGT TTC CCT GGA CCT CAG GGA CCT TA < 700

L Q K E V N W P L G W P I G G F P G P Q G P Y

C TAC TGT GGA ATT GGA GCT GCC AAT GCT TTT GGA CGC GAT ATA GTT GAC TCA CAT TAT AAG GCA TGT CTT < 770

Y C G I G A A N A F G R D I V D S H Y K A C L

TAC GCT GGA ATT AAC ATC AGC GGT GTC AAT GGG GAA GTG ATG CCT GGA CAG TGG GAA TTC CAA GTT GGT C < 840

Y A G I N I S G V N G E V M P G Q W E F Q V G P

CT GCT GTT GGT ATC TCA GCT GGT GAC GAA GTG TGG GCT GCA CGT TAC ATT CTC GAG AGG ATT GCT GAG GT < 910

A V G I S A G D E V W A A R Y I L E R I A E V

>SIGS1.2Fwd

|

T GCT GGA GTT GTT GTT TCA TTT GAC CCA AAA CCT ATC CCT GGT GAT TGG AAC GGT GCT GGT GCA CAC GCA < 980

A G V V V S F D P K P I P G D W N G A G A H A

AAC TAC AGT ACT AAG TCT ATG AGG GAA GAT GGA GGC TAT GAA ATC ATC AAA AAG GCT ATT GAG AAG CTT G < 1050

N Y S T K S M R E D G G Y E I I K K A I E K L G

<S1GS1.2Rev

|

GA TTA AGG CAC AAA GAG CAC ATT GCT GCA TAT GGT GAA GGC AAT GAA CGT CGT CTC ACT GGA AAA CAT GA < 1120

L R H K E H I A A Y G E G N E R R L T G K H E

A ACA GCT GAT ATC AAC TCC TTC AAA TGG GGT GTT GCC AAT CGT GGC TGC TCA GTT CGT GTA GGT AGA GAT < 1190

T A D I N S F K W G V A N R G C S V R V G R D

ACA GAG AAG GCA GGG AAG GGA TAT TTC GAG GAC AGG AGG CCT GCT TCG AAC ATG GAT CCT TAC ACT GTT A < 1260

T E K A G K G Y F E D R R P A S N M D P Y T V T

CA TCC ATG ATT GCT GAG ACC ACA ATT GTC TGG AAA CCT TAA GCC GTT CAT AAG CGT CTT GCT ATG TTT GC < 1330

S M I A E T T I V W K P *

T TGA ATC CTA CTC ATG TCT GAT TCT CTA AAA CTG CAT AGC TTT TGG AGG ATC TGA TAC ACA CTC GAC AGC < 1400

ATT TTT GAA GAG TTT TGA ACG ACA TAG CTA ACT TAG AGG ATT ATT GTT TCT TGA GTC AAT AAA TTG AAT A < 1470

GG GTA GTC TTA TTT TAT TTT CTT TGA ATA AAT GCA TTC ATC AAA GGC TTC GAT < 1523

GS1.3 (Solyc11g011380.1)

TTG GAA TAA TTA AGT TGT AAG TGT AAT AGT TTA ATA CAA GCA ACC CTG AAA ATC GCC TAT ATA AAG TGT A < 70

TA AAA ATT TAG TCT TTG CCT CAT CAA AGA AAA TTC ATC TTA TAG AGA ATT TTA ATT TAA GAA GTT TAT CA < 140

T CAT CAT GTC TCT GCT TTC AGA TCT TAT CAA CCT CAA TCT CTC AGG TGA TAC TCA GAA GAT CAT TGC TGA < 210

ATA CAT ATG TCT CTG CTT TCA GAT CTT ATC AAC CTC AAT CTC TCA GGT GAT ACT CAG AAG ATC ATT GCT G < 280

M S L L S D L I N L N L S G D T Q K I I A E

AA TAC ATA TGG ATT GGT GGA TCA GGC ATG GAC ATG AGG AGC AAA GCC AGG ACT CTC CCT GGT CCA GTT AC < 350

Y I W I G G S G M D M R S K A R T L P G P V T

T AGT CCT GCA GAA CTA CCC AAA TGG AAC TAC GAT GGA TCG AGC ACT GGT CAA GCT CCC GGA GAA GAC AGT < 420

S P A E L P K W N Y D G S S T G Q A P G E D S

GAA GTG ATC TTA TAT CCA CAA GCA ATC TTC AAG GAC CCA TTC AGA AGA GGC AAC AAC ATC TTG GTC ATG T < 490

E V I L Y P Q A I F K D P F R R G N N I L V M C

GT GAT GCC TAT ACT CCT GCT GGT GAG CCC ATC CCA ACA AAC AAG AGG CAC GCC GCC GCC AAG GTC TTC AG < 560

D A Y T P A G E P I P T N K R H A A A K V F S

C CAC CCT GAT GTG GCT GCT GAG GAA ACT TGG TAT GGT ATT GAA CAA GAA TAT ACC TTG CTG CAA AGG GAG < 630

H P D V A A E E T W Y G I E Q E Y T L L Q R E

GTC AAC TGG CCT CTT GGA TGG CCC ATT GGC GGT TTT CCT GGC CCC CAG GGA CCA TAC TAC TGT GGA ACC G < 700

V N W P L G W P I G G F P G P Q G P Y Y C G T G

GA GCT GAC AAG GCC TTT GGA CGT GAC ATT GTT GAC GCC CAT TAC AAG GCT TGT CTC TAT GCT GGG ATT AA < 770

A D K A F G R D I V D A H Y K A C L Y A G I N

C ATC AGC GGG ATC AAT GGT GAA GTC ATG CCG GGA CAG TGG GAA TTT CAA GTT GGA CCT TCT GTT GGC ATC < 840

I S G I N G E V M P G Q W E F Q V G P S V G I

>slgs1.3Fwd

|

TCA GCT GGT GAT GAA GTG TGG GTA GCT CGT TAC ATT CTA GAG AGG ATT GCA GAG ATT GCT GGG GTG GTC G < 910

S A G D E V W V A R Y I L E R I A E I A G V V V

TG TCA TTC GAC CCC AAG CCT ATT CCG GGC GAC TGG AAT GGT GCA GGT GCT CAC ACA AAT TAC AGC ACC AA < 980

S F D P K P I P G D W N G A G A H T N Y S T K

<slgs1.3Rev

|

G TCG ATG AGG GAA GAC GGA GGC TAT GAA ATA ATC TTA AAG GCT ATT GAG AAG CTT GGC TTG AAG CAC AAA < 1050

S M R E D G G Y E I I L K A I E K L G L K H K

GAA CAC ATA GCT GCA TAT GGT GAA GGC AAC GAG CGT CGT CTC ACT GGA AAG CAC GAA ACA GCC AAC ATC A < 1120

E H I A A Y G E G N E R R L T G K H E T A N I N

AC ACA TTC AAA TGG GGG GTT GCA AAC CGT GGT GCA TCT GTC CGT GTT GGA AGA GAC ACA GAG AAG GCA GG < 1190

T F K W G V A N R G A S V R V G R D T E K A G

C AAG GGA TAC TTT GAG GAC AGA AGG CCA GCC TCA AAT ATG GAC CCA TAC GTC GTT ACC TCC ATG ATT GCA < 1260

K G Y F E D R R P A S N M D P Y V V T S M I A

GAA ACC ACC ATC ATC GGT TAA < 1281

E T T I I G *

GS1.4 (Solyc12g041870.1)

```
TCT CTC CAT TTT TGT TTT CTA CAA ACT CGT CAC ACA TTA ATT CAG ATG AGA GCA ACC AAA ATT CAT GTG A < 70

AA ACA CAT TTT AAA TAT ATA TTA TAA GTT GAA GAA GAG AAA TTA AGA ATA TAT CAC TTG TAA CAT ATG GG < 140

T TGT GGT TTT AGC TGT TTA TAA AGA GTT CAA ATT AGC TTC TTA TAA TAA GAT TTT TTG CTT GAA AGT GAG < 210

TTA AGA AAC ATG TCA CTC TTG GAT CTT GTC AAC CTG GAT CTC TCT GAA TGC CAC GAG ACA AAC AAA AGT A < 280

      M  S  L  L  D  L  V  N  L  D  L  S  E  C  H  E  T  N  K  S  R

GA ATC ATT GCT GAA TAT ATA TGG ATT GAT GGA TCT GAT ATG AAC CTG AGA AGC AAA GGA AGG ACC CTG CA < 350

      I  I  A  E  Y  I  W  I  D  G  S  D  M  N  L  R  S  K  G  R  T  L  H

T GGT CCT GTT ACT AGT CCT TCT CAA ATT CCA AAT TGG AAC TAT GAT GGT TCG AGT ACT GGC CAA GCT CCT < 420

      G  P  V  T  S  P  S  Q  I  P  N  W  N  Y  D  G  S  S  T  G  Q  A  P

GGT GAA GAT AGT GAA GTC ATC TTA TAT CCC CAG GCA ATT TAC AAG GAC CCA TTC AGG GGA GGA AAT CAT A < 490

      G  E  D  S  E  V  I  L  Y  P  Q  A  I  Y  K  D  P  F  R  G  G  N  H  I

                                >SlGS1.4Fwd

                                |

TT CTT GTC ATG TGT GAT GCT TAT ACT CCA GCT GGA GAG CCC ATC CCA ACA AAC AAA AGG TTT AAT GCT GT < 560

      L  V  M  C  D  A  Y  T  P  A  G  E  P  I  P  T  N  K  R  F  N  A  V

A AAG ATA TTT AGC CAC CCT GAA GTC CTG GCT GAG ATA CCT TGG TTT GGT ATA GAG CAG GAG TAC ACT TTG < 630

      K  I  F  S  H  P  E  V  L  A  E  I  P  W  F  G  I  E  Q  E  Y  T  L

TTG CAG AAA AAT CTG AAT TGG CCC CTT GGT TGG CCA ATT GGA GGA TAT CGT GGA CCT CAG GGA CCA TAC T < 700

      L  Q  K  N  L  N  W  P  L  G  W  P  I  G  G  Y  R  G  P  Q  G  P  Y  F

                                <SlGS1.4Rev

                                |

TC TGT GGT GTT GGT GCA GAA AAA GCC TTT GGC CGG GAT ATT GTC AAC TCA CAC TAC AAA GCG TGT CTA TA < 770

      C  G  V  G  A  E  K  A  F  G  R  D  I  V  N  S  H  Y  K  A  C  L  Y

T GCT GGT GTC AAC ATT GGT GGA ATC AAT GCA GAA GTT ATG GCA GGC CAG TGG GAA TTT CAA GTT GGA CCA < 840

      A  G  V  N  I  G  G  I  N  A  E  V  M  A  G  Q  W  E  F  Q  V  G  P
```

ACA GTA GGC ATT TCT CCT TGT GAT GAC CTT TGG GTA GCG CGT TAC ATT CTA GTG AGG ATT GCA GAA GCA G < 910
T V G I S P C D D L W V A R Y I L V R I A E A A

CT GGT GTA ATT GTT TCT TTT GAT CCG AAA CCT GTT GAG GGT GAT TGC AAT GGT ACT GGT GCT CAT ACA AA < 980
G V I V S F D P K P V E G D C N G T G A H T N

T TAC AGT ACC AAG TCT ATG AGG GCC GAT GGA GGA CTA GAA GTA ATA AAC AAA GCC ATT GAG AAG CTA GGC < 1050
Y S T K S M R A D G G L E V I N K A I E K L G

AAG AGG CAC AAG GAA CAT ATT GTT GTT TAT GGT GTT GGC AAT GAA CGT CGT CTT ACA GGA GAA CAT GAA A < 1120
K R H K E H I V V Y G V G N E R R L T G E H E T

CA GCT GAT ATT AAC ACC TTC AAT TTT GGA ATT GCT GAT CGC GGA GCA TCG ATT AGG ATT GGA AGG GAG AT < 1190
A D I N T F N F G I A D R G A S I R I G R E M

G GAA AAA GCT GGA AAA GGA TAC TTG GAG GAT AGA AGG CCC TTT TCA AAC ATG GAT CCT TAT ATG GTA ACG < 1260
E K A G K G Y L E D R R P F S N M D P Y M V T

TTT ATG ATT GCA GAA ACA ACC ATC CTG TGG AAA CCA TGA CAC TTC TAT GAT TGC CTT CTT GCA TAT GAA T < 1330
F M I A E T T I L W K P *

GA AAA TTA ACA AAA AGG ATA GCA CAA AGG TGA ATT TTA TGC AGA TTT GAT CGA ACT TTA ATA TAA TAT TG < 1400

T TAG CCG CTA GCC AGG TTG TAC ATC ACA CCC CTT GAG GTG CGA TTC TTT TTT GGC CGA TGC TAA CAT GGG < 1470

ATA CTT TGT GTA GTA GGT TTT TTT TTA CAT AAT CTT GAG GTC TAC GTA AAT AGC TAC TAC TCT TTG TAT T < 1540

AG GTC AAT TTT CTA ATA AAA TAT TCT CTT TG < 1571

Supplemental data 2. Clustal omega's multiple sequence alignment with all SIGSs cDNAs.

GS2	ATGGCTCAGATCCTGGCTCCGTCTGCACAATGGCAGATGAGAATGACAAAGAGCTCAACC
GS1.4	-----
GS1.3	-----
GS1.1	-----
GS1.2	-----
GS2	GATGCTAGTCCCTTGACTTCAAAGATGTGGAGCTCTGTGGTGCTGAAGCAGAACAAAAGA
GS1.4	-----
GS1.3	-----

```

GS1.1 -----
GS1.2 -----

GS2      CACGCTCTTAAAAGCTCTGCCAAATTTAGAGTTTTTGGCCCTACAGTCTGACAAATGGCACC
GS1.4    -----ATGTCACTC
GS1.3    -----ATGTCTCTGCTT
GS1.1    -----ATGGCTCATCTT
GS1.2    -----ATGTCTATGATT

GS2      GTGAACAGAGTGGAAACAGCTGCTAAACTTGGACGTAACCTCCATACACTGATAAGATCATT
GS1.4    TTGGATCTTGTCAACCTGGATCTCTCTGAATGCCACGAGACAAAAGTAGAATCATT
GS1.3    TCAGATCTTATCAACCTCAATC-----TCTCAGGTGATACTCAGAAGATCATT
GS1.1    TCAGATCTTGTCAATCTTAATC-----TCTCTGATTCCTCTGAGAAAATCATT
GS1.2    TCAGATCTCATCAATCTTAATT-----TATCTGAATGCACTAAGAAAATTATT
          *       *   *   *                               *   **  ***

GS2      GCTGAATATATTTGGATCGGAGGGACTGGAATTGACATGCGCAGTAAATCAAGGACTATT
GS1.4    GCTGAATATATATGGATTGATGGATCTGATATGAACCTGAGAAGCAAAGGAAGGACCCTG
GS1.3    GCTGAATACATATGGATTGGTGGATCAGGCATGGACATGAGGAGCAAAGCCAGGACTCTC
GS1.1    GCTGAATACATATGGATTGGTGGATCAGGAATGGATGTAAGGAGCAAAGCCAGGACTCTA
GS1.2    GCCGAATACATATGGATTGGTGGATCAGGCACTGATCTCAGGAGCAAAGCCAGGACTCTT
          **  *****  **  *****  *   **  *  *  *   *   *  *  *  *  *  *  *  *  *  *  *

GS2      TCGAAACCAGTCAAGGATGCTTCTGAGCTCCCAAAGTGGAACTACGATGGATCAAGTACT
GS1.4    CATGGTCTGTACTAGTCCCTTCTCAAATTCCAAATGGAACTATGATGGTTTCGAGTACT
GS1.3    CCTGGTCCAGTTACTAGTCCCTGCAGAACTACCCAAATGGAACTACGATGGATCGAGCACT
GS1.1    TCTGGTCTGTGATGATCCTTCAAAGCTTCCCAAATGGAAATATGATGGTTCTAGCACA
GS1.2    TCAGGTCTGTTAAGGATCCTTCAAGCTTCCCAAATGGAACTATGACGGATCTAGCACA
          **  **          *  *  *  *  *  *  *  *  *  *  *  *  *  *  *  *  *  *

GS2      GGACAAGCACCTGGAGAAGACAGTGAAGTCATTCTATATCCTCAGGCAATATTTCAAAGAC
GS1.4    GGCCAAGCTCCTGGTGAAGATAGTGAAGTCATCTTATATCCCAGGCAATTTACAAGGAC
GS1.3    GGTCAAGCTCCCGGAGAAGACAGTGAAGTGATCTTATATCCACAAGCAATCTTCAAAGGAC
GS1.1    GGTCAAGCTCCTGGAGAAGACAGTGAAGTGATCCTATATCCTCAAGCAATTTTCAAAGGAT
GS1.2    GGGCAAGCTTCTGGAGAAGACAGTGAAGTGATCCTATATCCTCAAGCAATTTTCAAAGGAT
          **  *****  *  **  *****  *****  *  *  *****  **  *****  *  ***  **

GS2      CCTTTCCGTGGTGGTAACAACATCTTGGTTATCTGTGATGCCTACACACCAGCTGGAGAG
GS1.4    CCATTCAGGGGAGGAAATCATATTCTTGTGCATGTGTGATGCTTATACTCCAGCTGGAGAG
GS1.3    CCATTCAGAAGAGGCAACAACATCTTGGTCATGTGTGATGCCTATACTCCTGCTGGTGAG
GS1.1    CCATTCAGGAGGGGCAACAATATCTTGGTCATCTGTGATTGTTACACCCAGCTGGTGAA
GS1.2    CCATTCAGGAGAGGTGATAATATTTTGGTCATGTGTGATGCTTACACTCCAGCTGGTAAT
          **  ***  *  *  **  *  *  **  *  **  *  *  *  *  *  *  *  *  *  *  *

GS2      CCAATTCCTACAAACAAACGCCATAAAGCTGCTCAAATTTTTAGCGACCCAAAAGTTGCA
GS1.4    CCCATCCCAACAAACAAAAGGTTTAAATGCTGTAAAGATATTTAGCCACCCGAAAGTCCTG
GS1.3    CCCATCCCAACAAACAAGAGGCACGCCGCCCAAGGTCCTCAGCCACCCGATGTGGCT
GS1.1    CCAATTCCAACAAACAAGAGGCACAATGCTGCTAAAATATTTAGCAACCCGTAATGTTGTT
GS1.2    CCCATTCCAACAAACAAGAGGCACAATGCAGCCAAGATTTTCAGCAACCCGTTGTTGCT
          **  **  **  *****  *  *  *  *  *  *  *  *  *  *  *  *  *  *

GS2      GCTCAAGTTCATGGTTTGGAAATAGAACAAGAGTACACCTTACTCCAGCCAAATGTAAC
GS1.4    GCTGAGATACCTTGGTTTGGTATAGAGCAGGAGTACACTTGTGTCAGAAAAATCTGAAT
GS1.3    GCTGAGGAAACTTGGTATGGTATTGAACAAGAATATACCTTGTGCAAAGGGAGGTCAAC
GS1.1    GTTGAGGAACCATGGTATGGTCTTGAGCAAGAATACACCTTGTACAAAAGGAAATTAAT
GS1.2    GCTGAAGAACCATGGTATGGTATCGAGCAAGAGTACACGTTGTTGCAGAAAAGAGGTTAAC
          *  *  *  *  *  *  *  *  *  *  *  *  *  *  *  *  *  *  *  *  *  *

GS2      TGGCCCTTAGGTTGGCCTGTTGGAGGCTACCCCGACCTCAGGGTCCTTACTACTGTGGT
GS1.4    TGGCCCTTGGTTGGCCAAATGGAGGATATCGTGGACCTCAGGGACCATACTTCTGTGGT
GS1.3    TGGCCTCTTGGATGGCCCATTTGGCGGTTTTCCCTGGCCCCCAGGGACCATACTACTGTGGA
GS1.1    TGGCCTCTTGGATGGCCTATTGGTGGCTTTCCTGGACCACAGGGACCATACTACTGTGGA
GS1.2    TGGCCTCTCGGATGGCCTATTGGAGGTTTTCCCTGGACCTCAGGGACCTTACTACTGTGGA
          *****  *  **  *****  *****  *  *  *  *  *  *  *  *  *  *  *  *

GS2      GCTGGAGCGGAAAAGTCATTTGGCAGAGATATATCAGATGCTCACTACAAGGCTTGCCTG

```



```

GS2      GAAGCTCTTGCTGCCCAAAAGATCTCATTGAAGGTTTAG
GS1.4    -----
GS1.3    -----
GS1.1    -----
GS1.2    -----
    
```

Supplemental data 3. Results from SIGS sequencing using NCBI platform.

Sequences producing significant alignments:

Select: [All](#) [None](#) Selected: 0

Alignments [Download](#) [GenBank](#) [Graphics](#) [Distance tree of results](#)

Description	Max score	Total score	Query cover	E value	Ident	Accession
Solanum lycopersicum glutamine synthetase (GS2), transcript variant 1, mRNA	276	276	96%	1e-70	99%	NM_001323669.1
Lycopersicon esculentum clone 134810R, mRNA sequence	276	276	96%	1e-70	99%	BT013265.1
Solanum lycopersicum chromosome ch01, complete genome	267	267	91%	8e-68	100%	HG975513.1
Solanum lycopersicum strain Heinz 1706 chromosome 1 clone hbe-55e23 map 1, complete sequence	267	267	91%	8e-68	100%	AC239438.2
PREDICTED: Solanum pennellii glutamine synthetase, chloroplast (LOC107002042), transcript variant X1, mRNA	257	257	93%	5e-65	98%	XM_015199972.1

Figure 1. Results from the blast of the obtained products resulting from gene sequencing of SIGS2. The highlighted result corresponds the best match.

Sequences producing significant alignments:

Select: [All](#) [None](#) Selected: 0

Alignments [Download](#) [GenBank](#) [Graphics](#) [Distance tree of results](#)

Description	Max score	Total score	Query cover	E value	Ident	Accession
Solanum lycopersicum glutamine synthetase cytosolic isozyme 1-1 (gts1), mRNA	150	150	97%	4e-33	98%	NM_001323058.1
Solanum lycopersicum chromosome ch04, complete genome	150	150	97%	4e-33	98%	HG975516.1
Lycopersicon esculentum partial mRNA for putative glutamine synthase (gts1 gene)	145	145	97%	2e-31	97%	AJ277561.1
PREDICTED: Solanum pennellii glutamine synthetase cytosolic isozyme 1-1 (LOC107018296), mRNA	119	119	97%	1e-23	91%	XM_015218748.1
Solanum pennellii chromosome ch04, complete genome	119	119	97%	1e-23	91%	HG975443.1
PREDICTED: Solanum tuberosum glutamine synthetase cytosolic isozyme 1-1 (LOC102595103), mRNA	117	117	96%	4e-23	90%	XM_006346698.2

Figure 2. Results from the blast of the obtained products resulting from gene sequencing of SIGS1.1. The highlighted result corresponds the best match.

Sequences producing significant alignments:

Select: [All](#) [None](#) Selected: 0

Alignments [Download](#) [GenBank](#) [Graphics](#) [Distance tree of results](#)

Description	Max score	Total score	Query cover	E value	Ident	Accession
Solanum lycopersicum glutamine synthetase cytosolic isozyme 1-1 (gts1), mRNA	154	154	88%	4e-34	96%	NM_001323058
Solanum lycopersicum chromosome ch04, complete genome	154	154	88%	4e-34	96%	HG975516.1
Solanum tuberosum glutamine synthetase GS1 (qin) mRNA, complete cds	152	152	90%	1e-33	95%	AF302115.2
PREDICTED: Solanum pennellii glutamine synthetase cytosolic isozyme 1-1 (LOC107018296), mRNA	148	148	88%	2e-32	95%	XM_015218748.1
Solanum pennellii chromosome ch04, complete genome	148	148	88%	2e-32	95%	HG975443.1

Figure 3. Results from the blast of the obtained products resulting from gene sequencing of SIGS1.2. The highlighted result corresponds the best match.

Sequences producing significant alignments:

Select: All None Selected: 0

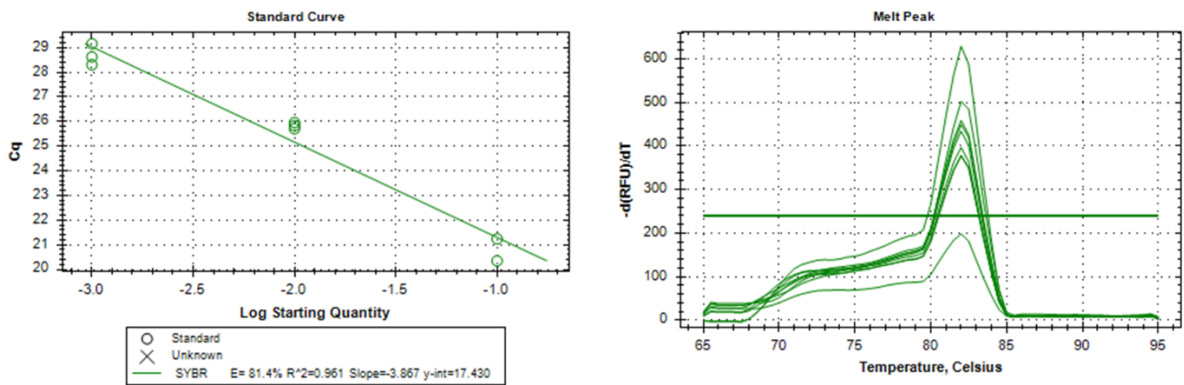
Alignments Download GenBank Graphics Distance tree of results

Description	Max score	Total score	Query cover	E value	Ident	Accession
Solanum lycopersicum glutamine synthetase (GS1), mRNA	220	220	98%	5e-54	100%	NM_001319855.1
Lycopersicon esculentum clone 113612F, mRNA sequence	220	220	98%	5e-54	100%	BT012720.1
Lycopersicon esculentum glutamine synthetase mRNA, partial cds	220	220	98%	5e-54	100%	U14754.1
PREDICTED: Solanum pennellii glutamine synthetase (LOC107004767), mRNA	215	215	98%	2e-52	99%	XM_015203118.1

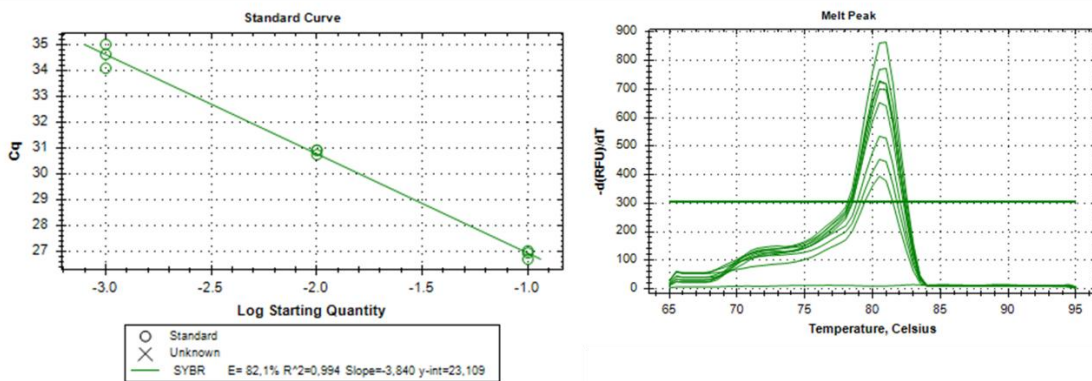
Figure 4. Results from the blast of the obtained products resulting from gene sequencing of SIGS1.3 using. The highlighted result corresponds the best match.

Supplemental data 4. Melting curves and calibration curves for SIGS2 (A) and SIGS1.1 (B) genes.

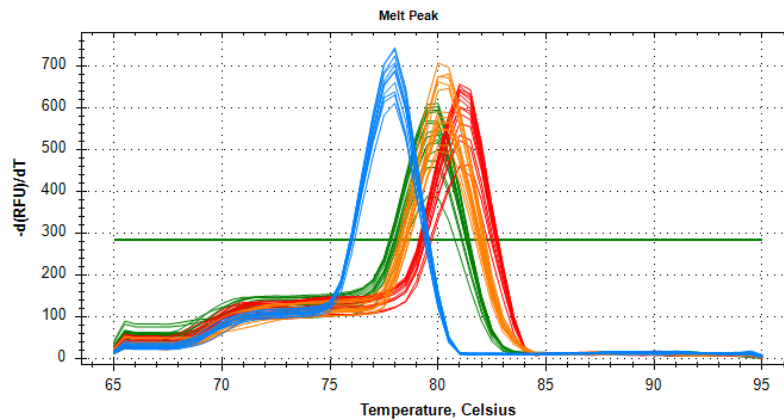
A



B



Supplemental data 5. Melting curves for *psIIA* (blue), *psIIB* (orange), *rbcL* and *rbcS* (red) genes.



Supplemental data 6. Solyc01g08280.2 full sequence, with annealing regions for Forward and Reverse primers (yellow) used for the full amplification of its coding region/cDNA, initial and stop codons (purple), the UTR (green) and the CDS (blue) highlighted.

ATATAGGAGAATATCAAATCTTTTTAAAAAAGAATATGAAATTTTAAAAAGTAATAATTTATACAAATCTTATTACTATCTTACGAAG
ATAACAATGTTAACCCCTCGACTTAATAATATATTTCAAATCAGAAATTAATAAAGAAATACAATAGTAATAAATGCATGATAAATAGATA
AAAAGATAAGTATCAACCATTAATAATAATAATATATTTTTTTAAAAATAATAGATGAGTTAATAACTTTGAACAGAAAAATTAGATAAT
ATTCAATTGTTTATCAATAAGTTATTATGTCTGAGAAACTGTAAAGTTTTACCCTTTTTTAATATTATTATTTTTATTCTTAATCTTT
AAGTCCTCTTGAATTAAGTAATTATAATTGGAAGAACTTCCAAAAAGTTTTTTTTTATAATAAAGAATAGATAATTAATTAATTAAGAA
GCCGATCATGAAAAACAACCTTTTTACCTTTTCTAAAACCTTTGAAGTATATCATCAATATCTGAACAAAGTTAAACAAAGACAAATAAT
GACAAAAGCCAGAGTTTTAAATACTAATTAATAGACTGATTAATTTACTAAAAAGATTATTTTTATTCAAATCTTGTCTTTATGAACT
GGTTACACTGGCAAAAAAACTATTTCTTTCTTAACAAGATATTTCAATTTCAAATCGTGAACAGAAAAATTAACATTATTATTAATG
AATGAAATGAACACAGTATAGATATGAATTAATCGAACTTTAACATGAAAAACGAAAAAAAATTAAGAAGAGAAGGCCCTTATCTTAA
ATGATAGGAGAAATATAGAAGTCATTGAATCTGGTAAAGGGTGACCTTATCAAACATAAACTATTTTCCGCCACTCAACAGACACC
CCTATCTACAATGAAAAAGCCAAGAACTTTCCATGTCCACTCAATTTTGTACCTTTAAATAGACTTCTCAAATAAGTTTTTGT
ACTCACCCATCTTCATCTTCTTCTCTCACTCTCAACACAACATTATTTCTGCATTGTCCACTTAGGTATGTAACCTATTTTCTACT
AACAGGGTCTGTTTTTTTTTCTTCTAAGACTGAAATGTGTGATTTTCATGCAAAAATAACACTGTTTTGTAAGTTTTGGGTTTGTGGGGTTT
TTAGTTTCTTGAGTATTGATTGCTGATAACAAAATGTGTGGATCAGAATGGGGTTTTAGTCACTGTTGTTTCAAGATTTCATCTTAAAGA
CCTAAATTGAATCTCAAGTACTATCTTTTTTCTTTCTTAGTGTGTGACCTTTGCATTATATGGATAAACTGCTAATAATGTTAGAGT
CATCATGTTAGTAGTCTTTGTTGTTCTTGTATCTGCTCTGTGAGATTTAAGGTATGCCTATGCTCTACCCTCCCCAGACCGCAC
TTGAGTGGGATTACAGTGGGAATGTTGTTGTTGTGGTACAATGGAGGATAACTCTAGTGGGAGGGTTTTGAGTTATGGTAGAAATTA
CATTTTCTCCTTGAATGATCATCTCGAAACAGAAAAGAGACAAAAGGTGAATTTTCTTTTTTCGAAACAGGACTGCATCCTTAACCTTA
GATTTAGATTGCAATATGATAAGTGTAGTTACATACTATATCTTATTCTGGAAGAGATCTTGGTTCCGGTATAGGGCTGCGCAGCAT
GGTTCATTACTCATTTTCATAGTTGATTTTTGACGGTAAATCCATTTCTCATTATTTTCGTAGTTCCCTGTCCCTTCGTTTCTGTTATTACC
TTTTGGTGCTTAAATATCGCATTATTTGGCTGTTATTACAGTTACTTTTCTCTGTATGTTATTGAATGTTTTCCCTGTTATTTGCTGTATC
CTCTTTGATTCTATTTTTTTGTCTAATTGCTTTGGTATGCATTACTTGAACCGAGGGTCTTTAGAAAACATCTCTACTACTACCTCCA
CGAGGCGAGGGTAAGGTCTGTGTACACCCTCTACCCTCCCCAACTCCACTACCCTCCCCAACTCCACCTGTGGAATTACACTGG
GTATGTTATCCATTAATGCCATGAAAATAAGATGACTTAAAAGTAGAATCCTGATAATTAGTTTGTCTGATGAGCATTGTTGATCTGATG
AGATTTTTAATCTTGATTGGTGATAAAGTTCCTTGTCTGTTATTTAACTTTTTTCAGTTGGTTAGGAGGTGAACGCTCAGATCTT
GGCTCCGCTGCACAATGGCAGATGAGAATGACAAGAGCTCAACCGATGCTAGTCCCTTGACTTCAAAGATGTGGAGCTCTGTGGT
GCTGAAGCAGAACAAAAGACACGCTCTTAAAAGCTCTGCCAAATTTAGAGTTTTGCCCCTACAGTCTGACAATGGCACCCTGAACAG
AGTGGAACAGCTGCTAAACTTGGACGTAACCTCATACACTGATAAGATCATTGCTGAATATATTTGATATATTCTTTGCTATATGCA
ATCTCATACTGTTTACTCAACATTGTCACTTGAAGATTTGTAGATCGTGTCTGTCAATTTCTTCACTTTCACTACCTTTACGAATGCCTAC
ATCTAGTTCTTTATGGATAGACTGACCTTGTGACATTTCTTCAAACAGGATCGGAGGGACTGGAATTGACATGCGCAGTAAATCAA
GGGTACATAGTCTGCTTCTTAATTAACCAACAAAAGTTTAGGAACTGAATTTGGATTATCTCATGTTATTTCTATTAATTGTTTCT

TTTGAATTTTCAGACTATTTTCGAAACCAGTCAAGGATGCTTCTGAGCTCCCAAAGTGGAACACGATGGATCAAGTACTGGACAAGCA
CCTGGAGAAGACAGTGAAGTCAATCTATAAGTAAGATCAGCAGCTGAATTTTTTTTTCTTTCTTTTTGAAGAATTTTCCTTTCTTTCTTT
ATTCCTTATTTTATTGTAAAAAAATCTTCTTTTCTTTTCCCATTTCTAAAGCTAACCTTGATCATTAACTCAGTCCTCAGGCAAT
ATTCAAAGACCCCTTCCGTGGTGGTAACAACATCTTGGTGAAGTTGTTTAGTAAACAATACTGATTCATGATGTTTTACTGAATCTTTAAT
CTCATTGGTTTTAAGTTTGGCACTATTGTTGTCTAAATTGAAACAGGTTATCTGTGATGCCTACACACCAGCTGGAGAGCCAATTCCT
ACAAACAAACGCCATAAAGCTGCTCAAATTTTAGCGACCCAAAAGTTGCAGCTCAAGTTCATGTAATTTTAAATTCATCTGCCTCA
CTTTTATAGTTTTATGTACCGTGTGGCTATTCTTCTGCATTATTTGTTGAGGTCTCTAAAACCAAGAGAACGCCAACTGTTCCCTTTG
AACAGTCAAAAATAAAATAAATGTGCTCATAGTTCATTTATCATGTAAAAACCTCATTAACTAACTCCAGGAAAATGAATTTTTGTTA
GACATTACGTTTCTCGCAAATAAATGCTAAGCTGGAAAGCTGCTTCTTATACTCTTTTAAACAACAACAACAACAAAATAAACCCGA
CGTATGTCCAAAAGTGTCTGCTGGGAAGTTAGTGTATACACAGACCTTACACCTACAAGGTAGAGAAGCTGTTTCGGCCTCAGCAG
TATTTAAAACCTGTTTCTTGTACTCTTTAACTGTTCCAGTTAAAGATCTCTCTTTAGCTGTTGGATGATAACATGATGAAACAATCA
TTTCTTGATGTTAGCAAGATCCTTTTTCTCCTGAAAATGGGATCAAAAAGAGTATATGTTGTTATTTGGTGCATTTTGCCTCCAG
TTTTGAATTTAATATCATATTGCTAATGTTGTCTAGCACTTGGTGTGACTAGGTTTGAATAGAACAAGAGTACACCTTACTCCAG
CCTAAATGTAACCTGGCCCTTAGGTTGGCCTGTTGGAGCTACCCCGACCTCAGGTAATTGTTTACACAAAAAGAATGGTACACAG
CTCAAAAATCATCCAGCACAAATGCAATCTAATGATGCTGTAATACTGTTCAATTTAATTAAGTGGAGATCTATTTATCTTTGTG
GAACTTTAGGGTCTTACTACTGTGGTGTGGAGCGGAAAAGTCAATTTGGCAGAGATATATCAGATGCTCACTACAAGGCTTGCCT
GTATGCTGGAATTAACATTAGTGGTACTAATGGAGAGGTTATGCCAGGACAGGTACCATTTCATCACTTCTATTCTAGTACAATAAA
ATCACTGTCACTTATAGTACTCTAATTTGGAGGATCAACGTAATTTGTTTTCAGTGGGAATTTCAAGTAGGTCCTAGTGTGGAATG
AAGGTGGAGATCATATCTGGTGTGCTAGATACCTCCTCGAGGTAATTAATCTTCCAAATCTGCATAAAATTTCTTTCAGGTTAGG
CATCTGGCAAGCATATCATCTAATTTCAACGAACAATACTTGAATACCTATTGACTCAGCTCCAGGTCCCGGCTGTGGGATTAAGG
AAATATTTTTCTAGTGGCATGAAATGATCGACTTATTACCTAAAGTGGTCTTTGACTGTTGCTGTGGTTTATGCTCTTGTATTGA
AGTGGTGTGCTGAACTAAGAAATCAGATTACTCATTCTTTTTTTTTTCCAAATCTTGATCTAACAGAGAATTAAGTACAATTAAGAA
GAGTTGTCTCTCACTCGATCCAAAACCAATTGAGGTGATCTAAAATCTTTATGATTTTTTTGTTATTCAAATTAAGTACAATTAAGAA
ACTCCATTTTTCTTCTCTGGTCTGGCATTACAGGGTACTGGAACGGTGCAGGATGCCACACTAACTACAGGTAGCTCCTTTTTG
CAAGAGAGAACTAGGAATCTTAAAGATAAGATTTGGGATGTGAATCTGTTAAGACCGAAATCACTTGCTCATTATGTTGGTATGTTGCT
ACAAC TAGGAATTAGTTGCAAGTACTTTTTACAATTCATTTTTGTTTATGTTTCGTAAGTCTTGTCTGTTTAAACCGCGCCC
CCTCTCCGTTTTTTCATTTTTCCAGTTTAGCAATTCTGTCTTCTGAAAACCAATGTATGGTTTCCATAGTAAAACCTTTGAAGGATTCA
CTTACTAGTTATTAATGGTTTGTGTTTGCAGTACACTGAGTATGAGAGAAGAGGGAGGTTTGAAGTTATAAGAAAAGCAATTTGAA
TCTATCCCTTCGCCACAAGGAACATATAAGTGCTTATGGAGAAGGAAATGAGAGAAGGTTGACCGGAAAGCATGAAACTGCTAGTAT
TGACCAATTTTCATGGGTATGCCTGCTGCTGATCTTCCCTTCAATTTGTACATAAAATAGTGTGTACCAATTATCCTCATTCTTCTGATT
TTCTAAATATGCAGGGAGTTGCTAACCGTGGTTGCTCAATCCGTGTGGGCGTGACACTGAGAAGGAAGGCAAGGTAAGTTTCTG
CTTTATTAGAGGGAGTAACATTAGCATCCTTGAGTTTATTGTGCAATGATGAAAAATGTAGCTTATTTTGGGACCACTTTTCTCAACA
TACATTTGCATAAAAAGAAAGTTAAAATACTGGATCTCAAAAATAAAAAGAGATGAATTAACCTTTTCTGAACAGTTATCCATGATCCAA
GCATCACTGTTTCTCATGGCCTTTTAAAGAATTTGCAACTATTTAGCTAAACACTTTGGCCTTGGCATTGATGGTCTTCTGATGCTGT
TTATTTCTCCTTTTTTGTCTGGGTTGGTGCATGCAGGTTATTTGGAAGACCGCCGCCAGCTTCAAACATGGACCCCTATGTTGT
GACTGGATTACTTGTGAACTACTATACTGTGGGAGCCAAACCCTTGAAGCTGAAGCTTGTCTGCCAAAAGATCTCATTGAAGGT
TTCAGTATATGAGGGGAAATTTGTTTTCATAAATACTCTTGAATTTATGAGATAAGTTCTGAAGCTTGTACCTTGTGAGGTTCC
TTATTTGGGAAAATCTTGTAAAGGAACCAAAATTTACCAGTTCATCCTAGAAAATAGGTTTCTTAAGACATGAGACTACTTTGGAGTTG
AGGTGTAATTTGGACTACTTTGAACATCTTTACCTTCTTTCTCCAGATGAATCCATTTCTCTGAAATCCAATGGTGTGCTCTTT
CCGAATGAAATCTTTGAACATATAATCAGTCAATTTTCAGTTTCTAACTAGCTAGTTAAGTTACTTATATGATGTTATCTTCTGTC
TACTATGTTCAAGTTCAGGTTCTTTAGAGAAATCATCATAAATGTTTATGATGTTGGCCATCAATCTGCCAGACTCTCGTCTTTAT
CTGGATTTGAACCTGGTTCTTTCCAGCATATATATTCATGTTACATGGACTTGAATATATGTGTCCAGCATGCTATTTTTAGTACT
TTGACTTGTGCAAAAGTAAATGAAGACTTCAAGTTAGTAAAGATGCATAATGTATGATGATAAGCTTGGCTTTCTTTCTTTAGAAAT
ATTTATTAATACCTTTTACATTTGTGTGAAGCCAAAGTATTCTTCCCTATCAGAATGCTTGTGTAACCTAGTCCAAGAGATTCTT
TTCATTTCTTTGGAGAAAAGCTACAAGCTGTCAATGTTGTCTAGATAAAGAAATGGAACAATCATGGCTTTA

Supplemental data 7. pJET1.2/blunt Map Vector.

